

TR 26-54

A STUDY OF PETROL AND DIESEL FUEL BLENDS WITH SPECIAL REFERENCE TO  
THEIR THERMODYNAMIC PROPERTIES AND PHASE EQUILIBRIA

Caroline Heyward

A thesis submitted to the Faculty of Science, Rhodes University,  
Grahamstown, in fulfilment of the requirements for the degree of  
Master of Science

December 1985

ACKNOWLEDGEMENTS

The author gratefully makes the following acknowledgements:

To Professor T.M. Letcher, under whose careful supervision this research was conducted, for his constant help and advice.

To Elna Dunnington for her assistance in the preparation of this text.

To Rhodes University and the C.S.I.R. for financial assistance.

ABSTRACT

The ternary phase behaviour of the n-heptane-1-propanol-water system was studied and compared with the theoretical prediction based on the UNIQUAC model for non-electrolyte solutions. The results showed that this model adequately approximated experimental studies.

The excess enthalpies and excess volumes for several binary mixtures were determined. The excess enthalpies were measured using a LKB flow microcalorimeter and the excess volumes determined using a PAAR densitometer. The study showed that no significant enthalpy or volume changes occurred when petrol/n-heptane were mixed with alcohols.

Ternary phase diagrams, including tie lines have been determined for a number of petrol-alcohol-water systems (including the Sasol blend of alcohols). The tie line results show that the concentration of water in the water-rich layer is strongly dependent on the type of alcohol used. The Sasol alcohol blended with petrol resulted in a high water concentration in the water-rich layer which forms on phase separation. This is believed to contribute significantly to the corrosion problems experienced by motorists using the Sasol blended fuel on the Witwatersrand. The effect of temperature on several of these blends was included in the study.

Diesel-alcohol blends and the co-solvent properties of ethyl acetate investigated. Ethyl acetate ensures miscibility at low concentrations for diesel-ethanol blends. Octyl nitrate and two cetane improvers from AECI were assessed in terms of their ability to restore cetane rating of blended diesel fuel to that of pure diesel fuel. The results indicated that all three samples were successful in this application.

CONTENTS

	<u>PAGE</u>
LIST OF TABLES	VI-VIII
LIST OF FIGURES	IX-XIII

SECTION

1. <u>INTRODUCTION</u>	1
1.1   TRANSPORTATION FUELS	1
1.2   TRENDS IN WORLD FUEL POLICY	3
1.3   LIQUID TRANSPORT FUEL FROM COAL	4
1.4   LIQUID TRANSPORT FUEL FROM NATURAL GAS	8
1.5   LIQUID TRANSPORT FUEL FROM OIL SHALES AND TARSANDS	9
1.6   PLANT OILS AS LIQUID TRANSPORT FUELS	10
1.7   ALCOHOLS AS LIQUID TRANSPORT FUELS	11
1.8   PROBLEMS ASSOCIATED WITH ALCOHOL FUEL BLENDS	14
1.8.1   Phase Separation	14
1.8.2   Corrosiveness	14
1.8.3   Exhaust Emissions	15
1.9   RESEARCH MOTIVATION	15
2. <u>THE PREDICTION OF PHASE EQUILIBRIA</u>	17
2.1   INTRODUCTION	17
2.2   APPLICATION OF THERMODYNAMICS TO PHASE EQUILIBRIA PROBLEMS	18
2.2.1   Activity and Activity Coefficients	19
2.2.2   Activity and Excess Gibbs Energy	20
2.2.3   Excess Gibbs Energy for a Binary System	21
2.2.4   Other Excess Gibbs Energy Relations	24
2.3   THE UNIQUAC EQUATION	26
2.3.1   Partition Function for a Binary Liquid Mixture	27
2.3.2   The Local Area Fraction	28
2.3.3   Combinatorial Factor	29
2.3.4   Average Local Area Fractions in Nonathermal Mixtures	30



CONTENTS - Continued

	PAGE
2.4 APPLICATION OF THE UNIQUAC EQUATION TO DETERMINE LIQUID-LIQUID PHASE EQUILIBRIA IN TERNARY SYSTEMS	33
2.4.1 Objectives	34
2.4.2 Evaluation of Pure-Component Structural Parameters	35
2.4.3 Determination of Binary Parameters	35
2.4.4 Pilot Investigations	36
2.4.4.1 Fitting of Activity Coefficient Data	36
2.4.4.2 Fitting of Solubility Data	36
2.4.5 Prediction of the Ternary Phase Diagram for the System Ethanol + Benzene + Water	39
2.4.6 Prediction of the Ternary Phase Diagram for the System 1-Propanol + n-Heptane + Water	48
2.5 DISCUSSION AND CONCLUSION	52
3. <u>EXCESS ENTHALPIES AND EXCESS VOLUMES OF HEPTANE/ PETROL + ALCOHOL BLENDS</u>	54
3.1 INTRODUCTION	
3.2 APPARATUS	54
3.3 EXCESS MOLAR ENTHALPIES OF BINARY LIQUID MIXTURES	54
3.3.1 Introduction	54
3.3.2 Flow Calorimeters	55
3.3.3 The LKB 2107 - 121 Flow Calorimeter	55
3.3.4 Determination of the Excess Enthalpy of Mixing for the Systems Heptane/Petrol + Alcohol	57
3.3.5 Operating Procedure	58
3.3.5.1 Determination of Flow Rates	58
3.3.5.2 Determination of Excess Molar Enthalpies of Mixing $H_m^E$	59
3.3.6 Results	59
3.4 EXCESS MOLAR VOLUMES OF BINARY LIQUID MIXTURES	67
3.4.1 Introduction	67
3.4.2 Vibrating Tube Densitometer	67

CONTENTS - Continued

	<u>PAGE</u>
3.4.3 Principle of Density Measurement	67
3.4.4 The PAAR DMA 601 Densitometer	68
3.4.5 Determination of the Excess Volume of Mixing for the Systems Heptane/Petrol + Alcohol	69
3.4.6 Operating Procedure	70
3.4.7 Results	72
3.5 DISCUSSION AND CONCLUSION	77
4. <u>WATER SOLUBILITY STUDIES IN PETROL AND HEPTANE + ALCOHOL BLENDS</u>	 78
4.1 INTRODUCTION	78
4.2 EXPERIMENTAL PROCEDURE	80
4.2.1 Materials	80
4.2.2 Binodal Curve and Tie Line Measurements	80
4.2.3 Conductivity Measurements	82
4.3 RESULTS	82
4.4 DISCUSSION	123
5. <u>DIESEL-ALCOHOL BLENDS</u>	127
5.1 INTRODUCTION	127
5.2 EXPERIMENTAL PROCEDURE	128
5.2.1 Materials	128
5.2.2 Method	128
5.3 RESULTS	128
5.4 DISCUSSION	138
6. <u>CONCLUSION</u>	140
7. <u>FUTURE STUDIES</u>	141
<u>REFERENCES</u>	143-147
APPENDIX 1	A1-A6
APPENDIX 2	A7-A11

LIST OF TABLES

<u>SECTION</u>		<u>PAGE</u>
1.	TABLE 1.1	RESERVES OF FOSSIL FUELS 4
	TABLE 1.2	PROPERTIES OF METHANOL AND ETHANOL COMPARED WITH PETROL 11
2.	TABLE 2.1	SOME MODELS FOR THE EXCESS GIBBS ENERGY AND SUBSEQUENT ACTIVITY COEFFICIENT FOR BINARY SYSTEMS 25
	TABLE 2.2	INTERACTION PARAMETERS FROM THE FITTING OF UNIQUAC COMPARED TO THOSE OF PRAUSNITZ 36
	TABLE 2.3	MUTUAL SOLUBILITIES OF HYDRO- CARBONS AND WATER AT 0 AND 25°C 38
	TABLE 2.4	INTERACTION PARAMETERS FROM THE FITTING OF UNIQUAC COMPARED WITH THOSE OF PRAUSNITZ 39
	TABLE 2.5	INTERACTION PARAMETERS FROM THE FITTING OF UNIQUAC COMPARED WITH THOSE OF PRAUSNITZ 40
	TABLE 2.6	INTERACTION PARAMETERS FROM THE FITTING OF UNIQUAC COMPARED WITH THOSE OF PRAUSNITZ 40
	TABLE 2.7	PHASE SEPARATION USING DERIVED INTERACTION PARAMETERS 41
	TABLE 2.8	PHASE SEPARATION USING PRAUSNITZ INTERACTION PARAMETERS 41
	TABLE 2.9	BINODAL CURVE DETERMINED BY BANCROFT AND HUBARD 42
	TABLE 2.10	EXPERIMENTALLY DETERMINED BINODAL CURVE 42
	TABLE 2.11	INTERACTION PARAMETERS 48
	TABLE 2.12	INTERACTION PARAMETERS 48
	TABLE 2.13	BINODAL CURVE DETERMINED USING CALCULATED $a_{12}$ AND $a_{21}$ 49
	TABLE 2.14	EXPERIMENTAL BINODAL CURVE 49

LIST OF TABLES - Continued

<u>SECTION</u>	<u>PAGE</u>		
3.	TABLE 3.1	EXPERIMENTAL EXCESS ENTHALPIES FOR THE PETROL/N-HEPTANE + ALCOHOL SYSTEMS AT 298,15 K	61
	TABLE 3.2	THE LIQUIDS USED IN THIS THESIS, THEIR SUPPLIERS AND THEIR DENSITIES	71
	TABLE 3.3	EXPERIMENTAL EXCESS MOLAR VOLUMES $V_M^E$ FOR PETROL + ALCOHOL SYSTEMS AT 298,15 K	72
4.	TABLE 4.1	EXPERIMENTAL DATA FOR THE BINODAL CURVES OF PETROL-ALCOHOL-WATER SYSTEMS AT 298,15 K	83
	TABLE 4.2	EXPERIMENTAL DATA FOR THE BINODAL CURVES OF N-HEPTANE-ALCOHOL-WATER SYSTEMS AT 298,15 K	87
	TABLE 4.3	CONCENTRATIONS OF THE TERNARY SOLUTIONS (a) AND (b) FOR THE PETROL TERNARY SYSTEMS AT 298,15 K	92
	TABLE 4.4	CONCENTRATIONS OF THE CONJUGATE TERNARY SOLUTIONS (a) AND (b) FOR THE HEPTANE TERNARY SYSTEMS AT 298,15 K	94
	TABLE 4.5	THE WATER CONCENTRATION $C_W$ OF THE WATER RICH LAYER AS CALCULATED FOR THE PETROL-ALCOHOL-WATER TERNARY SYSTEMS AT 298,15 K	96
	TABLE 4.6	CONCENTRATION OF WATER, $C_W$ , IN 10,0% AND 20,0% ALCOHOL-PETROL MIXTURES	97
	TABLE 4.7	CONDUCTIVITY, $\sigma$ OF, ALCOHOL-WATER MIXTURES OF WATER COMPOSITION $C_W$	98

LIST OF TABLES - Continued

<u>SECTION</u>		<u>PAGE</u>	
	TABLE 4.8	ELECTROSTATIC FACTORS FOR PURE LIQUID COMPONENTS	124
	TABLE 4.9	CLASSIFICATION OF SOLVENTS	124
5.	TABLE 5.1	EXPERIMENTAL DATA FOR THE BINODAL CURVES OF DIESEL-ALCOHOL-ETHYL ACETATE TERNARY SYSTEM AT 298,15 K	129
	TABLE 5.2	CETANE NUMBERS FOR DIESEL + ETHANOL + ETHYL ACETATE BLENDS	131
	TABLE 5.3	CETANE NUMBERS FOR DIESEL + ETHANOL + ETHYL ACETATE + OCTYL NITRATE BLENDS	132
	TABLE 5.4	CETANE NUMBERS FOR BLENDS CONTAINING OCTYL NITRATE (ON) OR AECI SAMPLES 1 AND 2	133

LIST OF FIGURES

<u>SECTION</u>		<u>PAGE</u>	
1.	FIGURE 1.1	THE HYDROGENATION AND SYNTHESIS ROUTE FOR COAL LIQUEFACTION	6
	FIGURE 1.2	THE FISCHER-TROPSCH PROCESSES EMPLOYED AT SASOL 1	7
	FIGURE 1.3	PROJECTED LIFETIMES OF ENERGY SOURCES	8
2.	FIGURE 2.1	STATEMENT OF PROBLEM	17
	FIGURE 2.2	THREE-STEP OF THERMODYNAMICS TO PHASE-EQUILIBRIA PROBLEMS	18
	FIGURE 2.3	GIBBS ENERGY FUNCTION FOR A PARTIALLY MISCIBLE LIQUID MIXTURE	33
	FIGURE 2.4	RESULTS OF FITTING BENZENE- ACETONE DATA TO VARIOUS EQUATIONS	37
	FIGURE 2.5	COMPARISON OF ACTIVITY COEFFICIENTS FOR THE ETHANOL- BENZENE SYSTEM	43
	FIGURE 2.6	COMPARISON OF ACTIVITY COEFFICIENTS FOR THE ETHANOL- WATER SYSTEM	44
	FIGURE 2.7	COMPARISON OF THE HYPOTHETICAL ACTIVITY COEFFICIENTS FOR THE PARTIALLY MISCIBLE BENZENE- WATER SYSTEM	45
	FIGURE 2.8	RESULTS OF THE $G_{MIX}^E$ COMPUTATION FOR THE BENZENE- ETHANOL-WATER SYSTEM	46
	FIGURE 2.9	TERNARY PHASE DIAGRAM OF THE PREDICTED BEHAVIOUR FOR THE BENZENE-ETHANOL-WATER SYSTEM	47
	FIGURE 2.10	RESULTS OF THE $G_{MIX}^E$ COMPUTATION FOR THE N-HEPTANE- 1-PROPANOL-WATER SYSTEM	50

LIST OF FIGURES - Continued

<u>SECTION</u>		<u>PAGE</u>
	FIGURE 2.11 TERNARY PHASE DIAGRAM OF THE N-HEPTANE-1-PROPANOL-WATER SYSTEM	51
3.	FIGURE 3.1 TOP VIEW OF LKB FLOW MICROCALORIMETER	56
	FIGURE 3.2 MIXING VESSEL OF A DIFFERENTIAL FLOW MICROCALORIMETER	56
	FIGURE 3.3 THE EFFECT OF INCREASING HYDROCARBON CHAIN OF THE ALCOHOL WHEN MIXED WITH N-HEPTANE AT 298,15 K	63
	FIGURE 3.4 A COMPARISON OF $H_M^E$ VALUES FOR THE SYSTEMS N-HEXANE, N-HEPTANE AND PETROL + ETHANOL AT 298,15 K	64
	FIGURE 3.5 A COMPARISON OF EXPERIMENTAL $H_M^E$ VALUES WITH LITERATURE DATA FOR THE SYSTEM N-HEPTANE + ISO-PROPANOL AT 298,15 K	65
	FIGURE 3.6 EXPERIMENTAL $H_M^E$ RESULTS FOR N-HEPTANE + ALCOHOLS AT 298,15 K	66
	FIGURE 3.7 LABORATORY ARRANGEMENT FOR THE MEASURING OF $V_M^E$ VALUES	68
	FIGURE 3.8 THE EFFECT OF INCREASING HYDROCARBON CHAIN OF THE ALCOHOL WHEN MIXED WITH N-HEPTANE AT 298,15 K	74
	FIGURE 3.9 A COMPARISON OF $V_M^E$ VALUES FOR THE SYSTEMS N-HEPTANE AND PETROL + ETHANOL AT 298,15 K	75

LIST OF FIGURES - Continued

<u>SECTION</u>		<u>PAGE</u>
	FIGURE 3.10 A COMPARISON OF $V_M^E$ VALUES FOR THE PETROL + ALCOHOL SYSTEMS AT 298,15 K	76
4.	FIGURE 4.1 LABORATORY ARRANGEMENT FOR THE DETERMINATION OF THE BINODAL CURVE AND ITS TIE LINES	81
	FIGURE 4.2 EXPERIMENTAL BINODAL CURVE FOR THE SYSTEM PETROL + METHANOL + WATER AT 298,15 K	100
	FIGURE 4.3 EXPERIMENTAL BINODAL CURVE FOR THE SYSTEM N-HEPTANE + METHANOL + WATER AT 298,15 K	101
	FIGURE 4.4 EXPERIMENTAL BINODAL CURVE FOR THE SYSTEM PETROL + ETHANOL + WATER AT 298,15 K	102
	FIGURE 4.5 EXPERIMENTAL BINODAL CURVE FOR THE SYSTEM N-HEPTANE + ETHANOL + WATER AT 298,15 K	103
	FIGURE 4.6 EXPERIMENTAL BINODAL CURVE FOR THE SYSTEM PETROL + 1-PROPANOL + WATER AT 298,15 K	104
	FIGURE 4.7 EXPERIMENTAL BINODAL CURVE FOR THE SYSTEM N-HEPTANE + 1-PROPANOL + WATER AT 298,15 K	105
	FIGURE 4.8 EXPERIMENTAL BINODAL CURVE FOR THE SYSTEM PETROL + ISO-PROPANOL + WATER AT 298,15 K	106
	FIGURE 4.9 EXPERIMENTAL BINODAL CURVE FOR THE SYSTEM N-HEPTANE + ISO-PROPANOL + WATER AT 298,15 K	107
	FIGURE 4.10 EXPERIMENTAL BINODAL CURVE FOR THE SYSTEM PETROL + 1-BUTANOL + WATER AT 298,15 K	108
	FIGURE 4.11 EXPERIMENTAL BINODAL CURVE FOR THE SYSTEM N-HEPTANE + 1-BUTANOL + WATER AT 298,15 K	109



LIST OF FIGURES - Continued

<u>SECTION</u>		<u>PAGE</u>
FIGURE 4.12	EXPERIMENTAL BINODAL CURVE FOR THE SYSTEM PETROL + SEC-BUTANOL + WATER AT 298,15 K	110
FIGURE 4.13	EXPERIMENTAL BINODAL CURVE FOR THE SYSTEM N-HEPTANE + SEC-BUTANOL + WATER AT 298,15 K	111
FIGURE 4.14	EXPERIMENTAL BINODAL CURVE FOR THE SYSTEM PETROL + TERT-BUTANOL + WATER AT 298,15 K	112
FIGURE 4.15	EXPERIMENTAL BINODAL CURVE FOR THE SYSTEM N-HEPTANE + TERT-BUTANOL + WATER AT 298,15 K	113
FIGURE 4.16	EXPERIMENTAL BINODAL CURVE FOR THE SYSTEM N-HEPTANE + ISO-BUTANOL + WATER AT 298,15 K	114
FIGURE 4.17	EXPERIMENTAL BINODAL CURVE FOR THE SYSTEM PETROL + 1-PENTANOL + WATER AT 298,15 K	115
FIGURE 4.18	EXPERIMENTAL BINODAL CURVE FOR THE SYSTEM N-HEPTANE + 1-PENTANOL + WATER AT 298,15 K	116
FIGURE 4.19	EXPERIMENTAL BINODAL CURVE FOR THE SYSTEM PETROL + 1-HEXANOL + WATER AT 298,15 K	117
FIGURE 4.20	EXPERIMENTAL BINODAL CURVE FOR THE SYSTEM N-HEPTANE + 1-HEXANOL + WATER AT 298,18 K	118
FIGURE 4.21	EXPERIMENTAL BINODAL CURVE FOR THE SYSTEM PETROL + SASOL ALCOHOL + WATER AT 298,15 K	119
FIGURE 4.22	EXPERIMENTAL BINODAL CURVE FOR THE SYSTEM N-HEPTANE + SASOL ALCOHOL + WATER AT 298,15 K	120

LIST OF FIGURES - Continued

<u>SECTION</u>		<u>PAGE</u>
FIGURES 4.23 4.24	THE EFFECT OF TEMPERATURE ON THE SOLUBILITY OF WATER IN 10% AND 20% MIXTURES (BY MASS) OF ALCOHOL IN PETROL	121
FIGURE 4.25	THE BINODAL CURVES FOR PETROL-ALCOHOL-WATER TERNARY SYSTEMS AT TWO TEMPERATURES 273,15 K AND 313,15 K	122
5. FIGURE 5.1	BINODAL CURVES FOR DIESEL-METHANOL-ETHYL ACETATE SYSTEMS	134
FIGURE 5.2	BINODAL CURVES FOR DIESEL-ETHANOL-ETHYL ACETATE SYSTEMS	135
FIGURE 5.3	CETANE NUMBER PLOTTED AGAINST DIESEL CONCENTRATION	136
FIGURE 5.4	CETANE NUMBER AS A FUNCTION OF OCTYL NITRATE CONCENTRATION FOR DIFFERENT CONCENTRATIONS OF DIESEL	136
FIGURE 5.5	THE DEGREE OF CETANE IMPROVEMENT PER PERCENT OF OCTYL NITRATE PLOTTED AGAINST THE DIESEL CONCENTRATION	137
FIGURE 5.6	THE CETANE NUMBER PLOTTED AGAINST CETANE IMPROVER CONCENTRATION FOR 60% AND 80% DIESEL CONCENTRATION	137

## 1.1. TRANSPORTATION FUEL

Energy for transportation has historically occurred naturally. Wind and muscle power served transportation needs on sea and land from pre-Christian times until the nineteenth century. The steam age saw solid fuels in the form of wood and coal power man into the industrial revolution. Railways and steamships served the needs of transportation and consumption of coal rocketed to keep pace with energy demands. The advent of the motor car at the turn of the century saw a significant demand for liquid transportation fuel emerge. The ready availability of Middle East oil and its cheapness supported the adoption of oil based fuels for road and air transport needs from the time of World War I <sup>(1)</sup>. Subsequent to the Second World War its use has been extended to almost all of the worlds sea and rail transport systems as well. Its natural advantage as a transport fuel has seen its demand increase by leaps and bounds in the second half of the twentieth century, reaching a level where Western Europe, Japan and the United States increased their oil imports by 95 percent between 1967 and 1973 <sup>(2)</sup>. In October 1973 the OPEC member countries raised the price of oil from \$ 3,11 to \$ 5,12 per barrel <sup>(2)</sup> and the oil crisis began. This, together with the fact that the world will exhaust its oil reserves within the next 60 - 100 years <sup>(3)</sup> has sparked off a world wide interest in alternative energy sources.

The three problems of replacing oil as a transport fuel relate to its high recoverable energy content, its easy transportability and the ninety years development of the motor vehicle. The automobile manufacturers have developed two highly specific engines refined to suit high quality petrol and diesel fuel so that any major change in energy sources must allow for a long transition period <sup>(4)</sup>.

When considering an alternate transport fuel one should consider the properties of the present fuels. They should:

- 1) be liquid at ambient temperatures and pressures
- 2) have a low vapour pressure to avoid vapour lock but some light components for easy vapourization in cold-starting
- 3) have high energy density (calorific value per mass unit)
- 4) have high density
- 5) have low levels of exhaust emissions (5)

In turn, conventional spark and compression ignition engines, should be improved using advanced technology. For example improved fuel economy is being sought by use of on-board computers, changes in combustion chamber shapes, more efficient emissions control devices, high compression ratios and reduced engine capacity and mass, through the use of turbochargers and the application of new materials (6). Improvements in fuel economy have already been achieved and in the five years after 1974, new cars sold in Britain used 10 percent less fuel (7). In West Germany and other European countries much the same is true.

It has been predicted that the end of the growth in oil supply is only ten years away and that this will be followed by ten years of fairly constant production giving governments and consumers some time in which to make the adjustments necessitated by a real decline in crude oil supply (3).

The need to conserve fuel because of uncertain availability and unpredictable prices is not the only problem the transportation industry faces. Additional uncertainty arises because fuel quality could begin to deteriorate significantly during this decade. The liquid hydrocarbons from which future petrol and diesel fuel will be made, whether from crude oil, coal, oil shales or tarsands are likely to contain increasing quantities of impurities such as sulphur and nitrogen, some of which may also appear in the refined motor fuel (8). There will be pressure to reduce the octane rating of petrol to increase the yield from crude oil and to reduce the energy used in refining.

For example, problems associated with a larger cut diesel fuel (at present - diesel fuel constitutes 18 percent of the crude oil barrel) will cause a drop in cetane value resulting in poor control of the combustion process, excessively high pressure in the combustion chamber, high stress levels, increased noise and difficult starting <sup>(9)</sup>.

Cetane and octane improvers could be added in larger quantities but this would not be cost effective since fuel additives contribute greatly to the cost of the fuel. As many as ten different additives are commonly included in a motor fuel. These include detergent dispersants, metal deactivators, rust and corrosion inhibitors, flow improvers, smoke suppressants, oxidation inhibitors, blending agents and deposit control substances <sup>(10)</sup>. These represent an important manufacturing sector of the fuel industry.

## 1.2 TRENDS IN WORLD FUEL POLICY

The crude oil situation has prompted much discussion and controversy with nations having to decide on definite fuel strategies. World communities have adopted different short term philosophies.

In Europe the attitude exists that crude oil is essential for just two major uses: transportation (including private vehicles, air-planes, ships and trucks) and petrochemical industries. This is due to the fact that road transport accounts for about one quarter of the total crude oil consumption, the other big users being industry (31 percent) and office heating (28 percent) <sup>(7)</sup>, both of which could utilise alternative energy sources such as coal and natural gas.

The United States instituted a synthetic fuel program in the 1970's. This has faltered as the crude oil prices have been maintained or reduced so that refined fuel costs have compared favourably with the production costs of synfuels <sup>(11)</sup>.

OPEC policy will probably remain constant in order to prevent a reducing dependence on oil due to increasing synfuel substitution. The result is that the U.S. has increased its dependence on OPEC for oil (2).

In the long term countries will have to recognise their resources and develop technologies to suit their needs. The potential non-petroleum sources from which liquid fuels may be obtained include enormous coal reserves (already being exploited in South Africa), natural gas, oil shale and tarsands, renewable biological materials and municipal waste. The first three non-renewable resources will be discussed. Appendix 1 deals with crude oil and its refining (4).

### 1.3 LIQUID TRANSPORT FUEL FROM COAL

It is accepted that the mainstay resource in the future will be coal. Examinations of Table 1.1 shows that whereas oil is absent in many of the world's industrial nations coal is readily available.

TABLE 1.1 - RESERVES OF FOSSIL FUELS

	Coal (hard + lignite) (Mg x 10 <sup>9</sup> )	Oil (m <sup>3</sup> x 10 <sup>9</sup> )	Gas (m <sup>3</sup> x 10 <sup>12</sup> )	Peat (Mg x 10 <sup>9</sup> )
Algeria	-	1,1	3,6	-
Argentina	-	0,4	-	-
Australia	111	0,2	0,9	-
Brazil	11	-	-	-
Canada	85	1,0	1,6	27,3
China	1011	3,2	0,7	-
Columbia	13	-	-	-
Cuba	-	-	-	0,9
Czechoslovakia	22	-	-	-
Finland	-	-	-	28,5
Germany (East)	30	-	-	11,4
Germany (West)	70	-	-	-
India	106	0,5	-	-



TABLE 1.1. - RESERVES OF FOSSIL FUELS - CONTINUED

	Coal (hard + lignite) (Mg x 10 <sup>9</sup> )	Oil (m <sup>3</sup> x 10 <sup>9</sup> )	Gas (m <sup>3</sup> x 10 <sup>12</sup> )	Peat (Mg x 10 <sup>9</sup> )
Indonesia	-	1,7	0,7	2,7
Japan	19	-	-	0,6
Libya	-	4,1	0,7	-
Malaysia	-	0,4	0,4	-
Middle East	-	36,0	14,1	-
Netherlands	-	-	1,8	-
Nigeria	-	3,1	1,3	-
Norway	-	0,9	0,5	2,1
Poland	51	-	-	6,9
South Africa	72	-	-	-
Sweden	-	-	-	10,2
USSR	5527	12,4	26	182
UK	16	2,7	0,8	10,5(inc Eire)
USA	1506	5,0	6,2	15
Venezuela	-	2,4	1,2	-

The conversion of coal to premium fuels is brought about by the application of heat (pyrolysis), by the use of solvents and by reaction with oxygen, steam or hydrogen. These, either alone or in combination constitute the processing technologies. The two broad divisions of the technology involve either hydrogenation or synthesis. Hydrogenation involves the combined effect of heat to breakdown the complex molecular structures in coal to simpler, but still ring structures; benzene, toluene and naphthalene represent possible products. The synthesis route involves a much more drastic breakdown of coal structures by total gasification with steam and oxygen, the intermediate product being a synthesis gas consisting mainly of hydrogen and carbon monoxide. By suitable choice of catalysts and conditions, the relative concentration of hydrogen and carbon monoxide can be adjusted to suit the final synthesis process which can produce, for example, methane, methanol, ammonia or a complex mixture of aliphatic hydrocarbon and alcohols obtained by the Fischer-Tropsch process. Figure 1.1 represents the two processes (12).

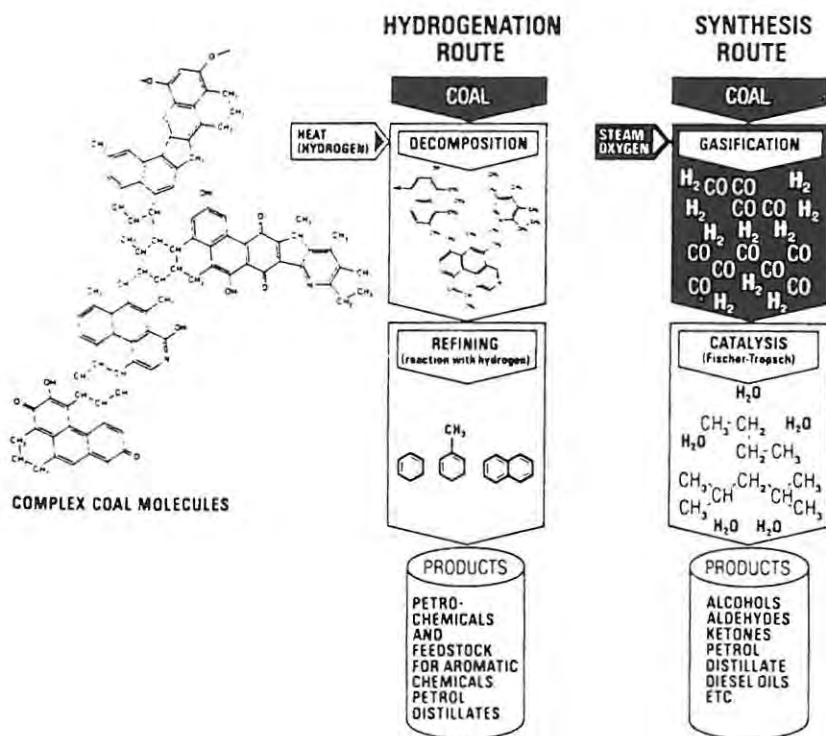


FIGURE 1.1 THE HYDROGENATION AND SYNTHESIS ROUTE FOR COAL LIQUEFACTION

South Africa decided to opt for the oil from coal programme during the 1950's when the SASOL organisation was established. The Fischer-Tropsch process was adopted for a number of reasons. Firstly, South African coals were found to have a high inherent ash content rendering them suitable for the existing hydrogenation process. A second reason was that mining operation and agriculture rely on diesel fuel as their machinery fuel and the Fischer-Tropsch process allows for the production of a satisfactory diesel fuel. Figure 1.2 is a schematic diagram of the process in operation at SASOL 1.



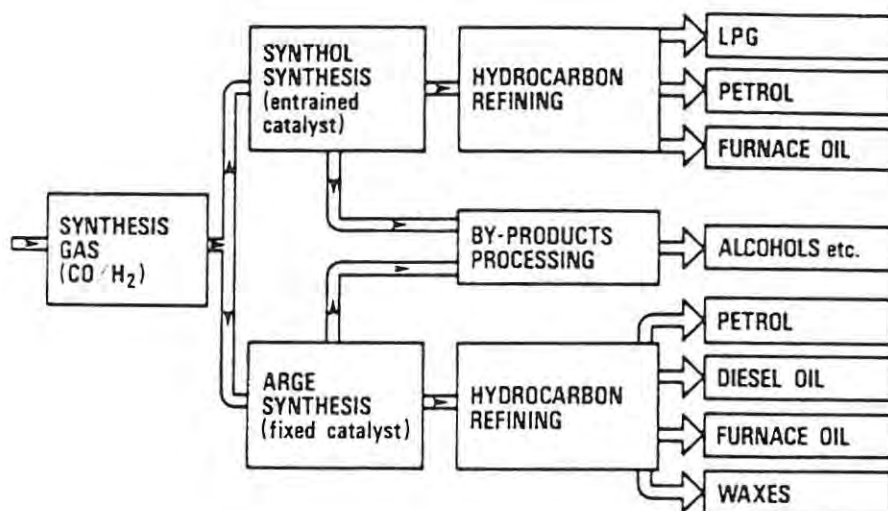


FIGURE 1.2 THE FISCHER-TROPSCH PROCESSES EMPLOYED AT SASOL 1

The disadvantages of the Fischer-Tropsch synthesis are the wide product spectrum and the low overall thermal efficiencies whereby twenty five percent of the energy in coal is lost in converting it to oil. The chemical market structure in South Africa is, however, able to accommodate the various products, for example, through the substitution of petrol with alcohols which will be dealt with later.

There are environmental and health factors to consider before developing a coal liquefaction industry. A large quantity of carbon dioxide escapes into the atmosphere while vegetation has to be restored to open-cast mined out areas. Coal liquefaction needs large quantities of water for power plant cooling towers, for generating electricity and for manufacturing the hydrogen gas essential for liquefaction. <sup>(13)</sup>. A 600-ton per day plant requires 4000 gallons per minute or about four gallons of water for every gallon of synthetic oil, which constitutes a significant factor in water scarce environments such as constitute much of South Africa. Despite these factors, SASOL in South Africa now has three plants and when SASOL 3 is fully operational should provide 50 percent of South Africa's transport fuels.

It is predicted that the coal reserves of the world could be used for another 500 years if the coal had to be used as a substitute for crude oil and natural gas <sup>(12)</sup>. (Refer to figure 1.3 for a forecast of the world's energy sources).

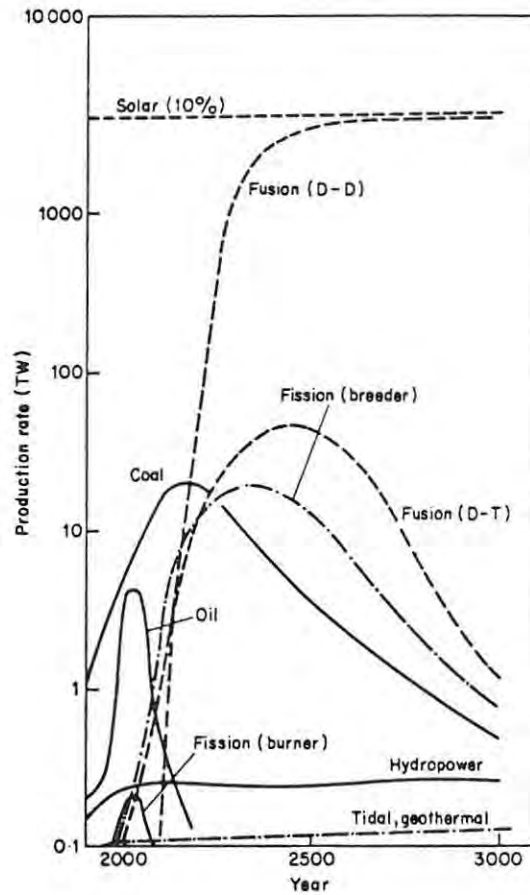


FIGURE 1.3 PROJECTED LIFETIMES OF ENERGY SOURCES. (McMullan et al. 1976)

#### 1.4 LIQUID TRANSPORT FUEL FROM NATURAL GAS

Natural gas is being used as a experimental transport fuel in many parts of the world. In the United States, Ford Motor Company has an experimental fleet of vehicles. This includes a propane (liquid petroleum gas) and a methane (major component of natural gas or a product of coal gasification) driven vehicles. These types of vehicles are available in many parts of the world although they are

dangerous (high pressure cylinders) and may be inconvenient (due to a low energy density requiring frequent refuelling) <sup>(15)</sup>.

In New Zealand, the use of Maui gas to produce petrol via the Mobil process has become an economic proposition and the plant is now productive operating at 13000 barrels a day <sup>(4)</sup>. Metals are added to the shape selective zeolite catalysts that catalyse the formation of methanol from carbon dioxide and hydrogen. As the methanol is formed, it is transformed by the zeolite to hydrocarbon in the range for petrol. The process produces a high octane petrol which contains no sulphur or nitrogenous compounds <sup>(16)</sup>. It, too, like SASOL produces large quantities of alcohol.

This methanol-to-gasoline (MTG) process can be linked to commercial methanol producing processes. An example is a hundred barrels a day pilot plant at Wessiling in West Germany which is linked to a coal gasification processing plant.

#### 1.5 LIQUID TRANSPORT FUEL FROM OIL SHALES AND TARSANDS

In the United States shale oil has received much attention. It is seen as a natural feedstock for the refineries and is hoped to replace imported fuel. There is an astonishing amount of shale oil in the United States but it is situated in remote regions of Utah and Colorado <sup>(17)</sup>. It has to be mined which is expensive and this requires a lot of water. The Union Oil Company in Colorado is, however, proceeding with the project <sup>(11)</sup>.

It is difficult to obtain useful oil from tarsands, since first the tar must be driven from the tarsand by heating, then condensed leaving the resulting product low in hydrogen. Moreover, the sulphur content is high at 25 percent. Oil shale is even less attractive yielding only 3 percent crude oil per mass of shale <sup>(12)</sup>.

## 1.6 PLANT OILS AS LIQUID TRANSPORT FUELS

Diesel wrote in 1911 that the diesel engine can be fed with vegetable oils. Anything, even powdered charcoal can fuel a diesel engine if it can be injected into a cylinder and will ignite at the temperature generated by high compression. Sunflower oil and peanut oil have high energies of combustion being high molecular mass hydrocarbons and can be used as diesel fuels <sup>(18)</sup>. These plants need only be squeezed to extract the oil. Problems do develop with some oils as they are too viscous and can produce excessive carbon when they burn. This results in injection nozzles becoming clogged and such vegetable oils, therefore, do require processing.

Vegetable oils as liquid transport fuel represent a renewable fuel source and can be used as extenders to diesel fuel. For example, the Phillipines uses a 5 percent coconut oil diesel oil blend.

## 1.7 ALCOHOLS AS LIQUID TRANSPORT FUELS

Alcohols can be considered to be major alternate fuels. They can be derived from low grade crude oil, coal and biomass. \* The small molecular mass alcohols, ethanol and methanol have received much attention during the past decade regarding their production and use in transportation vehicles. They have been handled in industry for many years so that their toxicology, flammability and hazards are well-known. Engines designed to burn pure alcohol produce good results in driving performance, horsepower to mass ratios, efficiency and emission compared with today's internal combustion engines fuelled with unleaded petrol <sup>(6)</sup>.

Unfortunately, neither ethanol nor methanol has particularly good fuel properties in current unmodified compression or spark ignition engines so that blending petrol and diesel with methanol and ethanol is being extensively researched.

\* Biomass-a term which includes all products of photosynthesis i.e. all vegetable and animal material as well as agricultural forestry, municipal and industrial waste products.

Furthermore, methanol and ethanol have high octane numbers and low cetane numbers so that cetane improvers are necessary when blending with diesel fuel. For a comparison of the properties of methanol and ethanol with petrol refer to table 1.2 <sup>(5)</sup>.

TABLE 1.2 PROPERTIES OF METHANOL AND ETHANOL COMPARED WITH PETROL

	<u>Methanol</u>	<u>Ethanol</u>	<u>Petrol</u>
Research Octane Number	106-135	106-110*	91
Motor Octane Number	87,4-94,6	90-92*	82
Pre-ignition Rating	0	-28	ca 70
Calorific Value (lower) MJ/kg	19,7	27	44
Latent Heat MJ/kg	1,0	0,85	0,33
Stoichiometric Air-Fuel			
Mass Ratio	6,46	9	14,6
Boiling Point °C	64,6	78,5	35-200**
Vapor Pressure at 70°F, Bar	0,13	0,06	0,6
Relative Density	0,79	0,79	0,75
Molecular Weight	32,04	46,07	100-105 avg.

\* Depending on the source reference

\*\* Full boiling range

The octane numbers of alcohol are significantly higher than petrol and permit an increase in compression ratio of the order of between two and four to one. However, these fuels have much worse pre-ignition tendencies than petrol. Ethanol's properties appear to be more favourable than methanol's due to its higher calorific and lower latent heat values. Generally, alcohols' much lower calorific values lower their stoichiometric air/fuel ratios, requiring more fuel for a given volume. This, and their much higher latent heats, make the fuels' cooling effect on the intake charge much greater than with petrol. Charge temperatures at full load are reduced, resulting in increased volumetric efficiencies and more torque and power from the engine <sup>(5)</sup>.

## ETHANOL

Petrol can be blended with anhydrous ethanol to form a homogeneous blend but low temperatures or water contamination does cause phase separation (see Section 4). Ethanol can be produced from any material which can be hydrolyzed to produce fermentable sugars. Unfortunately, there is no present economical process for converting cellulose to glucose, so feedstocks are limited to sugar or starch crops. In Brazil, energy farming is attractive and both cane and cassava are grown as fuel feedstocks. The Brazilians have developed large scale processes for the fermentations of these crops to produce ethanol which is used to supplement petrol. Fuel blends of up to 20 percent ethanol are used successfully in modified Volkswagen engines whilst fleets of cars are testing 100 percent alcohol fuels <sup>(21)</sup>. Other parts of the world find this strategy incompatible with food production, however. A programme was instituted in the United States for the production of ethanol from corn and a 10 percent ethanol in petrol blend known as Gasohol is marketed in many parts of the country. Use of this fuel is however mainly confined to farmers.

Although ethanol has a low cetane number and is not very soluble in diesel, a diesel-ethanol blend is being tested in the United States. It contains 4 percent butanol (to ensure miscibility) as well as an alkyl nitrate to act as a cetane improver <sup>(22)</sup>. The total amount of ethanol is kept below 35 percent by volume. This blend results in a higher fuel consumption and a reduced smoke content in exhaust emissions.

## METHANOL

Methanol can be produced from the pyrolysis of wood, coal and natural gas. The world's methanol situation is at present catastrophic <sup>(23)</sup> since the world capacity in 1983 exceeded demand by 21 percent and the excess is expected to rise to 29 percent this year. The reason for this surplus is largely due to the fact that methanol is a by-product in many industries and that optimistic projections were made on methanol's use in fuel.



A fuel market has been developed to utilise some of this excess production. Germany is using a 5 percent methanol in petrol blend and in the United States methanol petrol blends are dispensed alongside straight petrol. The 5 percent blend increases road octane rating by two points which is significant for countries facing a lead phasedown. In the United States "gas stations" are also selling 15 percent methanol blends, the effects of which on engine operation are unknown and effective control is still being sought <sup>(24)</sup>.

This higher percentage blend is a very attractive commercial proposition since methanol costs half as much as petrol by volume, although its energy value (refer to table 1.2) is much lower than that of petrol. Methanol is also used as an additive in the United States in a product known as oxinol. It is a 1 : 1 mixture of methanol and tertiary butyl alcohol and is added to petrol upto a 9 percent composition <sup>(25)</sup>. The tertiary butanol is used to prevent phase separation due to methanol's hydroscopic properties. Another advantage of using the higher alcohol content is the increase in volumetric heat content as the enthalpy of combustion of methanol is half that of petrol.

Research into a methanol-diesel fuel is continuing. Methanol is assimilated badly in diesel and a suitable blending agent such as dodecanol must be present to ensure miscibility. The use of blending agents in ensuring stable alcohol fuel blends results in increased costs and thus places an upper limit on the amount of alcohol that can be used in a fuel.

It is generally accepted that methanol produced by gasification and resynthesis is considerably cheaper than ethanol produced by fermentation <sup>(26)</sup>, although ethanol represents a more favourable alternate fuel choice if the fact that it is derived from renewable energy sources is considered <sup>(27)</sup>.

## 1.8 PROBLEMS ASSOCIATED WITH ALCOHOL FUEL BLENDS

### 1.8.1. Phase Separation of Alcohol Blends

The presence of water constitutes a mixing problem with petrol and diesel fuels since hydrocarbon/alcohol/water compositions typically separate into two phases, one water-rich and one water-poor.

In fact, a great number of alcohols contain water (as much as a few percent) as a result of the manufacturing processes. For example, ethanol, produced by fermentation followed by distillation, contains a water content of 4,5 percent <sup>(28)</sup>. The removal of this water necessitates complex azeotropic distillation with aromatic hydrocarbons. All short chain alcohols are hydroscopic and an equilibrium water content is formed after storage due to the uptake of atmospheric moisture. This is usually small (less than one percent) but it can be important in phase separation.

The higher alcohols, propanol and butanol, are more soluble than methanol and ethanol in hydrocarbons but are less volatile. They are also more expensive to produce and not generally considered a feasible alternative. They can be included as a third component in methanol or ethanol hydrocarbon blends as they create an average molecular environment providing solubility to both water and hydrocarbon. For example, iso-propanol can solubise water in hydrocarbons. Other substances such as tetrahydrofuran (THF) and ethyl acetate have been added to diesel/ethanol blends to allow the two to mix even at low temperatures <sup>(29)</sup>. Alternative approaches include the formation of stable microemulsions from the two-phase mixtures of diesel and aqueous ethanol by the addition of surfactants, ionic or non-ionic <sup>(30)</sup>.

### 1.8.2. Corrosiveness

Alcohols are corrosive and react with lead, magnesium, aluminium and some plastics and elastomers <sup>(31)</sup>.



The components in a conventional vehicle system likely to be attacked are, therefore, the fuel tank, "terneplate", fuel pump diaphragms, carburettor and fuel gauge floats, carburettor and pump castings and some sealing rings and washers. These problems are severe with 100 percent alcohol fuels <sup>(32)</sup> but appear to be generally tolerable in blends of 10-20 percent methanol or ethanol.

In South Africa, however, problems associated with the SASOL alcohol substituted fuel (12 percent alcohol mixture added to petrol) have arisen and some carburettors have corroded severely. This has been attributed to either phase separation (as a result of the presence of water) or corrosion by the alcohols (so-called dry corrosion).

### 1.8.3. Exhaust Emissions

Methanol and ethanol have high octane numbers and thus can be used as octane improvers in petrol in countries where use of lead octane improvers is prohibited. There is usually a negligible quantity of sulphur present in these alcohols, so that there are no increased sulphur emissions with them. Carbon dioxide emissions are reduced as is the formation of oxides of nitrogen ( $\text{NO}_x$ ). Exhaust emissions of hydrocarbons are also reduced <sup>(31)</sup>. Methanol, however, does have one major exhaust disadvantage. Emissions of aldehydes occur. Formaldehyde is a major constituent and is known to cause eye irritation and the formation of smog.

## 1.9. RESEARCH MOTIVATION

Much of this project relates to the South African fuel situation. Work has been done on:

- 1) Theoretical prediction of ternary phase behaviour. The system used here was a model system - heptane-1-propanol-water. This involved an assessment of liquid-liquid equilibria models. Literature data was then used to determine parameters necessary for the calculation of Gibbs energy function. The UNIQUAC model was used and proved successful.

2) Thermodynamic properties of excess enthalpy and volume in order to investigate the possible heating and expansion effects on mixing petrol with alcohols.

3) Investigating the phase properties, including tie lines of petrol-alcohol-water in an attempt to understand the severe corrosion problems experienced by motorists in South Africa. Different isomers of the  $C_3$  and  $C_4$  alcohols were tested to determine whether the position of the hydroxyl group could contribute to water solubility. The tie line results proved most successful and demonstrated why South Africa blended petrol-alcohol fuels were potentially more corrosive than the simple ethanol and methanol blends used elsewhere.

4) Diesel-alcohol blends examining methanol and ethanol as prospective extenders relating to their miscibility in diesel with the co-solvent ethyl acetate. A comparison of three cetane improvers was included.

2 THE PREDICTION OF PHASE EQUILIBRIA

2.1 INTRODUCTION

Phase equilibrium thermodynamics quantify the variables which describe the state of equilibrium of two or more homogeneous phases which are free to interchange energy and matter. A homogeneous phase at equilibrium is any region in space where the intensive properties (e.g. temperature and pressure) are the same throughout. The problem under investigation here is to describe the state of two phases which are free to interact and which have reached a state of equilibrium so that given some of the equilibrium properties of the two phases, it is possible to predict the remaining ones. The problem can be represented schematically in figure 2.1 (33).

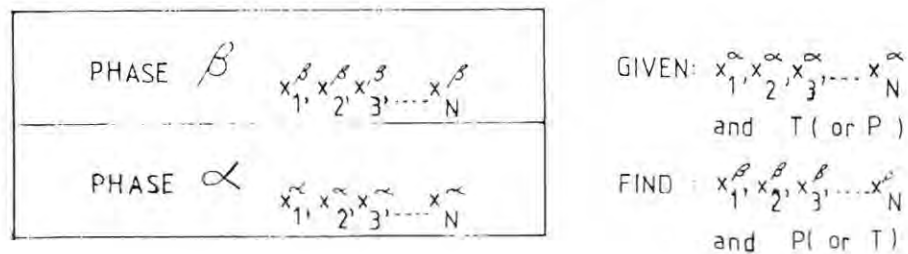


FIGURE 2.1 STATEMENT OF PROBLEM

Let us consider the two multicomponent phases,  $\alpha$  and  $\beta$ , which have reached an equilibrium at temperature  $T$ , the mole fractions  $x_1^\alpha, x_2^\alpha$  of phase  $\alpha$  are known. The mole fractions of phase  $\beta$ ,  $x_1^\beta, x_2^\beta$  and the pressure of the system,  $P$ , are thus required. The number of intensive properties which must be specified to fix the state of equilibrium is given by the Gibbs phase rule (with  $P, T$  and  $x$  as the only variables).

Number of independent intensive properties = (number of components - number of phases + 2)

The determination of ternary phase equilibria which permits the formation of two phases therefore requires all three intensive properties.

## 2.2 APPLICATION OF THERMODYNAMICS TO PHASE EQUILIBRIA PROBLEMS

Application of thermodynamics to phase equilibria in multicomponent systems is shown schematically in figure 2.2

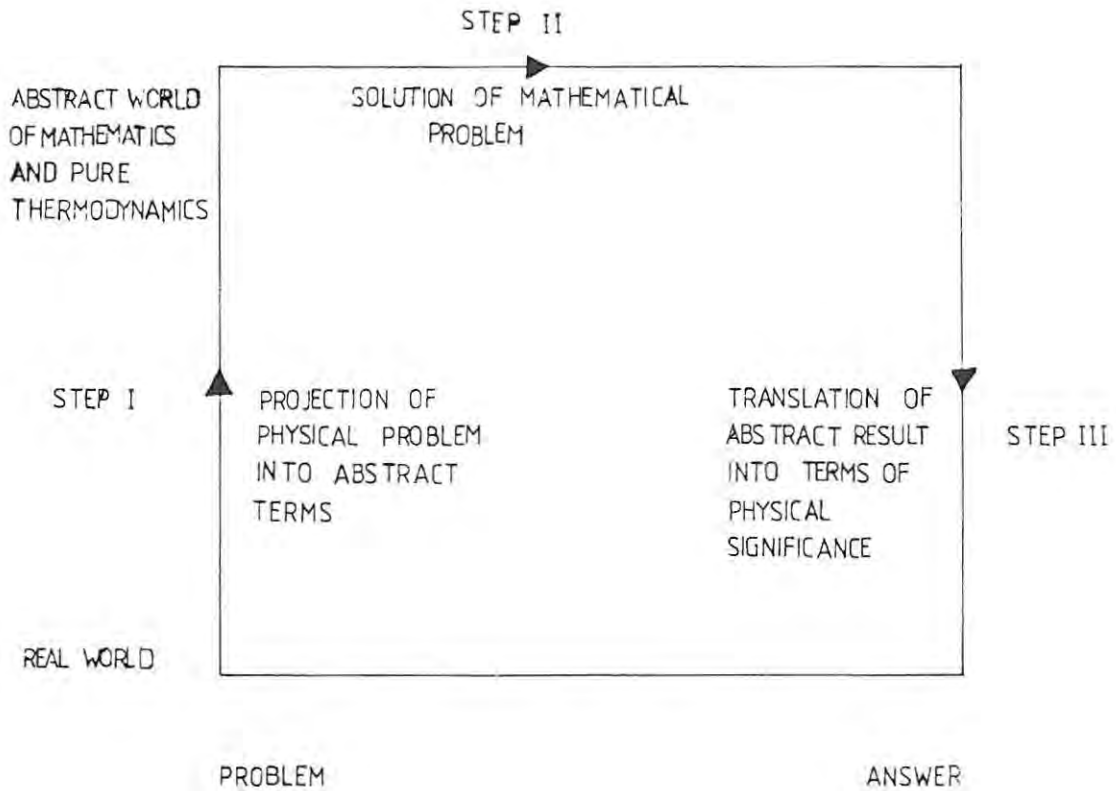


FIGURE 2.2 THREE-STEP APPLICATION OF THERMODYNAMICS TO PHASE-EQUILIBRIA PROBLEMS

Step 1 requires the definition of appropriate and useful mathematical functions in order to facilitate Step 2. Gibbs' 1873 definition of chemical potential makes Step 1 possible as the chemical potential of each component must be equal in every phase. The most difficult step is Step 3 as thermodynamics gives severely limited information on the relation between abstract chemical potential and the real experimentally accessible quantities of temperature, pressure and composition.

Any problem concerning equilibrium distribution of some component  $i$  between two phases,  $\alpha$  and  $\beta$ , begins with the relation:

$$\mu_i^\alpha = \mu_i^\beta \quad \text{eqn. 2.1}$$

where  $\mu$  is the chemical potential. How  $\mu_i^\alpha$  is related to  $T$ ,  $P$  and  $x_1^\alpha, x_2^\alpha, \dots$  and  $\mu_i^\beta$  is related to  $T$ ,  $P$  and  $x_1^\beta, x_2^\beta, \dots$  then becomes the problem. Auxiliary functions such as fugacity and activity are then introduced which give a better notion than the abstract concept of chemical potential.

### 2.2.1 Activity and Activity Coefficients

The activity of a substance gives an indication of how "active" a substance is relative to its standard state, since it provides a measure of the difference between the substance's chemical potential at the state of interest and that at its standard state. The activity of component  $i$  at some pressure, temperature and composition is defined as the ratio of the fugacity of  $i$  ( $f_i$ ) at these conditions to the fugacity of  $i$  in the standard state which is a state at the same temperature as that of the mixture and at some specified condition of pressure and composition.

$$a_{i(T,P,x)} = \frac{f_{i(T,P,x)}}{f_{i(T,P^0,x^0)}} \quad \text{eqn. 2.2}$$

where  $P^0$  and  $x^0$  are respectively arbitrary but specified pressure and composition.

The activity coefficient  $\gamma_i$  is the ratio of the activity of  $i$  to the mole fraction of  $i$ .

$$\gamma_i = \frac{a_i}{x_i} \quad \text{eqn. 2.3}$$

The activity coefficient is also related to  $x_i$  and to the standard state fugacity  $f_i^0$  by

$$\gamma_i = \frac{f_i^L}{x_i f_i^0} \quad \text{eqn. 2.4}$$

where  $f_i^L$  is the fugacity of component  $i$  in a liquid solution.

The standard state fugacity  $f_i^0$  frequently refers to a hypothetical state since it does happen that component  $i$  cannot physically exist as a pure liquid at system temperature and pressure. The value can be calculated by extrapolation with respect to pressure and since liquid-phase properties remote from the critical region are not sensitive to pressure such extrapolation introduces little uncertainty.

### 2.2.2 Activity Coefficient and Excess Gibbs Energy

The relation between partial excess Gibbs energy and activity coefficient is obtained by consideration of the definition of fugacity.

$$\mu_i - \mu_i^0 = RT \ln \frac{f_i}{f_i^0} \quad \text{eqn. 2.5}$$

This equation represents an isothermal change for any component in any system where  $\mu_i^0$  or  $f_i^0$  is arbitrary but may not be chosen independently, when one is chosen, the other is fixed.

At constant temperature and pressure for a component  $i$  in solution,

$$\bar{g}_i \text{ (real)} - \bar{g}_i \text{ (ideal)} = RT [\ln f_i \text{ (real)} - \ln f_i \text{ (ideal)}] \quad \text{eqn. 2.6}$$

The partial excess function  $\bar{g}_i^E$  is introduced by differentiation of:

$$G^E = G_{\text{actual solution}} - G_{\text{ideal solution}} \text{ (at constant } T, P, n_j) \quad \text{eqn. 2.7}$$

Substitution then gives

$$g_i^E = RT \ln \frac{f_i \text{ (real)}}{f_i \text{ (ideal)}} \quad \text{eqn. 2.8}$$

An ideal solution exists, where at constant temperature and pressure, the fugacity of every component is proportional to some suitable measure of its concentration which is usually taken to be the mole fraction. That is, at constant temperature and pressure, for any component  $i$  in an ideal solution

$$f_i^L = R_i x_i \quad \text{eqn. 2.9}$$

where  $R_i$  is a proportionality constant dependent on temperature and pressure but independent of  $x_i$ .

Substitution of this equation into equation 2.8 gives

$$\bar{g}_i^E = RT \ln \frac{f_i}{R_i x_i} \quad \text{eqn. 2.10}$$

It is known that an ideal solution is one where the activity is equal to the mole fraction, if the standard state fugacity  $f_i^0$  is set equal to  $R_i$  the activity becomes

$$a_i = \gamma_i x_i = \frac{f_i}{R_i} \quad \text{eqn. 2.11}$$

But for an ideal solution  $f_i = R_i x_i$  and therefore  $\gamma_i = 1$  and  $a_i = x_i$ . Substitution of equation 2.11 into 2.10 gives the important result.

$$\bar{g}_i^E = RT \ln \gamma_i \quad \text{eqn. 2.12}$$

which leads to

$$g^E = RT \sum x_i \ln \gamma_i \quad \text{eqn. 2.13}$$

from the extensive excess property equation

$$M^E = \sum_j n_j m_j^E \quad \text{eqn. 2.14}$$

$g^E$  is the molar excess Gibbs energy

### 2.2.3. Excess Gibbs Energy for a Binary System

The total excess Gibbs energy  $G^E$  for a binary solution, containing  $n_1$  moles of component 1 and  $n_2$  moles of component 2 is defined by

$$G^E = RT (n_1 \ln \gamma_1 + n_2 \ln \gamma_2) \quad \text{eqn. 2.15}$$

The excess Gibbs energy is that over and above what the observed Gibbs energy for an ideal solution would be at the same temperature, pressure and composition. By definition an ideal solution is one where all  $\gamma_i = 1$ .



Equation 2.15 gives  $G^E$  as a function of both  $\gamma_1$  and  $\gamma_2$ . By differentiation the individual activity coefficients  $\gamma_1$  and  $\gamma_2$  can be related to  $G^E$ .

$$RT \ln \gamma_1 = \left( \frac{\partial G^E}{\partial n_1} \right)_{T, P, n_2} \quad \text{eqn. 2.16}$$

$$RT \ln \gamma_2 = \left( \frac{\partial G^E}{\partial n_2} \right)_{T, P, n_1} \quad \text{eqn. 2.17}$$

These two equations allow limited data to be interpolated and extrapolated with respect to composition.

To illustrate the procedure, consider a binary mixture. Activity coefficients for a binary mixture over the entire range of composition are required at a fixed temperature  $T$ . However, experimental data is available for only one composition  $x_1 = x_2 = 0,5$ . From that one data point  $\gamma_1 (x_1 = 0,5)$   $\gamma_2 (x_2 = 0,5)$  is calculated; for simplicity symmetrical behaviour is assumed so that  $\gamma_1 = \gamma_2$  at  $x_1 = x_2$ .

An expression relating  $G^E$  to the composition and subject to the condition that at fixed composition  $G^E$  is proportional to  $n_1$  and  $n_2$  and that  $G^E = 0$  when  $x_1 = 0$  or  $x_2 = 0$  is required.

The simplest expression obtained is:

$$G^E = (n_1 + n_2) g_E = (n_1 + n_2) A x_1 x_2 \quad \text{eqn. 2.18}$$

where  $g_E$  is the excess Gibbs energy per mole of mixture and  $A$  is a constant dependent on temperature. The mole fraction  $x$  is simply related to mole number  $n$  by:

$$x_1 = \frac{n_1}{n_1 + n_2} \quad \text{eqn. 2.19}$$

$$x_2 = \frac{n_2}{n_1 + n_2} \quad \text{eqn. 2.20}$$



The constant A is found from substituting equation 2.18 into equation 2.15 and using the experimentally determined  $\gamma_1$  and  $\gamma_2$  at the composition midpoint.

$$A = \frac{RT}{(0,5)(0,5)} \left[ 0,5 \ln \gamma_1(x_1=0,5) + 0,5 \ln \gamma_2(x_2=0,5) \right]$$

eqn. 2.21

Upon differentiating equation 2.18 as indicated by equations 2.16 and 2.17:

$$\begin{aligned} \frac{\partial A}{\partial n_1} & \frac{(n_1 - n_2)}{(n_1 + n_2)} \\ &= A n_2 \frac{\partial}{\partial n_1} \left( \frac{n_1}{n_1 + n_2} \right) \\ &= A n_2 \left( \frac{1 \cdot (n_1 + n_2) - n_1}{(n_1 + n_2)^2} \right) \\ &= A n_2 \left( \frac{n_2}{(n_1 + n_2)^2} \right) \\ &= A \frac{n_2^2}{(n_1 + n_2)^2} \\ &= A x_2^2 \end{aligned}$$

So that  $RT \ln \gamma_1 = A x_2^2$  eqn. 2.22

and  $RT \ln \gamma_2 = A x_1^2$  eqn. 2.23

Equation 2.22 and 2.23 allow for the calculation of activity coefficients  $\gamma_1$  and  $\gamma_2$  at any desired x even though experimental data is limited.

This simple example illustrates how the concept of excess functions, coupled with the Gibbs - Duhem equation can be used to interpolate or extrapolate experimental data with respect to composition.

The equations 2.22 and 2.23 represent the two-suffix Margules equations and provide a good representation for many simple liquid mixtures i.e. for mixtures molecules which are similar in size, shape and chemical nature. The two equations are symmetrical: when  $\gamma_1$  and  $\gamma_2$  are plotted against  $x_2$  (or  $x_1$ ) the two curves are mirror images. At infinite dilution the activity coefficients of both components are equal

$$\gamma_1^\infty = \lim_{x_1 \rightarrow 0} \gamma_1 = \exp \frac{A}{RT}$$

$$\gamma_2^\infty = \lim_{x_2 \rightarrow 0} \gamma_2 = \exp \frac{A}{RT}$$

#### 2.2.4 Other Excess Gibbs Energy Relations

Many expressions relating  $g^E$  (per mole of mixture) to composition have been proposed. All contain adjustable constants which, at least in principle, depend on temperature. That dependence may in some cases be neglected, especially if the temperature change is not large. In practice the number of adjustable constants per binary is typically two or three; the larger the number of constants, the better the representation of the data but at the same time, the larger the number of reliable experimental data points required to determine the constants. Extensive and highly accurate experimental data is required to justify more than three empirical constants for a binary system. Table 2.1 represents six mathematical models of  $g^E$  and the corresponding activity coefficient equation. These are applicable to non-electrolyte solutions.

TABLE 2.1 SOME MODELS FOR THE EXCESS GIBBS ENERGY AND SUBSEQUENT ACTIVITY COEFFICIENTS FOR BINARY SYSTEMS

Name	$g^E$	Binary Parameters	$\ln \gamma_1$ and $\ln \gamma_2$
Two-suffix Margules	$g^E = Ax_1x_2$	A	$RT \ln \gamma_1 = Ax_2^2$ $RT \ln \gamma_2 = -Ax_1^2$
Three-suffix Margules	$g^E = x_1x_2 [A + B(x_1 - x_2)]$	A, B	$RT \ln \gamma_1 = (A + 3B)x_2^2 - 4Bx_2^3$ $RT \ln \gamma_2 = (A - 3B)x_1^2 + 4Bx_1^3$
van Laar	$g^E = \frac{Ax_1x_2}{x_1(A/B) + x_2}$	A, B	$RT \ln \gamma_1 = A \left[ 1 + \frac{A}{B} \frac{x_1}{x_2} \right]^{-2}$ $RT \ln \gamma_2 = B \left[ 1 + \frac{A}{B} \frac{x_2}{x_1} \right]^{-2}$
Wilson	$\frac{g^E}{RT} = -x_1 \ln(x_1 + \Lambda_{12}x_2) - x_2 \ln(x_2 + \Lambda_{21}x_1)$	$\Lambda_{12}, \Lambda_{21}$	$\ln \gamma_1 = -\ln(x_1 + \Lambda_{12}x_2) + x_2 \frac{\Lambda_{12}}{x_1 + \Lambda_{12}x_2} - \frac{\Lambda_{21}}{\Lambda_{21}x_1 + x_2}$ $\ln \gamma_2 = -\ln(x_2 + \Lambda_{21}x_1) - x_1 \frac{\Lambda_{12}}{x_1 + \Lambda_{12}x_2} - \frac{\Lambda_{21}}{\Lambda_{21}x_1 + x_2}$
NRTL	$\frac{g^E}{RT} = x_1x_2 \frac{\tau_{21}G_{21}}{x_1 + x_2G_{21}} + \frac{\tau_{12}G_{12}}{x_2 + x_1G_{12}}$ where $\tau_{12} = \frac{\Delta g_{12}}{RT}$ $\tau_{21} = \frac{\Delta g_{21}}{RT}$ $\ln G_{12} = -\alpha_{12} \tau_{12}$ $\ln G_{21} = -\alpha_{21} \tau_{21}$	$\Delta g_{12}, \Delta g_{21}, \alpha_{12}$	$\ln \gamma_1 = x_2^2 \left[ \tau_{21} \left( \frac{G_{21}}{x_1 + x_2G_{21}} \right)^2 + \frac{\tau_{12}G_{12}}{(x_2 + x_1G_{12})} \right]$ $\ln \gamma_2 = x_1^2 \left[ \tau_{12} \left( \frac{G_{12}}{x_2 + x_1G_{12}} \right)^2 + \frac{\tau_{21}G_{21}}{(x_1 + x_2G_{21})} \right]$

UNIQUAC

AS DISCUSSED IN TEXT

For moderately non ideal binary mixtures, all equations for  $g^E$  containing two (or more) binary parameters give good results. For strongly non ideal binary mixtures e.g. solutions of alcohols with hydrocarbons the Wilson, NRTL (Non Random Two Liquid) and UNIQUAC equations are useful <sup>(34)</sup>.

The Wilson's equation appears to provide a good representation of excess Gibbs energies for a variety of miscible mixtures, particularly for highly asymmetric systems such as solutions of polar or associating components such as alcohols in non polar solvents. However it is not applicable to a mixture which exhibits a miscibility gap <sup>(34)</sup>. It is inherently unable, even quantitatively, to account for phase splitting although it may be used for mixtures where miscibility is incomplete provided attention is confined to the one phase region. For this reason it was not considered in this study.

The NRTL and UNIQUAC equations are applicable to both vapour-liquid and liquid-liquid equilibria permitting the use of solubility data for the determination of binary parameters.

This investigation deals only with the UNIQUAC equation.

### 2.3 THE UNIQUAC EQUATION

The UNIQUAC theory is based on an entropic solution model. This treatment emphasises differences in structure or arrangements in solution, ordering or disordering, the mixing of large and small molecules, or local ordering. (The NRTL and Wilson equations are similarly based).

In the UNIQUAC theory, the quasi-chemical lattice model of Guggenheim, previously applicable to small molecules of essentially the same size is extended to mixtures containing molecules of different size and shape by utilising the local composition concept <sup>(35)</sup>.

### 2.3.1 Partition Function for a Binary Liquid Mixture

The liquid state is represented by a three dimensional lattice of equi-spaced sites, the volume in the immediate vicinity of a site is called a cell. Each molecule in the liquid is divided into attached segments such that each segment occupies one cell. The total number of cells is equal to the total number of segments.

The configurational partition function  $Z$  is given by:

$$Z = Z_{\text{lattice}} Z_{\text{cell}} \quad \text{eqn. 2.24}$$

Where  $Z_{\text{lattice}}$  refers to where the centre of every segment is coincident with a lattice site and where  $Z_{\text{cell}}$  provides those contributions to  $Z$  which are caused by motions of a segment about this central position.

For non electrolytes removed from critical conditions, it is assumed that  $Z_{\text{cell}}$  is independent of composition. For a binary mixture containing  $N_1$  molecules of component 1 and  $N_2$  molecules of component 2, the Helmholtz energy of mixing  $\Delta A$  is given by:

$$\Delta A = -kT \ln \frac{Z_{\text{lattice}}(N_1, N_2)}{Z_{\text{lattice}}(N_1, 0) Z_{\text{lattice}}(0, N_2)} \quad \text{eqn. 2.25}$$

The molar excess Gibbs energy,  $g^E$ , is given by:

$$g^E \approx a^E = \frac{A}{n_1 + n_2} - RT \ln (x_1 \ln x_1 + x_2 \ln x_2) \quad \text{eqn. 2.26}$$

where  $a^E$  is the excess Helmholtz energy per mole of mixture

The lattice partition function is given by:

$$Z_{\text{lattice}} = \sum_{\theta} W(\theta) \exp -u_0/kT \quad \text{eqn. 2.27}$$

where  $W$  is the combinatorial factor and  $u_0$  is the potential energy of the lattice.

Both  $W$  and  $u_0$  depend on the molecular configuration, designated by the variable  $\theta$ . The summation in equation 1.27 is over all values of  $\theta$  which are permitted within the constraints of the overall stoichiometry.

For mixtures of polysegmented molecules differing in size and shape, the local area fraction is used to describe the micro-composition of the lattice.

### 2.3.2 The Local Area Fraction

A molecule of component 1 is represented by a set of bonded segments, the number of segments per molecule is  $r_1$ . While all segments have the same size, they differ in their external contact area.

For a molecule of component 1 the number of external nearest neighbours is given by  $z q_1$ , where  $z$  is the co-ordination number of the lattice, and  $q_1$  is a parameter proportional to the molecule's external surface area.

The local area fraction  $\theta_{21}$  is the fraction of external sites around molecule 1 which are occupied by segments of molecule 2. Similarly, local area fraction  $\theta_{11}$  is the fraction of external sites around molecule 1 which are occupied by segments of another molecule 1. Similar definitions for  $\theta_{12}$  and  $\theta_{22}$  can be obtained.

For a binary mixture, four local area fractions describe the microstructure of the lattice; however only two of these are independent because:

$$\theta_{11} + \theta_{21} = 1 \quad \text{eqn. 2.28}$$

and

$$\theta_{12} + \theta_{22} = 1 \quad \text{eqn. 2.29}$$

The lattice energy  $u_0$  is the sum of all the interaction energies between pairs of nonbonded segments.

$$- u_0 = (z/2)q_1N_1(\theta_{11}u_{11} + \theta_{21}u_{21}) + (z/2)q_2N_2(\theta_{22}u_{22} + \theta_{12}u_{12}) \quad \text{eqn. 2.30}$$

where  $u_{ij}$  characterises the energy of interaction between sites  $i$  and  $j$ .

For convenience  $u_{ij} = (z/2) u_{ij}$  so that equation 2.30 becomes:

$$- u_0 = q_1 N_1 (\theta_{11}u_{11} + \theta_{21}u_{21}) + q_2 N_2 (\theta_{22}u_{22} + \theta_{12}u_{12}) \quad \text{eqn. 2.31}$$

The energy parameters  $u_{ij}$  represent averages since, in a given molecule, all segments are not necessarily chemically identical.

### 2.3.3 Combinatorial Factor

For a given set of local area fractions the number of possible configurations for a mixture of  $N_1$  molecules of component 1 and  $N_2$  molecules of component 2 must be calculated. The assumption made is that

$$W = W_1 W_2 h (N_1, N_2) \quad \text{eqn. 2.32}$$

when  $W_i$  refers to the number of configurations associated with a site occupied by a segment of molecule  $i$ . The function  $h$  depends only on  $N_1$  and  $N_2$  and is introduced as a normalisation factor to ensure that the combinatorial factor  $W$  satisfies a physically reasonable boundary condition. The boundary condition chosen is the combination factor of Staverman for mixtures of molecules with arbitrary size and shape but no attractive forces.

The summation in equation 2.27 can be replaced by its maximum term. The number of distinguishable configurations  $W_1$  and  $W_2$  are approximated by

$$W_1 = \frac{(q_1 N_1 \theta_{11} + q_2 N_2 \theta_{12})!}{(q_1 N_1 \theta_{11})! (q_2 N_2 \theta_{12})!} \quad \text{eqn. 2.33}$$

$$W_2 = \frac{(q_2 N_2 \theta_{22} + q_1 N_1 \theta_{21})!}{(q_2 N_2 \theta_{22})! (q_1 N_1 \theta_{21})!} \quad \text{eqn. 2.34}$$



To find  $h_1$  the athermal case is considered (all  $u_{ij} = 0$  and therefore  $u_0 = 0$ ) and the maximum term in the summation is found by separate differentiations with respect to  $\theta_{11}$  and  $\theta_{22}$  and by setting the result equal to zero.

The average local area fractions for an athermal (superscript (0)) mixture are then given by:

$$\theta_{11}^{(0)} = \frac{q_1 N_1}{q_1 N_1 + q_2 N_2} \quad \text{eqn. 2.35}$$

$$\theta_{22}^{(0)} = \frac{q_2 N_2}{q_2 N_1 + q_2 N_2} \quad \text{eqn. 2.36}$$

Mass balance constraints give

$$\theta_{12}^{(0)} = \theta_{11}^{(0)} = \theta_1 = \frac{q_1 N_1}{q_1 N_1 + q_2 N_2} \quad \text{eqn. 2.37}$$

$$\theta_{21}^{(0)} = \theta_{22}^{(0)} = \theta_2 = \frac{q_2 N_2}{q_2 N_2 + q_1 N_1} \quad \text{eqn. 2.38}$$

This illustrates that in the zeroth approximation the average local area fractions are the same as the average area fractions denoted by  $\theta_1$  and  $\theta_2$ .

The normalisation factor  $h$  can now be found by substituting equations 2.33 to 2.36 into equation 2.32 giving

$$h(N_1, N_2) = \frac{w^{(0)}(q_1 N_1 \theta_{11}^{(0)})!(q_1 N_1 \theta_{21}^{(0)})!(q_2 N_2 \theta_{22}^{(0)})!(q_2 N_2 \theta_{12}^{(0)})!}{(q_1 N_1 \theta_{11}^{(0)} + q_2 N_2 \theta_{12}^{(0)})!(q_2 N_2 \theta_{22}^{(0)} + q_1 N_1 \theta_{21}^{(0)})!} \quad \text{eqn. 2.39}$$

where  $w^{(0)}$  is the combinatorial factor given by Staverman.

#### 2.3.4 Average Local Area Fractions in Nonathermal Mixtures

The summation in equation 2.27 is replaced by its maximum term.

Equations 2.30, 2.31 and 2.32 are used but in this case the approximation is not set to zero. The resulting expression for  $Z_{\text{lattice}}$  is separately differentiated with respect to  $\theta_{11}$  and  $\theta_{22}$  and the results are set to zero. Using the constraining equations 2.37 and 2.38 the local average areas are given by

$$\theta_{11}^{(1)} = \frac{\theta_1}{\theta_1 + \theta_2 \exp \left\{ -(u_{21} - u_{11})/RT \right\}} \quad \text{eqn. 2.40}$$

$$\theta_{22}^{(1)} = \frac{\theta_2}{\theta_2 + \theta_1 \exp \left\{ -(u_{12} - u_{22})/RT \right\}} \quad \text{eqn. 2.41}$$

The superscript (1) denotes the first approximation. Substituting equations 2.25, 2.27, 2.31 to 2.34 and 2.38 into equation 2.26 the following is obtained

$$g^E = g^E (\text{combinatorial}) + g^E (\text{residual}) \quad \text{eqn. 2.42}$$

where  $g^E (\text{combinatorial})$  is the contribution due to the differences in sizes and shapes of the molecules, and  $g^E (\text{residual})$  is due to the energetic interactions.

For a binary mixture

$$g^E (\text{combinatorial}) = x_1 \ln \frac{\Phi_1}{x_1} + x_2 \ln \frac{\Phi_2}{x_2} + \frac{(z/2)(q_1 x_1 \ln \frac{\theta_1}{\Phi_1} + q_2 x_2 \ln \frac{\theta_2}{\Phi_2})}{\quad} \quad \text{eqn. 2.43}$$

and

$$g^E (\text{residual}) = -q_1 x_1 \ln \theta_1 + \theta_2 \tau_{21} - q_2 x_2 \ln \theta_2 + \theta_1 \tau_{12} \quad \text{eqn. 2.44}$$

where the co-ordination number  $Z$  is set equal to 10 and segment fractions  $\Phi$  and area fractions  $\theta$  are given by

$$\Phi_i = \frac{r_i x_i}{\sum_j r_j x_j} \quad \text{eqn. 2.45}$$

$$\theta_i = \frac{q_i x_i}{\sum_j q_j x_j} \quad \text{eqn. 2.46}$$

The parameters  $r$  and  $q$  are pure component molecular structure constants dependent on molecular size and external surface areas.

For each binary combination in a multicomponent system there are two adjustable parameters  $\tau_{ij}$  and  $\tau_{ji}$ . These, in turn, are given in terms of characteristic energies  $u_{ij}$  and  $u_{ji}$  by

$$\tau_{ij} = \exp(-\Delta u_{ij} / RT) = \exp(-a_{ij} / T) \quad \text{eqn. 2.47}$$

where  $\Delta u_{ij} = u_{ij} + u_{jj}$

For any component  $i$  the activity coefficient is obtained by differentiation and becomes

$$\ln \gamma_i = \ln \frac{\phi_i}{x_i} + (z/2)q_i \ln \frac{\theta_i}{\phi_i} + \phi_j \left( l_i - \frac{r_i}{r_j} l_j \right) - q_i \ln (\theta_i + \theta_j \tau_{ji}) + \theta_j q_i \left( \frac{\tau_{ji}}{\theta_i + \theta_j \tau_{ji}} - \frac{\tau_{ij}}{\theta_j + \theta_j \tau_{ij}} \right)$$

eqn. 2.48

where  $l_j = z (r_j - q_j) - (r_j - 1)$

eqn. 2.49

The above form of the UNIQUAC equation is that according to the original formulation. The later version included a value  $q'$  which permitted better agreement for water and alcohol containing systems<sup>(36)</sup>. For alcohols, the surface of interaction  $q'$  is smaller than the geometric external surface  $q$ , indicating that the intermolecular interaction is determined primarily by the hydroxyl group. For water  $q' = 1.00$ . The term  $\theta_i$  becomes  $\theta_i'$  in these systems where

$$\theta_i' = \frac{q_i' x_i}{\sum_j q_j x_j} \quad \text{eqn. 2.50}$$

## 2.4 APPLICATION OF THE UNIQUAC EQUATION TO DETERMINE LIQUID-LIQUID PHASE EQUILIBRIA IN TERNARY MIXTURES

The UNIQUAC equation can be used to predict whether one or two phases exist at equilibrium for a known composition. Provided that the binary parameters are known, the activity coefficients can be calculated from equation 2.48 for each component at any composition. The molar Gibbs energy of mixing can then be calculated at any composition from

$$G_{mix}^E = RT \sum_i x_i \ln \gamma_i x_i \quad \text{eqn. 2.51}$$

For a ternary system the mole fraction of component 1 ( $x_1$ ) is held constant and  $G_{mix}^E$  is calculated from knowledge of activity coefficients and is then plotted as a function of the mole fraction of component 2 ( $x_2$ ).

The condition for equilibrium is that the total free energy can be minimised, if the free energy of the system can be reduced by separation into two phases, then phase separation will take place.

This is seen in the following diagram - figure 2.3.

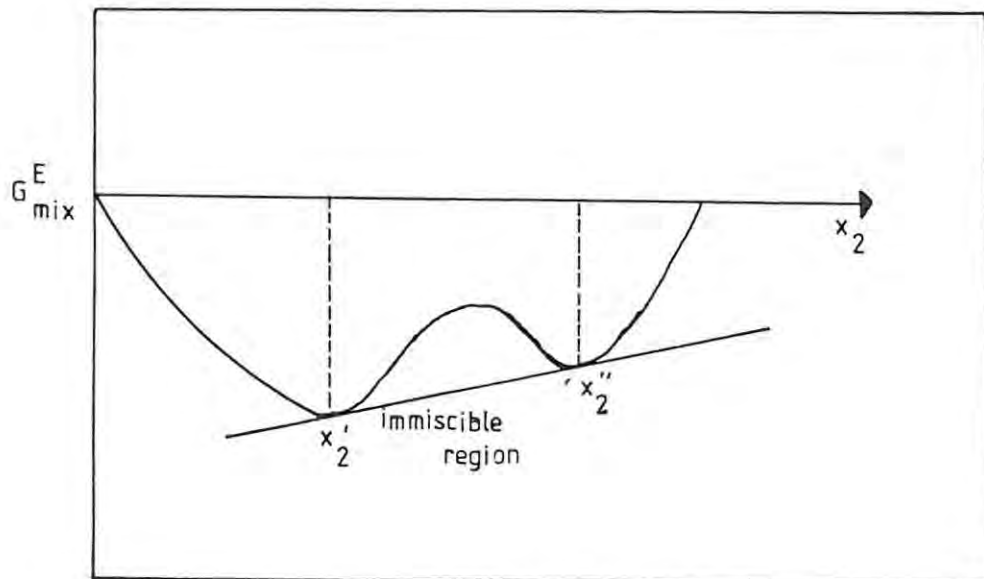


FIGURE 2.3 GIBBS ENERGY FUNCTION FOR A PARTIALLY MISCIBLE LIQUID MIXTURE

The mathematical condition for phase separation is that a straight line can be placed in such a way that it is simultaneously tangent to the free energy curve at two points  $x_2^I$  and  $x_2^{II}$ . This is shown schematically in figure 2.3.

Any intermediate point on this straight line represents a lower free energy than a point on the unstable one phase curve, and a mixture having such a composition will separate into two phases having compositions  $x_2^I$  and  $x_2^{II}$ .

From each curve of  $G_{mix}^E$  plotted as a function of  $x_2$ , for constant  $x_1$ , the two points with a common tangent define two points on the ternary phase diagram. By varying  $x_1$  the whole phase diagram can be determined.

#### 2.4.1 Objectives

As much of this work was concentrated on water solubility studies in petrol-alcohol blends it was decided to devote attention to the prediction of ternary phase behaviour in a system which approximated the petrol-1-propanol-water system. Petrol is a mixture of hydrocarbons and therefore was not suitable for theoretical work. A pure alkane was selected as a model compound. Ternary phase behaviour of n-hexane, n-heptane and n-octane with 1-propanol and water was compared with that of petrol. n-Heptane was found to be the better representative compound. 1-Propanol was selected for investigation as an important system in this field and also since ternary phase predictions are more accurate the broader the two phase region. Solubility studies (see section 4) revealed that 1-propanol allowed for the greatest solubilisation of water. The n-heptane + 1-propanol + water system represents a type 1 ternary system. Two binaries i.e. 1-propanol and n-heptane and 1-propanol and water are completely miscible whereas water and n-heptane are only partially miscible<sup>(37)</sup>.

Unfortunately binary parameters for heptane and 1-propanol and for heptane and water were not available. It was necessary to determine

these so that relevant binary data was obtained and fitted using computer programs. The binary data (activity coefficients at various compositions) was fitted to the UNIQUAC equation and the resulting binary parameters (in the form  $a_{ij}$ ) compared with known values determined by Prausnitz and Abrams for related binary systems.

The evaluation of structural parameters  $r$ ,  $q$  and  $q'$  and the determination of binary parameters will be presented before the methods used to calculate binary parameters for the system investigated are discussed.

#### 2.4.2 Evaluation of Pure - Component Structural Parameters $r$ , $q$ and $q'$

The structural parameters  $r$  and  $q$  are respectively, the van der Waals volume and area of the molecule relative to those of a standard segment.

$$r_i = \frac{V_{wi}}{V_{ws}} \quad \text{eqn. 2.52}$$

$$q_i = \frac{A_{wi}}{A_{ws}} \quad \text{eqn. 2.53}$$

where  $V_{wi}$  and  $A_{wi}$  are the van der Waals volumes and areas of the molecule, and where  $V_{ws}$  and  $A_{ws}$  are the van der Waals volume and area of a standard segment.

#### 2.4.3 Determination of Binary Parameters

Parameters  $a_{ij}$  and  $a_{ji}$  are found from binary experimental data. Sources of data include:

- a) vapour-liquid equilibrium at constant temperature
- b) vapour-liquid equilibria at constant pressure
- c) total pressure data at constant temperature
- d) boiling point (or dew point) data at constant pressure
- e) mutual (liquid-liquid) solubilities
- f) azeotropic data
- g) activity coefficients at infinite dilution



#### 2.4.4 Pilot Investigations

##### 2.4.4.1 Fitting of Activity Coefficient Data

Activity coefficient data was used to obtain interaction parameters for the completely miscible binary systems. The ZXSSQ subroutine from the IMSL library was used. This derivative-free version of the Levenberg-Marquardt <sup>(38)</sup> algorithm reduced the available data and allowed for the fitting of the interaction parameters according to the UNIQUAC equation.

The accuracy of this approach was tested by obtaining the source data as Prausnitz and Abrams for a miscible system. The system acetone and benzene studied by Brown and Smith was used and fitted to five equations in table 2.1. The activity coefficients of each component over the whole composition range were then calculated using the appropriate interaction parameters and are represented on figure 2.4.

The UNIQUAC equation for activity coefficients appears to yield the closest approximation of the original data. The interaction parameters calculated are very similar to those determined by Prausnitz and are given in table 2.2.

---

Table 2.2. INTERACTION PARAMETERS FROM THE FITTING OF UNIQUAC COMPARED TO THOSE GIVEN BY PRAUSNITZ

---

System: Acetone (1) + Benzene (2) at 318 K		
	Fitted	Prausnitz
$a_{12}$	174,00	181,94
$a_{21}$	-108,70	-114,19

---

##### 2.4.4.2. Fitting of Mutual Solubility Data

Solubility data is readily available and reliable. Table 2.3 is a typical example and the discrepancy between results is negligible. When two liquid phases are in equilibrium, the composition of the two phases are related by a set of equations, one for each component  $i$ .  $(x_i \gamma_i)^\alpha = (x_i \gamma_i)^\beta$  where  $x$  is the liquid phase mole



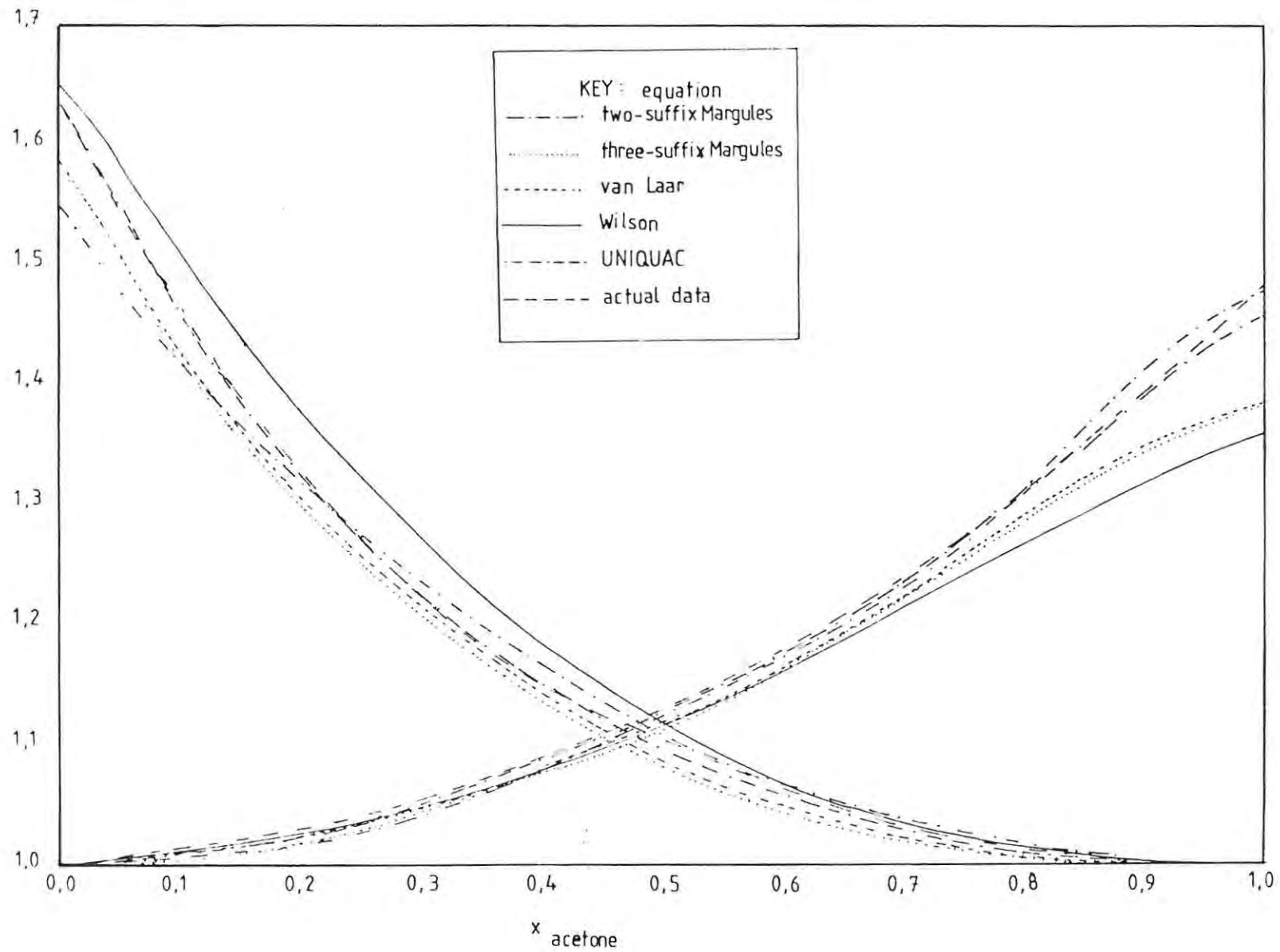


FIGURE 2.4 RESULTS OF FITTING BENZENE-ACETONE DATA TO VARIOUS EQUATIONS

Table 2.3 MUTUAL SOLUBILITIES OF HYDROCARBONS AND WATER AT 0 AND 25°C

Compound	<u>Solubility of hydrocarbon in water (p.p.m.)*</u>			<u>Solubility of water in hydrocarbon (p.p.m.)*</u>		
	<u>Experimental</u>		Literature 25°C	<u>Experimental</u>		Literature 25°C
	0°C	25°C		0°C	25°C	
n-Pentane	65,7	47,6	38,5, 40.4	26	101	120
n-Hexane	16,5	12,4	12,3, 9,5, 18,3	28	90	140
n-Heptane	4,39	3,37	2,93, 2,66	26	82	134, 91, 151
n-Octane	1,35	0,85	0,66, 0,88	23	79	132
Benzene	1678	1755	1770, 1780, 1795	302	691	666, 522, 694
Toluene	724	573	515, 629	228	543	538
Ethylbenzene	197	177	152, 209	178	442	438

\* Grams in 10<sup>6</sup> grams of solution (p.p.m. by mass)

fraction,  $\gamma$  is the liquid phase activity coefficient and  $\alpha$  and  $\beta$  indicate equilibrium phases. The data in table 2.3 is given in parts per million which is converted to mole fraction.

An assumption is made setting the activity coefficient at unity when  $x$  is nought i.e. at infinite dilution. The activity coefficients are then calculated using the UNIQUAC equation and the interaction parameters determined by reiterative technique. The subroutine ZSCNT (also from the IMSL library) was used for this purpose.

The accuracy was tested using two different systems: 1-butanol + water and toluene + water, the former representing a more miscible system. The results are shown in table 2.4.

Table 2.4 INTERACTION PARAMETERS FROM THE FITTING OF UNIQUAC COMPARED WITH THOSE OF PRAUSNITZ

System: 1-Butanol (1) + Water (2) at 323 K		
	Fitted	Prausnitz
$a_{12}$	1278,88	1254,65
$a_{21}$	-81,74	-127,48
System: Toluene (1) + Water (2) at 323 K		
	Fitted	Prausnitz
$a_{12}$	1522,69	1371,36
$a_{21}$	365,50	305,71

The interaction parameters were of the same order as those determined by Prausnitz although a different data source and fitting technique were used.

#### 2.4.5. Prediction of the Ternary Phase Diagram for the System Ethanol + Benzene + Water at 298,15 K

The experimental data for the two miscible binary systems was obtained from the following papers

1. benzene (1) + ethanol (2) Smith and Robinson J. Chem. Eng. Data 15 No. 3 391-395
2. ethanol (1) + water (2) Hansen and Miller J. Phys. Chem. 58 No. 3 193-196

The fitting procedure yielded the following interaction parameters:

Table 2.5 INTERACTION PARAMETERS FROM THE FITTING OF UNIQUAC  
COMPARED WITH THOSE OF PRAUSNITZ

System: Benzene (1) and Ethanol (2) at 298 K		
	Fitted	Prausnitz
$a_{12}$	1008,71	1131,13
$a_{21}$	-115,89	-149,34

System: Ethanol (1) + Water (2) at 298 K		
	Fitted	Prausnitz
$a_{12}$	-36,36	-163,72
$a_{21}$	293,84	573,61

The solubility data for the immiscible benzene-water binary yielded the following interaction parameters given in table 2.6.

Table 2.6 INTERACTION PARAMETERS FROM THE FITTING OF UNIQUAC  
VALUES COMPARED WITH PRAUSNITZ

System: Benzene (1) + Water (2) at 298 K		
	Fitted	Prausnitz
$a_{12}$	1328,24	2057,42
$a_{21}$	355,125	115,13

These interaction parameters together with the structural parameters were substituted into the UNIQUAC expression for  $G^{E_{mix}}$ . The mole fraction benzene  $x_1$  was held constant at 0,05 mole fraction units so that if phase separation occurred two  $x_2$  values were determined from the graph of  $G^{E_{mix}}$  against  $x_2$  (refer to Appendix 2 for the computer program). Figure 2.8 represents the results of this computation. The results were tabulated and can be compared with results obtained using Prausnitz interaction parameters in tables 2.7 and 2.8. These are represented on ternary phase diagrams in figure 2.9 and compared with the binodal curves determined by Hubard and Bancroft<sup>(39)</sup> and experimentally (refer to Section 4). The activity coefficients were calculated for each binary system and are represented by figures 2.5 - 2.7. Tables 2.9 and 2.10 compare the binodal curve found in the literature and that determined experimentally.

Table 2.7 PHASE SEPARATION USING DERIVED INTERACTION PARAMETERS

$x_1$	$x_2$	
0,10	0,0	0,90
0,15	0,0	0,830
0,20	0,005	0,750
0,25	0,015	0,700
0,30	0,028	0,620
0,35	0,042	0,550
0,40	0,077	0,465
0,41	0,085	0,440
0,43	0,10	0,380

Table 2.8 PHASE SEPARATION USING PRAUSNITZ INTERACTION PARAMETERS

$x_1$	$x_2$	
0,10	0,0	0,700
0,15	0,0	0,800
0,20	0,0	0,730
0,25	0,020	0,660
0,30	0,040	0,570
0,35	0,060	0,490
0,40	0,110	0,380
0,41	0,120	0,360
0,43	0,170	0,290

Table 2.9 BINODAL CURVE DETERMINED BY BANCROFT AND HUBARD

$x_1$	$x_2$	$x_3$
0,0032	0,1703	0,8265
0,0109	0,2416	0,7555
0,0148	0,2621	0,7231
0,0200	0,2828	0,6972
0,0246	0,2968	0,6786
0,0340	0,3185	0,6475
0,0457	0,3423	0,6119
0,0605	0,3612	0,5783
0,0998	0,3956	0,5046
0,1349	0,4106	0,4545
0,2550	0,4142	0,3308
0,3507	0,3918	0,2575
0,5222	0,3225	0,1553
0,6970	0,2265	0,0765

Table 2.10 EXPERIMENTALLY DETERMINED BINODAL CURVE

$x_1$	$x_2$	$x_3$
0,0064	0,0734	0,9201
0,0147	0,1623	0,8221
0,0543	0,3294	0,6163
0,0259	0,2218	0,7522
0,0816	0,3831	0,5352
0,1009	0,4071	0,4919
0,1521	0,4258	0,4220
0,1718	0,4229	0,4053
0,2299	0,4166	0,3535
0,4928	0,3480	0,1604
0,6395	0,2699	0,0906

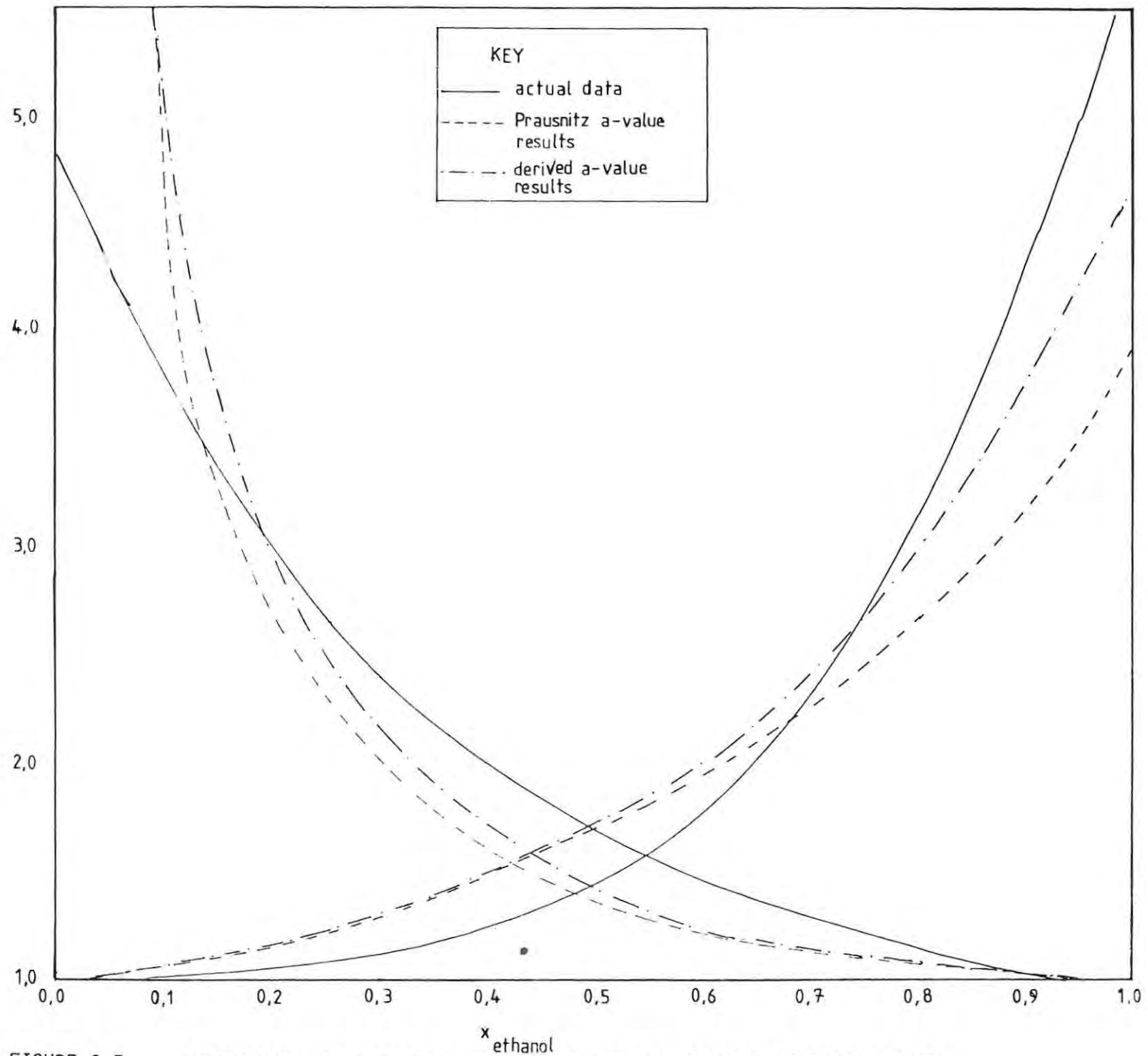


FIGURE 2.5 COMPARISON OF ACTIVITY COEFFICIENTS FOR THE ETHANOL-BENZENE SYSTEM



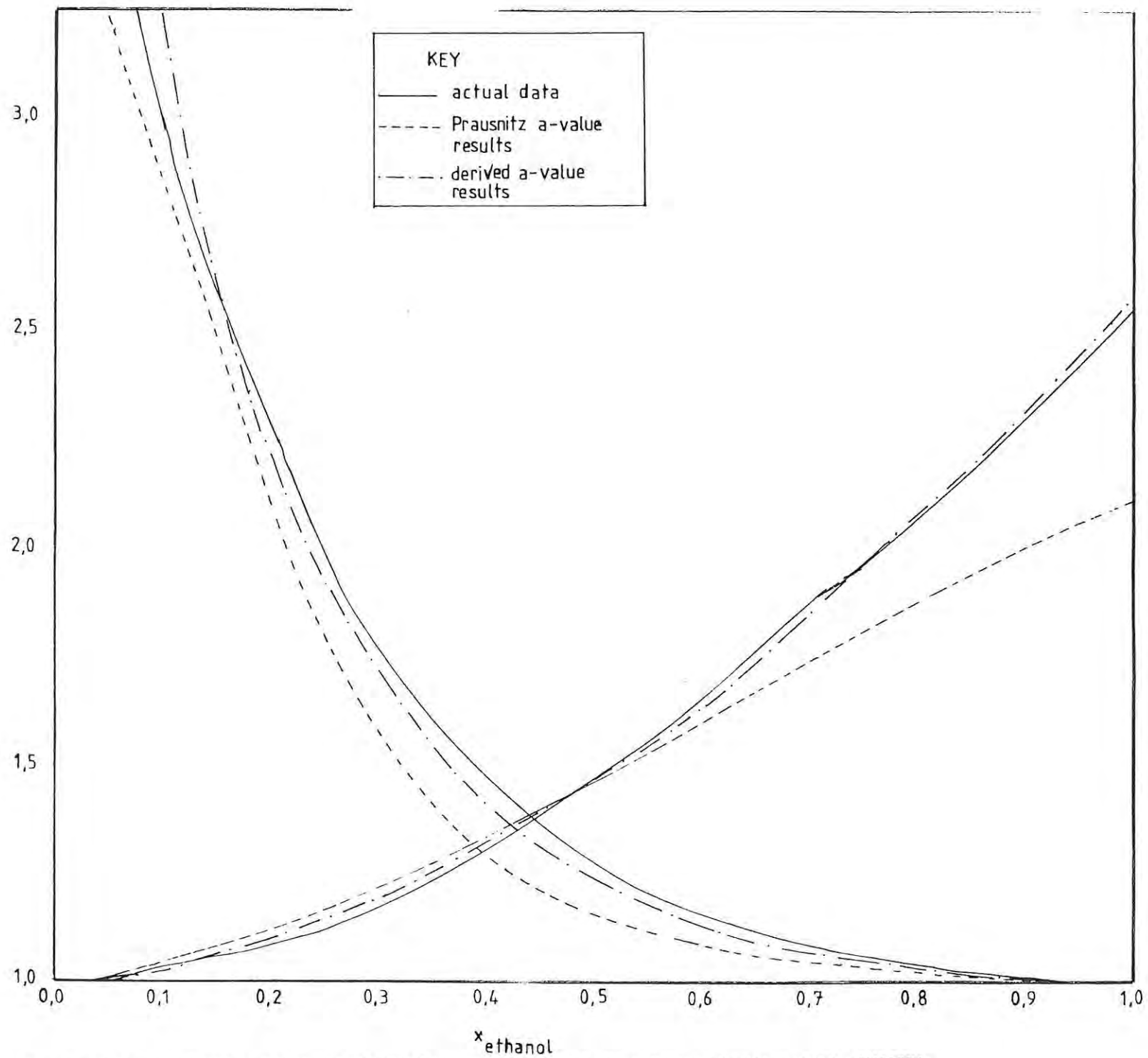


FIGURE 2.6 COMPARISON OF ACTIVITY COEFFICIENTS FOR THE ETHANOL-WATER SYSTEM

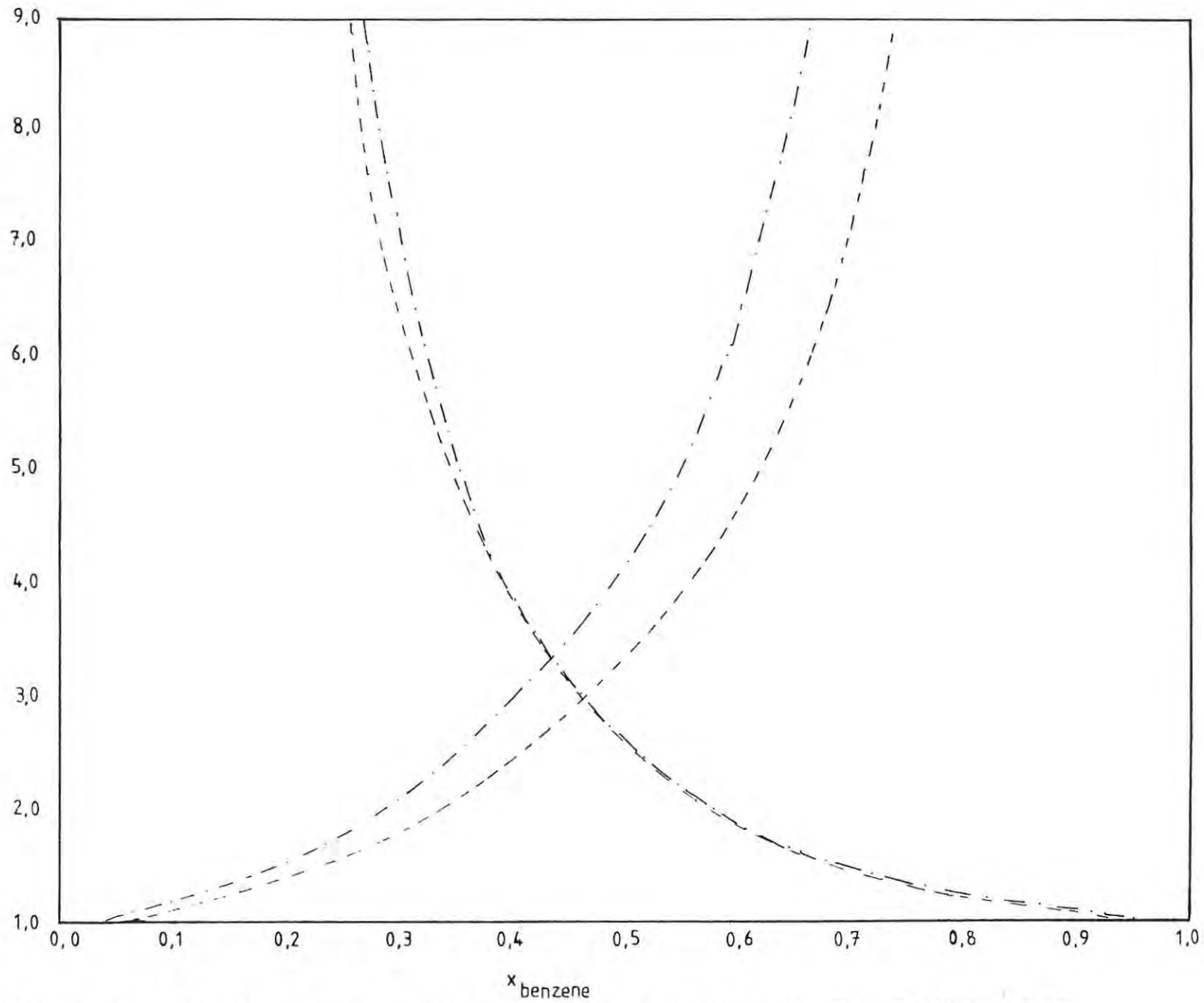


FIGURE 2.7 COMPARISON OF THE HYPOTHETICAL ACTIVITY COEFFICIENTS FOR THE BENZENE-WATER PARTIALLY MISCIBLE SYSTEM

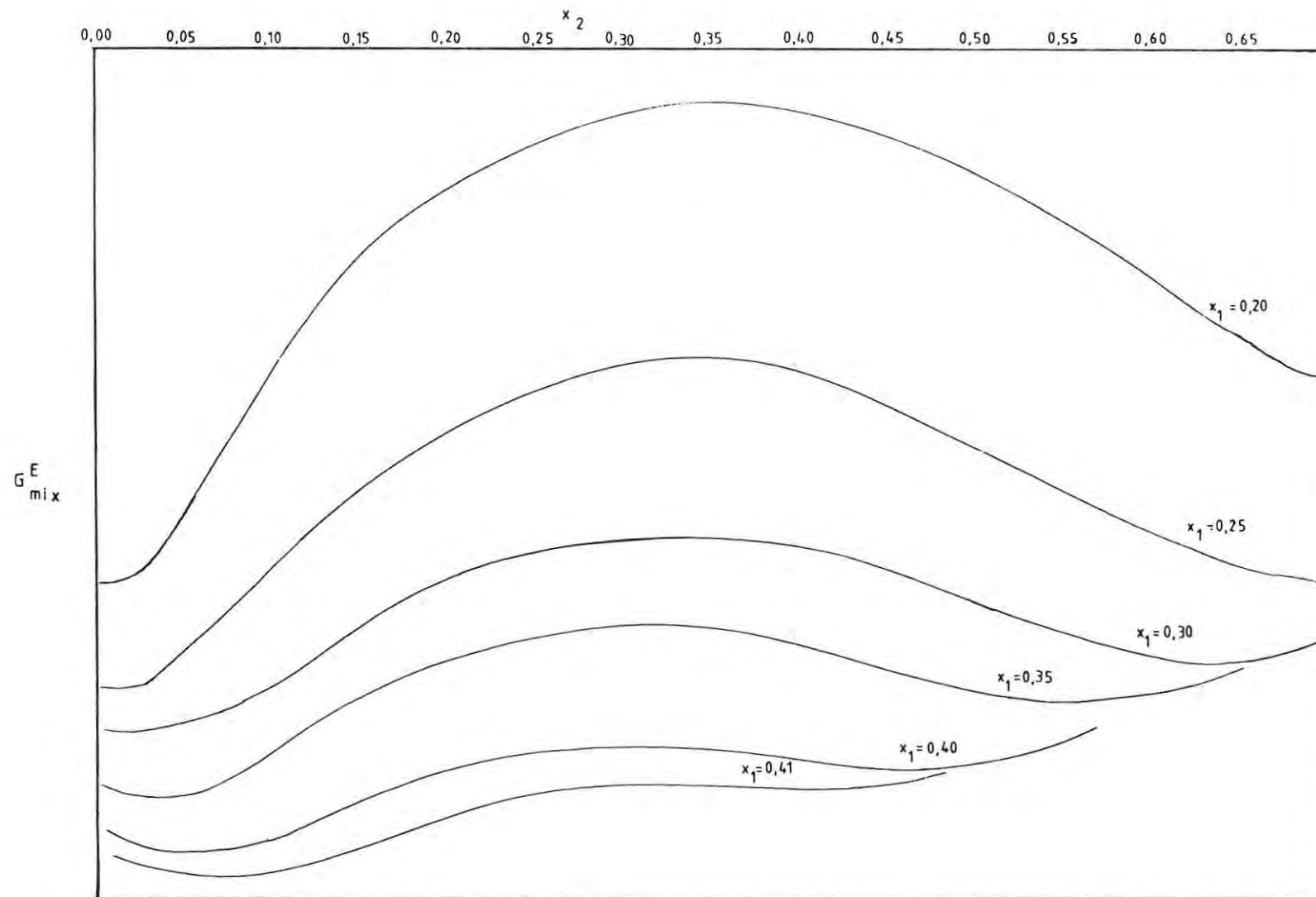


FIGURE 2.8 RESULTS OF  $G_{MIX}^E$  COMPUTATION FOR THE BENZENE-ETHANOL-WATER SYSTEM

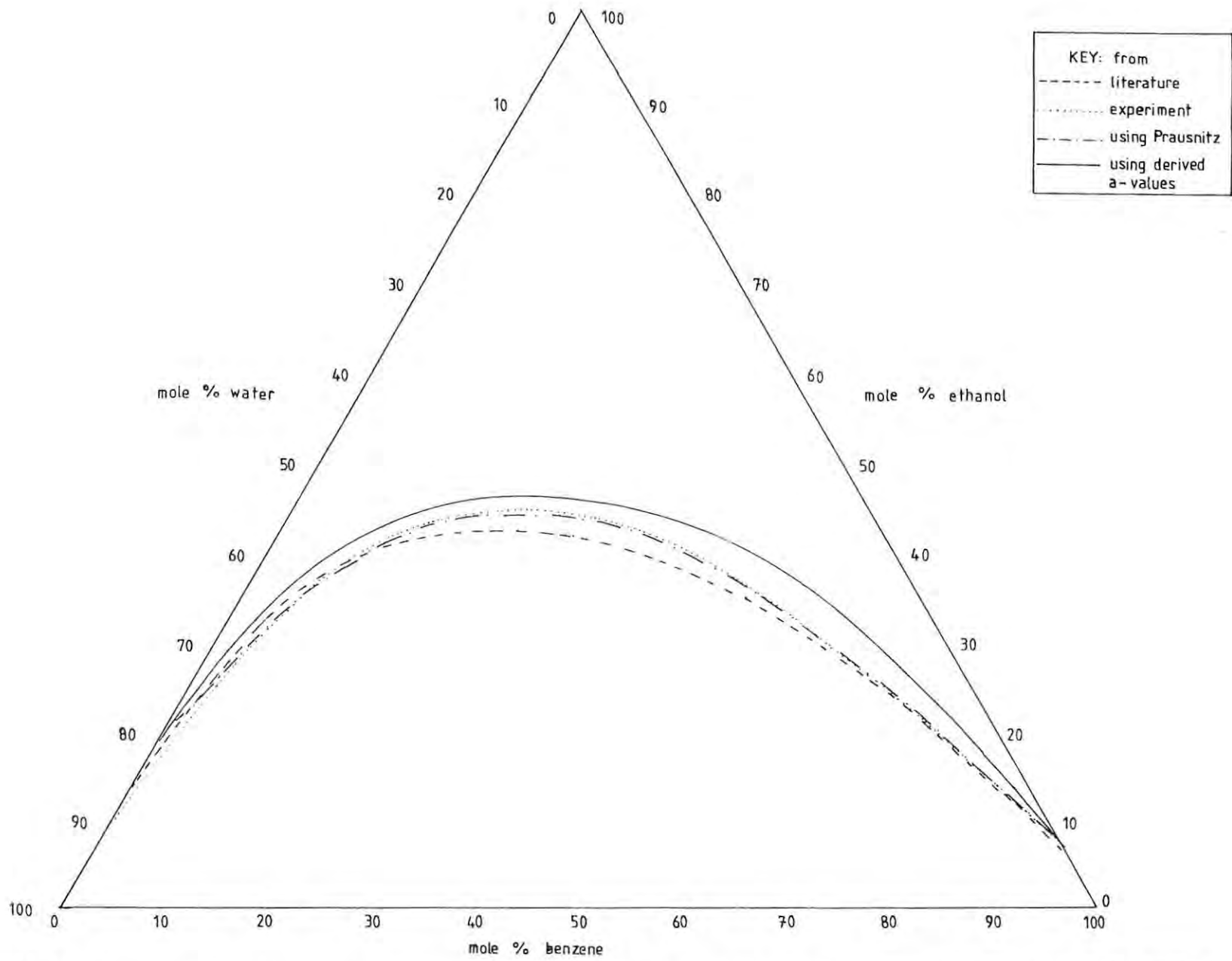


FIGURE 2.9 TERNARY PHASE DIAGRAM OF THE PREDICTED BEHAVIOUR FOR THE BENZENE-ETHANOL-WATER SYSTEM

### 2.4.6 Prediction of the Ternary Phase Diagram for the System

1-Propanol + Heptane + Water at 298,15 K

The interaction parameters for the two miscible binary systems were derived from the following experimental data:

1. n-heptane (1) + 1-propanol (2) Van Ness et al J. Chem. & Eng. Data 2 No. 12 217-225
2. 1-propanol (1) + water (2) Hansen and Miller J. Phys. Chem. 58 No. 3 193-196

These values were compared with Prausnitz values for the binary systems at 303 K.

Table 2.11 INTERACTION PARAMETERS

System: n-heptane (1) + 1-propanol (1)		
	Fitted	Prausnitz (303 K)
$a_{12}$	592,82	1340,00
$a_{21}$	-163,31	-151,85

System: 1-propanol (1) + water (2)		
	Fitted	Prausnitz (303 K)
$a_{12}$	58,26	100,17
$a_{21}$	564,23	539,63

Solubility data fitting yielded results shown in table 2.12.

Table 2.12 INTERACTION PARAMETERS

System: heptane (1) + water (2)	
$a_{12}$	2079,22
$a_{21}$	559,72

Figure 2.10 represents  $x_2$  plotted against the UNIQUAC expression for  $G_{mix}^E$ . The table 2.13 describes the results which are compared with experimentally defined ternary phase diagram on figure 2.10 and table 2.14.

Table 2.13 BINODAL CURVE DETERMINED USING CALCULATED  $a_{12}$   
AND  $a_{21}$

$x_1$	$x_2$	
0,20	0,0	0,800
0,25	0,0	0,740
0,30	0,010	0,660
0,35	0,022	0,595
0,40	0,035	0,540
0,45	0,065	0,405
0,47	0,110	0,270

Table 2.14 EXPERIMENTAL BINODAL CURVE

$x_1$	$x_2$	$x_3$
0,0340	0,3130	0,6524
0,0813	0,4234	0,4953
0,1092	0,4324	0,4584
0,1593	0,4473	0,3934
0,2332	0,4472	0,3196
0,4190	0,3940	0,1870
0,5716	0,3396	0,0888
0,6256	0,3197	0,0547
0,7352	0,2214	0,0436
0,8749	0,1235	0,0015

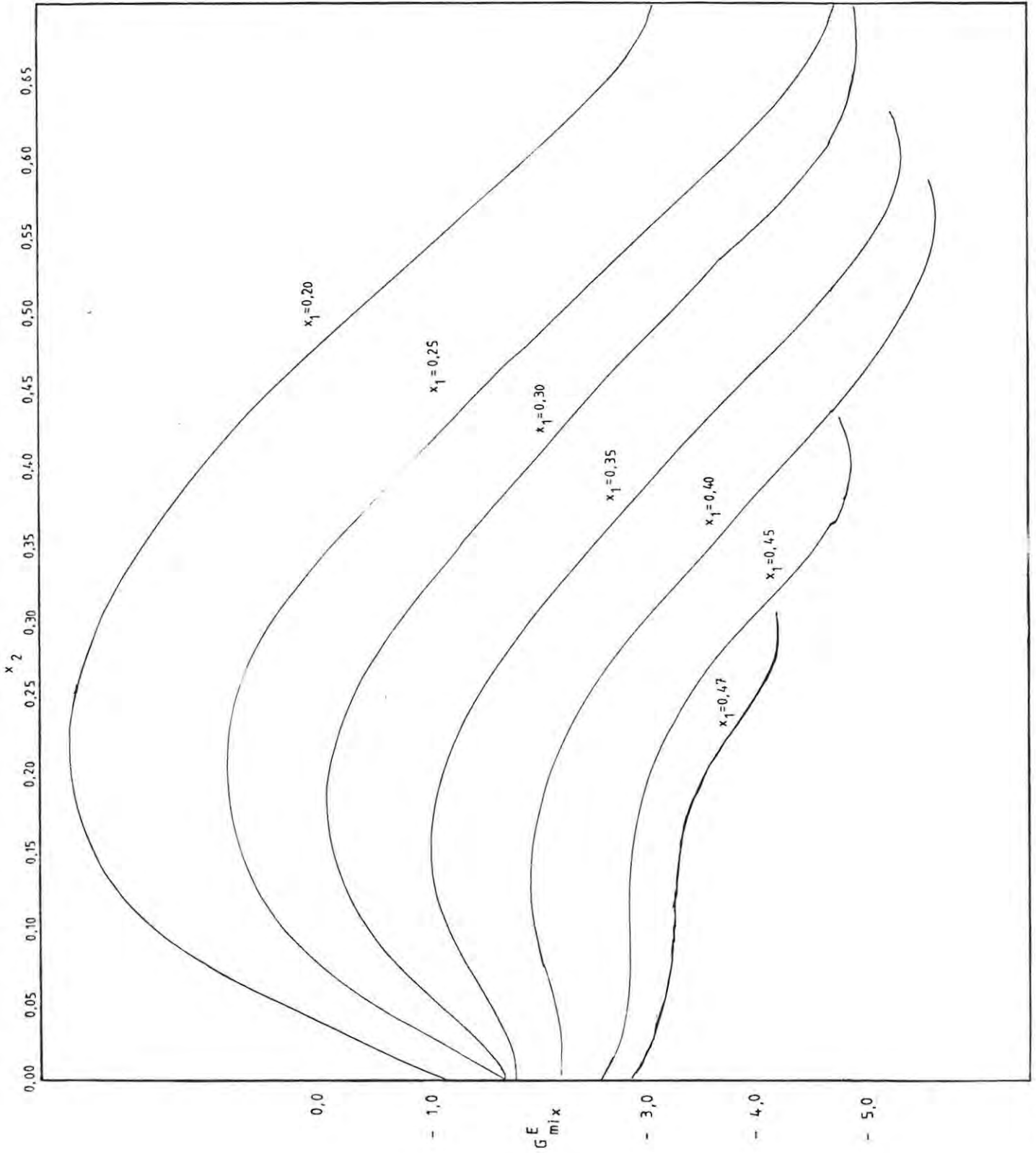


FIGURE 2.10 RESULTS OF THE  $G^E_{MIX}$  COMPUTATION FOR THE N-HEPTANE-1-PROPANOL-WATER SYSTEM



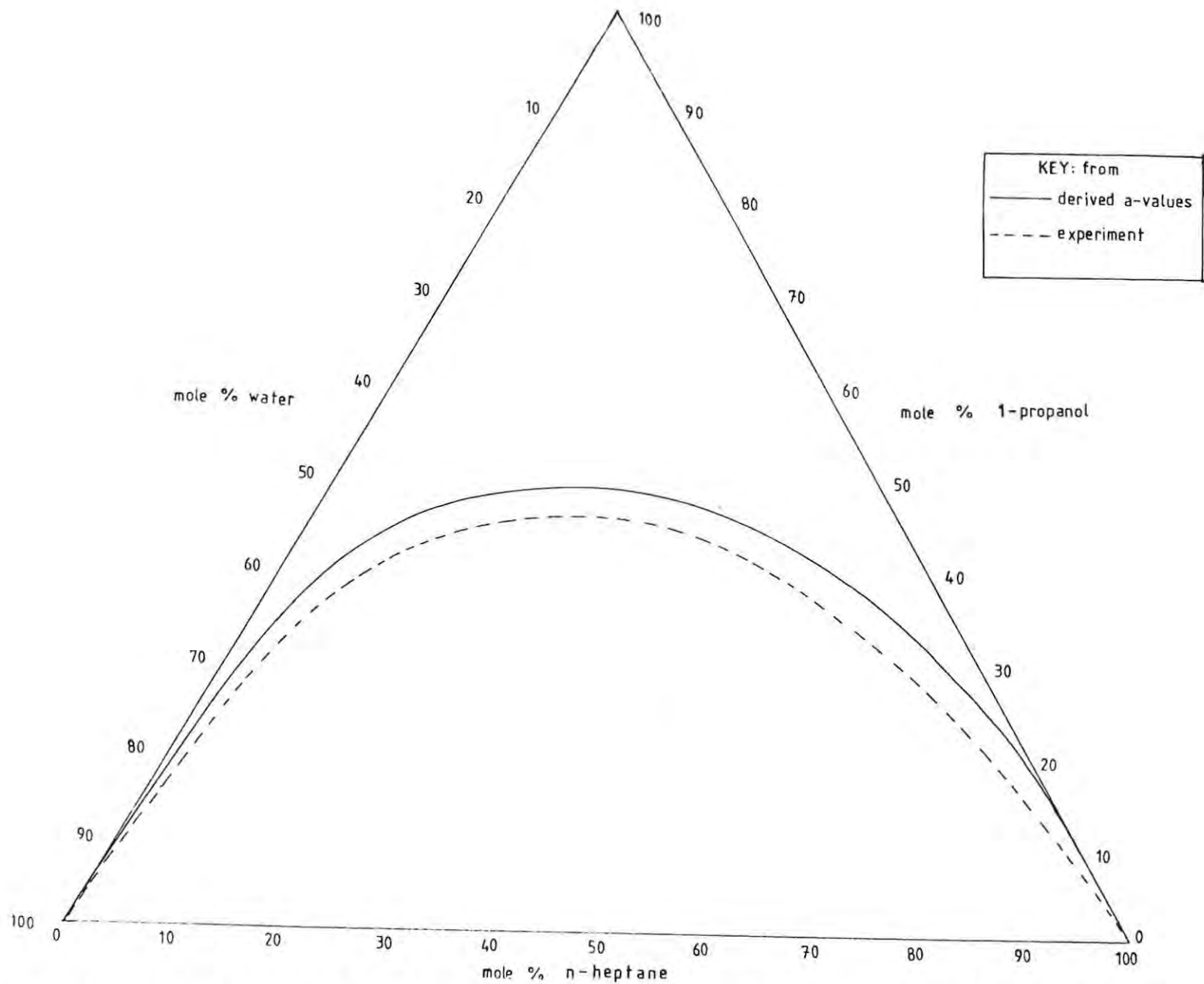


FIGURE 2.11 TERNARY PHASE DIAGRAM OF THE BEHAVIOUR OF THE N-HEPTANE-1-PROPANOL-WATER SYSTEM

## 2.5 DISCUSSION AND CONCLUSION

Liquid-liquid equilibria are much more sensitive to small changes in activity coefficients than vapour-liquid equilibria and small inaccuracies can cause serious errors. Therefore, much care must be exercised in determining interaction parameters from experimental data. The experimental data must be of very high accuracy.

Data of insufficient precision no doubt prompted Nagata to state that the prediction of ternary phase liquid-liquid diagram having one partially miscible (immiscible) pair is very difficult using only binary data <sup>(40)</sup>. However, despite the choice of a Group I system the system studied here does have a broad two phase region which allows for more accurate prediction <sup>(38)</sup>.

Ternary systems containing one partially miscible binary and two completely miscible binaries (as above) are of particular interest because of their importance in extractive and azeotropic distillations.

The UNIQUAC equation was modified in 1978 by including another binary parameter <sup>(41)</sup>. However, in many practical cases, the quantity and quality of experimental data do not justify the use of more than two binary parameters per binary. It is significant to note that in the application to ternary liquid-liquid equilibria, the NRTL equation requires nine adjustable parameters whilst the UNIQUAC equation requires six. Obviously the more parameters one uses the better will be the fit.

Maurer and Prausnitz have stated that modifications and refinements of the UNIQUAC equation are not likely to relax the initial stringent assumptions i.e. that UNIQUAC considers only the effect of changing positional co-ordinates while neglecting the effect of mixing on what are erroneously called "internal" degrees of freedom, rotation and vibration <sup>(41)</sup>. Recent work has shown that mixing influences a molecules ability to exercise rotation and vibration, primarily because the free volume of a molecule in the pure liquid is very different from that in a mixture. Flory's "equation of state contributions" to the excess functions should therefore be included whenever polyatomic molecules are considered.

The UNIQUAC model and all models for excess properties are based on a drastically oversimplified picture. One simple effect which could be considered is the change in free volume which accompanies mixing. If this is considered we can expect a significant improvement in results. The equations based on lattices or other simple geometric arrangements assume that when molecules are mixed they are simply exchanging nearest neighbours in an otherwise constant environment.

Prediction of liquid-liquid equilibria of ternary mixtures based on the constituent binaries is a rigorous test of an activity coefficient equation. No equations presently known are completely satisfactory in meeting the test for all systems. For the system studied the modified UNIQUAC equation was found to be applicable and adequate.

### 3 EXCESS ENTHALPIES AND EXCESS VOLUMES OF HEPTANE/PETROL + ALCOHOL BLENDS

#### 3.1 INTRODUCTION

Excess enthalpies and excess volumes are two of the many thermodynamic quantities essential for use in chemical engineering for the design of plant and equipment. This knowledge of thermodynamic non-ideality of liquids and liquid mixtures can often modify the flow sheet of a plant significantly <sup>(42)</sup>.

During the last decade many papers have been presented relating to the values of oxygenates in motor fuel. Alcohols were found to serve a dual function in conserving fuel and supplying some antiknock quality important when lead phasedown is considered. In the process of blending it is possible that significant heat and volume changes take place. For these reasons it was considered of interest to investigate the excess enthalpies and excess volumes of petrol/n-heptane + alcohol binary mixtures. The theory and experimental methods to be discussed are applicable to binary liquid mixtures of non-electrolytes.

#### 3.2 APPARATUS

The excess enthalpy of mixing  $H_m^E$  measurements were determined using a commercial LKB 2107 flow calorimeter. Excess volume of mixing  $V_m^E$  measurements were made by the vibrating tube densitometer (PAAR DMA601) method.

The purity of the hydrocarbons and alcohols used in this thesis are presented in table 3.2 and their experimental densities determined using the above densitometer, are compared with literature values.

#### 3.3 EXCESS MOLAR ENTHALPIES OF BINARY LIQUID MIXTURES

##### 3.3.1 Introduction

In an ideal solution there is no enthalpy change on mixing. In real solutions, however, interactions between liquids often result in a change in enthalpy. A means of investigating these interactions between component molecules in the liquid state is achieved by a study of the excess molar enthalpy of binary mixtures <sup>(42)</sup>.

The excess enthalpy  $H^E$  can be represented by

$$H^E = H (\text{real mixture}) - H (\text{ideal mixture}) \quad \text{eqn. 3.1}$$

If the value of  $H$  (ideal mixture) is assumed to be zero, then the excess molar enthalpy is given by

$$H_m^E = H (\text{real mixture}) / (n_A + n_B) \quad \text{eqn. 3.2}$$

where  $n_A$  and  $n_B$  are the number of moles of components A and B respectively.

### 3.3.2 Flow Calorimeters (43)

In a flow calorimeter, the two liquids are introduced into a mixing vessel at a steady determinable rate. The flow rates are determined by weighing the component reservoirs before and after a calorimetric run, and recording the duration of the run.

Considering an endothermic system in the mixing vessel, the power  $P$  in the heater needed to restore the temperature of the mixed liquids to that of the unmixed liquids, is measured. The molar excess enthalpy of mixing and the mole fraction  $x_A$ , of one of the liquids, A (assume two liquids A and B) are given by the formulae.

$$H_m^E = P / (f_A + f_B) \quad \text{eqn. 3.3}$$

$$x_A = f_B / (f_A + f_B) \quad \text{eqn. 3.4}$$

$$\text{where } P = i^2 R \text{ (J s}^{-1}\text{)} \quad \text{eqn. 3.5}$$

$i$  = current (amps) through resistance  $R$  (ohms)

$f_A$  = flow rate of component A ( $\text{mol s}^{-1}$ )

$f_B$  = flow rate of component B ( $\text{mol s}^{-1}$ )

$x_A$  = mole fraction of component A

### 3.3.3. The LKB 2107-121 Flow Calorimeter (44)

The arrangement of the apparatus is shown in figure 3.1 and figure 3.2 is a diagrammatic representation of the mixing vessel.

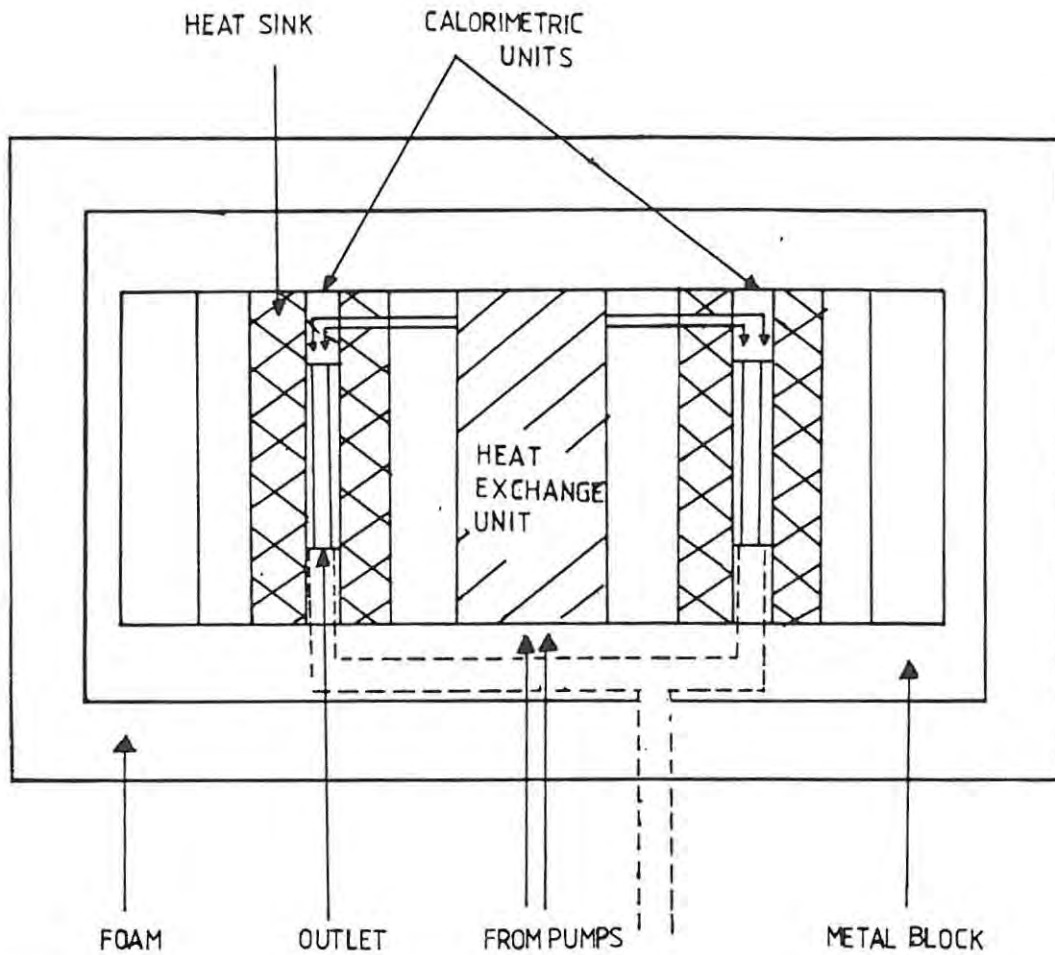


FIGURE 3.1 TOP VIEW OF LKB FLOW MICROCALORIMETER

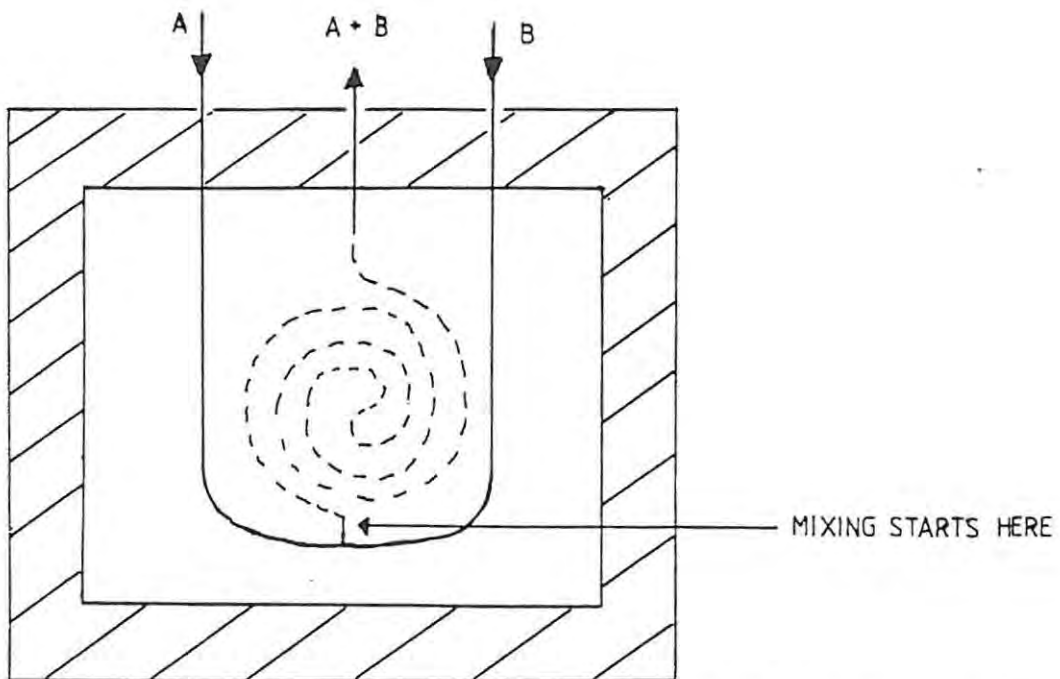


FIGURE 3.2 MIXING VESSEL OF A DIFFERENTIAL FLOW MICROCALORIMETER

The mixing vessel is a special wound gold tube 1mm in diameter and 60mm long, through which the liquids flow after mixing. The mixing cell is sandwiched between a pair of thermocouples and is in contact with a heat sink assembly. If heat is absorbed by an endothermic reaction in the tube, heat will flow from the heat sink into the tube. Heat generated by an exothermic reaction in the gold tube will flow from the tube to the heat sink assembly. In each case the temperature difference causes a heat flow across the thermopiles and an electromotive force proportional to the temperature difference is generated. The output voltage from the thermopiles is amplified and can be fed either to a recorder or a digital readout system, or both.

A heat exchanger (consisting of a coiled teflon tube 1m long placed inside the LKB thermostat and through which the liquids are pumped on their way to the mixing cell) ensures that the liquids are at the required mixing temperature by the time they reach the mixing vessel.

The LKB thermostat consists of a controlled air bath which maintains a preset air temperature a few degrees above the ambient temperature.

The control unit incorporates a power supply which provides an adjustable current for calibrating the microcalorimeter. The power supply also includes a facility for heating the calorimeter heat sink and monitoring the heat sink temperature. A digital readout system is also fitted.

#### 3.3.4. Determination of the Excess Enthalpy of Mixing for the Systems Heptane/Petrol + Alcohol

The flow calorimeter was used in conjunction with two LKB Varioperpex peristaltic pumps, the LKB 2107/210 thermostat, the LKB 2107/310 control unit and a Perkin-Elmer 561 chart-recorder. LKB veton and teflon tubing was used throughout. To achieve a constant temperature of 303,15 K ethylene glycol cooled to 279,15 K in a bath by a Tecam refrigerator coil was pumped through the external LKB thermostat.



### 3.3.5. Operating Procedure

It was first necessary to obtain a steady baseline before operation with no liquid flowing through the mixing vessel. This was recorded on a chart recorder for reference. The system was then flushed with a liquid similar in properties to the experimental fluids. Absolute alcohol was used.

The two liquids were then pumped through the mixing vessel at the desired flow rates, until a baseline deflection and a new steady state was obtained. The residence time in the mixing vessel is approximately 1,5 minutes at normal flow rates of  $20 \text{ cm}^3 \text{ hr}^{-1}$ .

The necessary current for restoring baseline response for each individual experiment was recorded in order to calculate the heat effect. If the mixing was endothermic the calibration current was switched on during the experiment and adjusted until the deflection on the recorder was nullified and the original baseline re-established. If the heating was exothermic, the steady state recorder deflection was noted and a heating current was applied to double this deflection.

The rate of heating (supplied to the mixing cell) was calculated using the following equation:

$$P = i^2 R \quad \text{eqn. 3.6}$$

Once the original baseline was re-established, the pumps were switched off and the flow rates determined.

#### 3.3.5.1 Determination of Flow Rates

The flow rates were measured by weighing the two  $25 \text{ cm}^3$  conical flasks containing the pure liquids, before and after each run. The time lapse between the start and finish of each run was measured on a stopwatch. The flow rate was thus given by:

$$\text{flow rate}_A = \frac{\text{mass of liquid A/molar mass liquid A}}{\text{time lapse}} \quad \text{eqn. 3.7}$$

where A corresponds to one of the pure liquids of the mixture. In order to minimise evaporation, the conical flasks were equipped with quickfit stoppers with two narrow inlets, one for the teflon tubing and the other open to the atmosphere. The resulting effluent mixture was collected in a suitable container and its mass compared to the combined mass of the pure liquids consumed at the end of each run. This provided a constant check for leaks in the tubing within the calorimeter apparatus.

3.3.5.2 Determination of Excess Molar Enthalpies of Mixing  $H_m^E$   
The molar excess enthalpy was calculated from

$$H_m^E = (i^2 R) / (f_A + f_B) \quad \text{eqn. 3.8}$$

when  $i$  = current (m amps) required to nullify the heating effect and regain the baseline.

$R$  = resistance of the heater coil (50,18  $\Omega$  for this apparatus).

$f_A + f_B$  = molar flow rates of liquids A and B.

### 3.3.6. Results

The results are tabulated in table 3.1 and are graphically represented in figures 3.3 - 3.4.

The use of petrol in the microcalorimeter caused problems as it was impossible to maintain consistent flow rates. Heptane was therefore substituted and the results are compared with literature results <sup>(45)</sup>.

Figure 3.3 shows the effect of increasing the hydrocarbon chain of the alcohol from ethanol to 1-butanol. Isopropanol when mixed with n-heptane elicits the greatest excess enthalpy effect and 1-butanol the least. Ethanol and 1-propanol results are very similar but the position of the hydroxyl group in isopropanol appears to result in a slightly larger excess enthalpy.

Figure 3.4 compares the experimentally determined excess enthalpies obtained with heptane/petrol and ethanol with literature values for

heptane and ethanol and for hexane and ethanol <sup>(46)</sup>. The results determined here are very similar to those derived from the literature and petrol closely resembles n-heptane in its enthalpy properties when mixed with ethanol. In order to compare these literature values with petrol the assumption was made that the molecular mass of petrol was the same as n-heptane.

Figure 3.5 shows a further comparison between experimental results and literature data <sup>(45)</sup>. The determined values are slightly lower than those in the literature. A reason for this could be a difference in the purity of the samples. The alcohols were all dried as described in Section 4.2.1.

Figure 3.6 is a representation of the results with a different set of axes. The X-axis is percentage mass heptane and the Y-axis is the excess enthalpy in units of joules per gram mixture.

Isopropanol is shown to effect the highest enthalpy of mixing i.e. approximately 9J per gram of heptane (considering an equimolar mixture). The specific heat of heptane is 44,8 cal<sup>s</sup> K<sup>-1</sup> mol<sup>-1</sup> which is equivalent to 0,45 cal<sup>s</sup> K<sup>-1</sup> g<sup>-1</sup> or 1,8 JK<sup>-1</sup> g<sup>-1</sup>

knowing that  $q = mx C_p X \quad t$  eqn. 3.8

$$t = \frac{9}{1 \times 1,8}$$
$$= 5K$$

This small rise in temperature on mixing is probably negligible in blending procedures.

Table 3.1 EXPERIMENTAL EXCESS ENTHALPIES FOR THE PETROL/N-HEPTANE  
+ ALCOHOL SYSTEMS AT 298,15 K

System: Petrol (Petrol = C<sub>7</sub> H<sub>16</sub>) + Ethanol

$x_{\text{petrol}}$	$H_m^E/\text{J mol}^{-1}$	% petrol	$H^E/\text{Jg}^{-1}$
0,100	200	19,46	3,891
0,200	350	35,21	6,162
0,300	485	48,23	7,797
0,400	565	59,17	8,358
0,500	615	68,49	9,425
0,600	605	76,53	7,717
0,700	570	83,53	6,802
0,800	500	89,69	5,605
0,900	515	95,14	3,329

System: Heptane + Ethanol

$x_{\text{heptane}}$	$H_m^E/\text{J mol}^{-1}$	% heptane	$H^E/\text{Jg}^{-1}$
0,100	295	19,46	5,739
0,200	432	35,21	7,606
0,300	525	48,23	8,441
0,400	570	59,17	8,432
0,500	600	68,49	8,219
0,600	630	76,53	8,036
0,700	580	83,53	6,921
0,800	515	89,69	5,773
0,900	345		

System: Heptane + 1-Propanol

$x_{\text{heptane}}$	$H_m^E/\text{J mol}^{-1}$	% heptane	$H^E/\text{Jg}^{-1}$
0,100	195,0	15,63	3,047
0,200	353,6	29,41	5,200
0,300	485,1	41,67	6,738
0,400	590,4	52,63	7,768
0,500	667,5	62,50	8,344
0,600	708,2	71,43	8,431
0,700	707,7	79,55	8,042
0,800	654,4	86,96	7,113
0,900	529,2	93,75	5,513

System: Heptane + iso-Propanol			
x heptane	$H_m^E / \text{J mol}^{-1}$	% heptane	$H^E / \text{Jg}^{-1}$
0,10	250	15,63	3,910
0,20	420	29,41	6,176
0,30	570	41,67	7,917
0,40	670	52,63	8,816
0,50	730	62,50	9,125
0,60	760	71,43	9,048
0,70	735	79,55	8,352
0,80	655	86,96	7,120
0,90	500	93,75	5,208
System: Heptane + 1-Butanol			
x heptane	$H_m^E / \text{J mol}^{-1}$	% heptane	$H^E / \text{Jg}^{-1}$
0,10	162,9	13,05	2,13
0,20	313,6	25,25	3,96
0,30	447,3	36,67	5,47
0,40	559,2	47,39	6,63
0,50	642,5	57,47	7,39
0,60	686,4	66,96	7,66
0,70	686,7	75,92	7,44
0,80	632,0	84,39	6,67
0,90	514,8	92,46	5,29

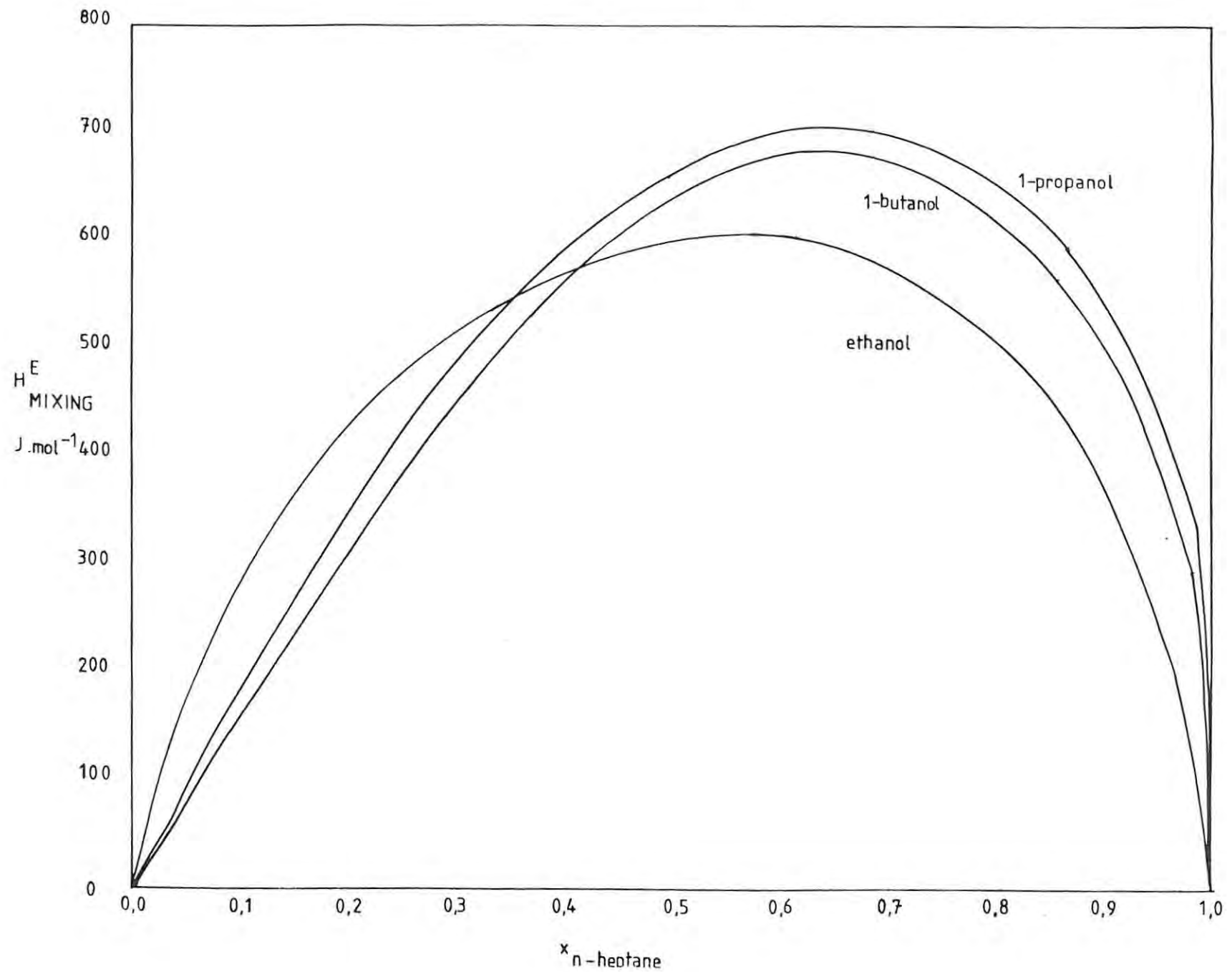


FIGURE 3.3 THE EFFECT OF INCREASING HYDROCARBON CHAIN OF THE ALCOHOL WHEN MIXED WITH N-HEPTANE AT 298,15 K

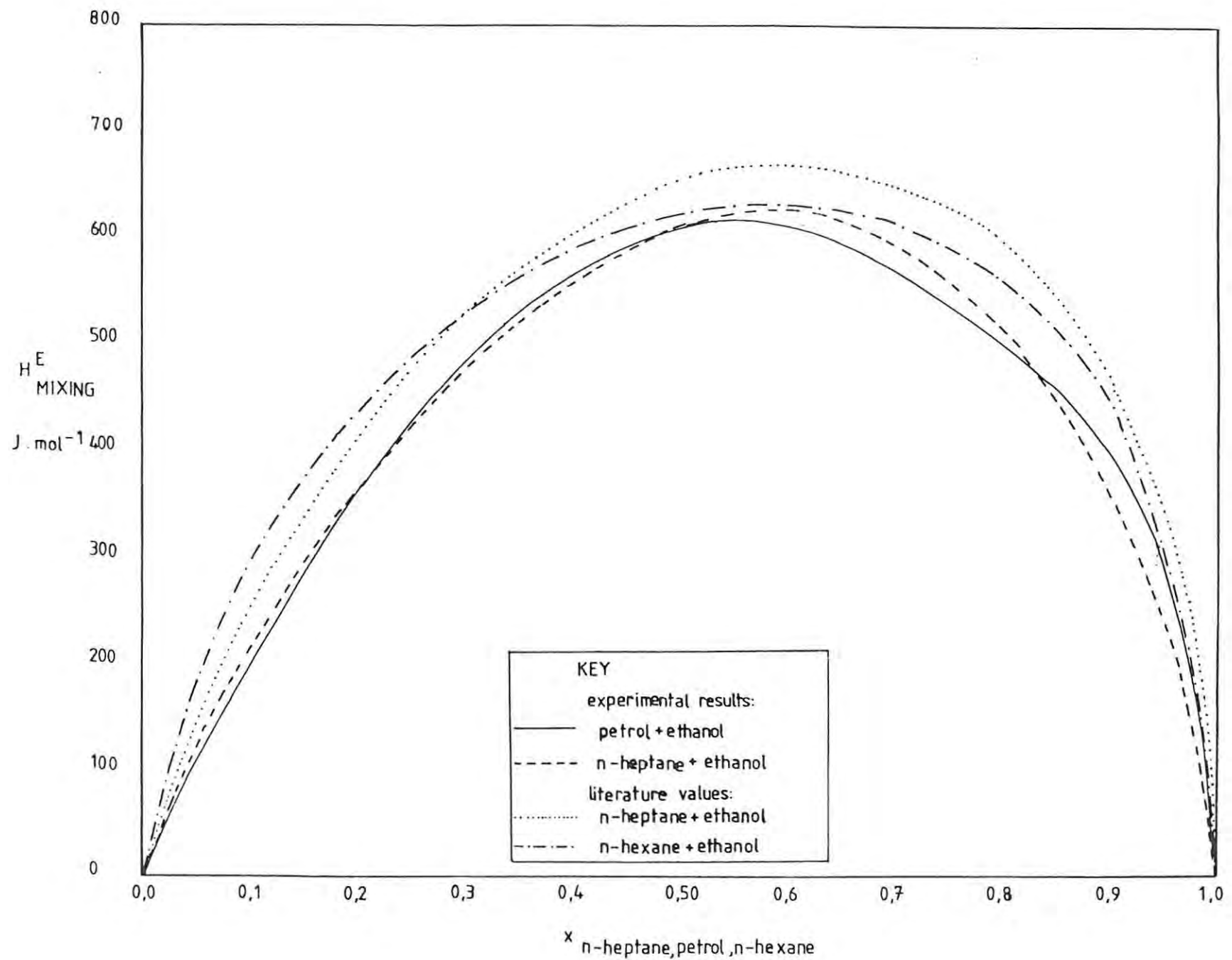


FIGURE 3.4 A COMPARISON OF  $H_M^E$  VALUES FOR THE SYSTEMS N-HEXANE, N-HEPTANE AND PETROL + ETHANOL AT 298,15 K



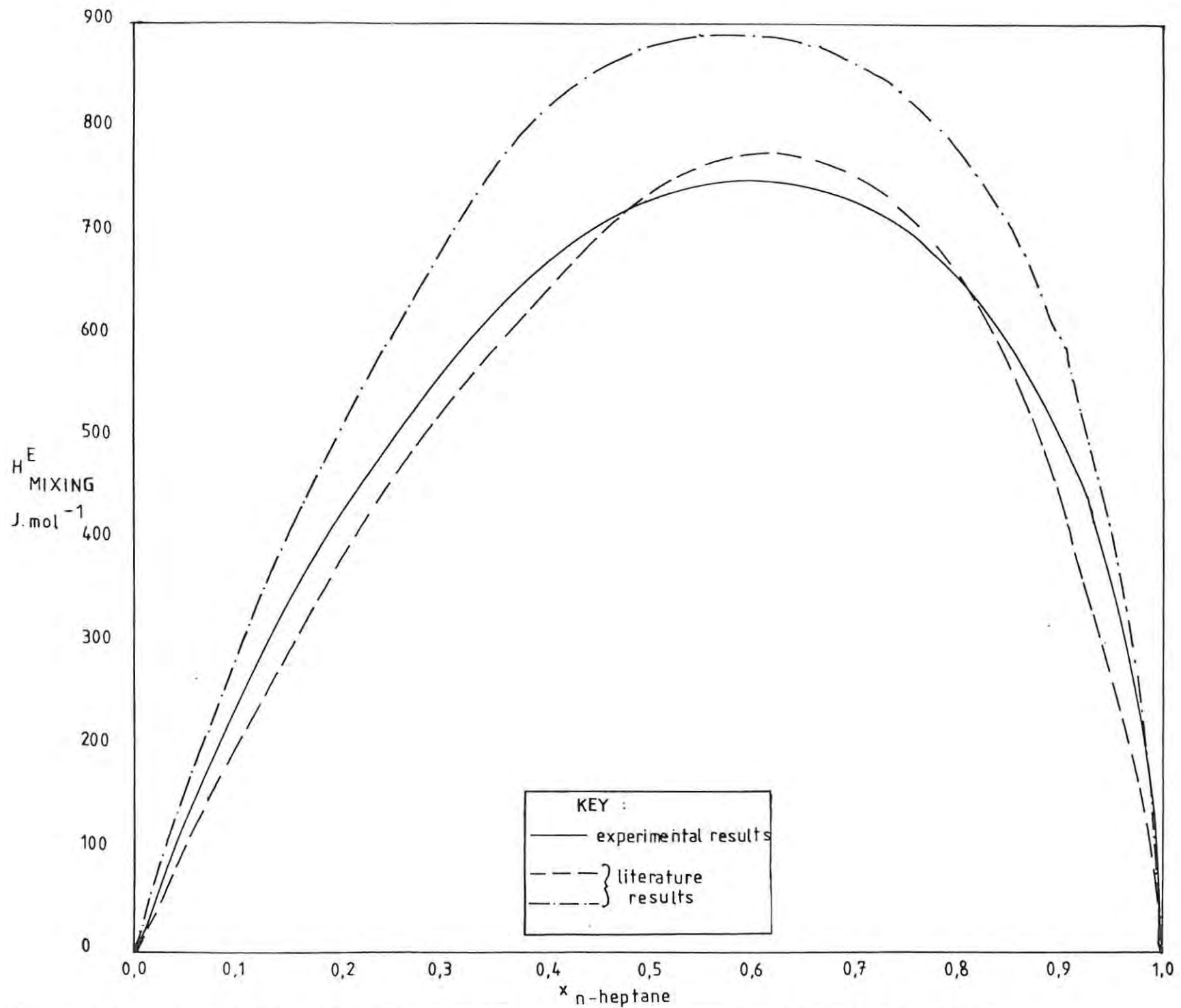


FIGURE 3.5 A COMPARISON OF EXPERIMENTAL  $H_M^E$  VALUES WITH LITERATURE DATA FOR THE SYSTEM N-HEPTANE + ISOPROPANOL AT 298,15 K

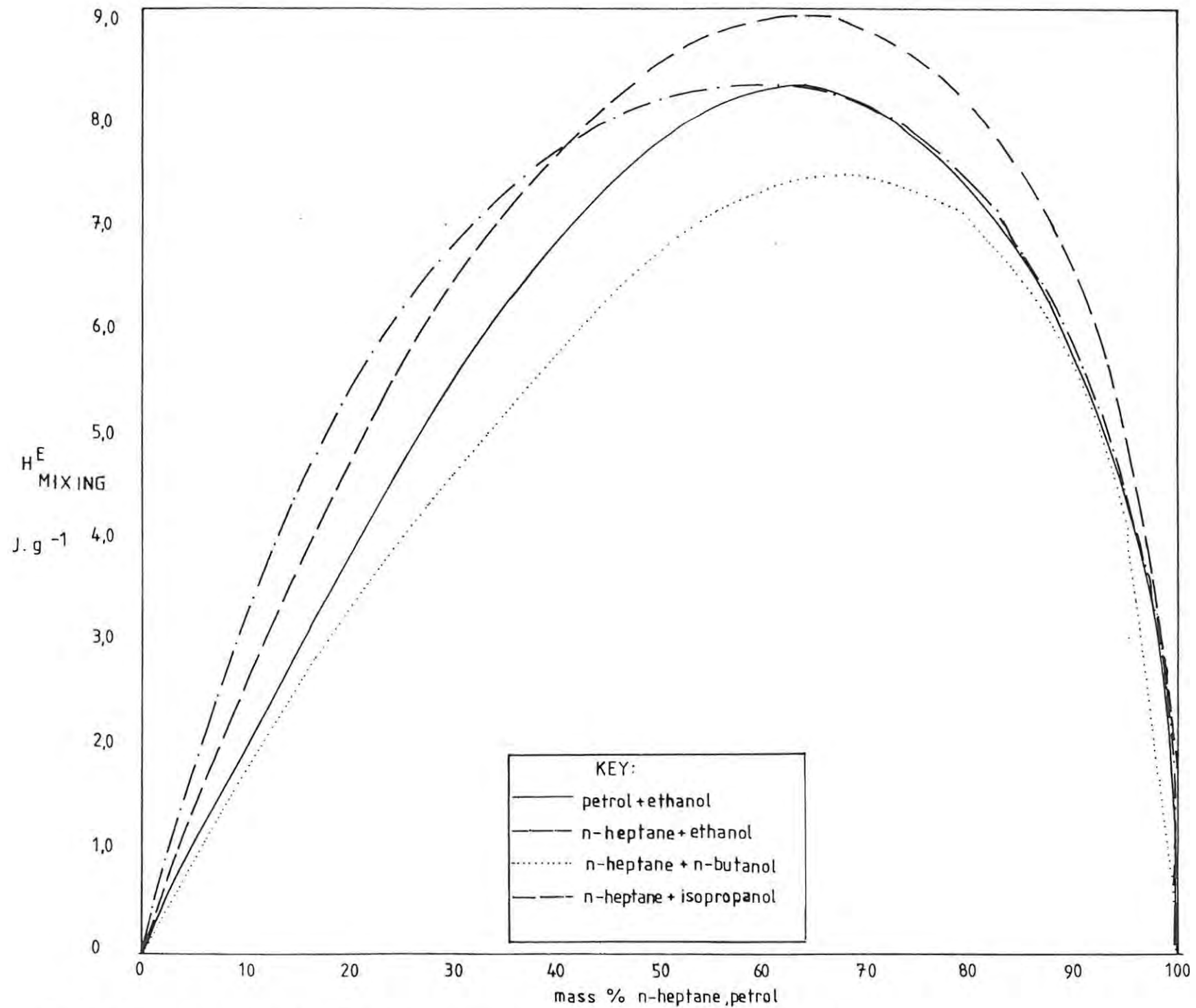


FIGURE 3.6 EXPERIMENTAL  $H^E_M$  RESULTS FOR N-HEPTANE + ALCOHOLS AT 298,15 K

### 3.4 EXCESS MOLAR VOLUMES OF BINARY LIQUID MIXTURES

#### 3.4.1 Introduction

There are two principle methods for the determination of volume changes: 1 - directly by mixing the liquids and observing volume changes.

2 - indirectly, by measuring the density of liquid mixtures and hence determining the excess volume.

In composing mixtures, care must be taken to account for evaporation into the vapour spaces of the mixing contained. Mole fractions of component in compositions are determined by weighing each component. Therefore, for two components A and B of a binary mixture

$$x_A = \frac{m_A / M_A}{(m_A / M_A) + (m_B / M_B)} \quad \text{eqn. 3.9}$$

where  $x_A$  = mole fraction of component A.

$m_A$  = mass of A /g.

$M_A$  = molar mass of A.

It was essential that complete mixing occurred.

#### 3.4.2 Vibrating Tube Densitometer (47)

This method for obtaining densities of mixtures is based on the principle that the density of a fluid contained in a small U-shaped tube is related to the natural vibrational frequency of that tube. The density,  $\rho$ , of the liquid is linearly related to the period of the vibration,  $T$ , of the tube the equation

$$\rho = a + bT^2 \quad \text{eqn. 3.10}$$

where  $a$  and  $b$  are constants

#### 3.4.3 Principle of the Density Measurement

The natural frequency of the U-tube is influenced by the mass of the sample, and also the sample density. The system is analogous to a hollow body of mass,  $m$ , which is suspended on a spring with a spring constant  $c$ .

Its volume  $v$ , is assumed to be filled with a sample of density  $p$ .  
The natural frequency of such a system is given by:

$$f = \frac{1}{2\pi} \left( \frac{c}{(m + pv)} \right)^{1/2} \quad \text{eqn. 3.11}$$

The period of oscillation  $T$  is the reciprocal of the frequency so that

$$T^2 = \frac{1}{f^2} = 4\pi^2 \left( \frac{(m + pv)}{c} \right) = Ap + B \quad \text{eqn. 3.12}$$

$$\text{where } A = 4\pi^2 \frac{v}{c} \quad \text{eqn. 3.13}$$

$$B = 4\pi^2 \frac{m}{c} \quad \text{eqn. 3.14}$$

A and B are thus instrument constants for each individual oscillator.

Measurements on two standard substances (std1 and std 2) allow for an equation relating to density in terms of standards to be set up.

$$p_{\text{unknown}} = p_{\text{std}} + b(T_{\text{unknown}}^2 - T_{\text{std}}^2) \quad \text{eqn. 3.15}$$

$$\text{where } b = \frac{(p_{\text{std1}} - p_{\text{std2}})}{(T_{\text{std1}}^2 - T_{\text{std2}}^2)} \quad \text{eqn. 3.16}$$

The standard substance 1 is usually water.

#### 3.4.4 PAAR DMA 601 Densitometer (47)

This is an example of a vibrating tube densitometer and the laboratory arrangement is represented diagrammatically in figure 3.7.

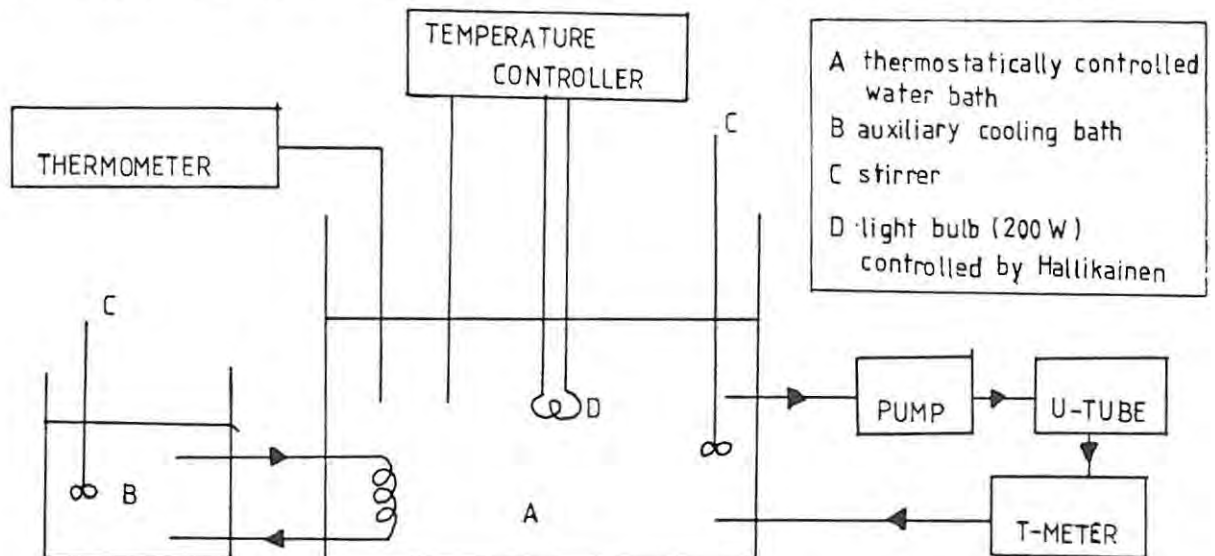


FIGURE 3.7 LABORATORY ARRANGEMENT FOR THE MEASURING OF  $V_M^E$  VALUES

The system employs an oscillating sample tube. Two cells generate a frequency in synchronism with the zero amplitude positions of the oscillating sample tube. The built-in time base gives a clock pulse every  $10^{-5}$  seconds so that by counting the number of clock pulses for the number of oscillations the time for the number of preselected oscillator periods can be determined. This makes possible high resolution period measurements in a very short time.

The sample tube is U-shaped and water-jacketed. The required operating temperature is maintained by circulating water from a thermostatically controlled water bath. The water is pumped from the water bath, through the densitometer apparatus and back. An auxiliary cooling bath is added to cool the main batch as the water temperature tends to rise. A standard light bulb is sufficient to maintain the water at operating temperature. Three mechanical stirrers were employed to ensure ready mixing of the water.

#### 3.4.5 Determination of the Excess Volumes of Mixing for the System Petrol + Alcohol

In the calculation of  $V_m^E$  the densities of the two components A and B were required. These were calculated using the following equation:

$$P_A = b (T_A^2 - T_{H_2O}^2) + P_{H_2O} \quad \text{eqn. 3.17}$$

$$P_B = b (T_B^2 - T_{H_2O}^2) + P_{H_2O} \quad \text{eqn. 3.18}$$

where b is given in equation 3.16.

The  $V_m^E$  values were given by the equation (7)

$$V_m^E = \left[ \frac{(X_A m_A) + (X_B m_B)}{P_{\text{unknown mixture}}} - \frac{(X_A m_A)}{P_A} - \frac{(X_B m_B)}{P_B} \right] \quad \text{eqn. 3.19}$$

A computer program was written to calculate these values.

### 3.4.6 Operating Procedure

Solutions of approximately 15 cm<sup>3</sup> volume were prepared by adding petrol (the more volatile component of the mixture) to varying amounts of alcohol. The alcohols were dried using the procedure described in Section 4. The mass of the empty container, container plus component A, and container + component A and B were determined in each case to determine  $x_A$ . The stoppered container was then swirled to ensure mixing of the two components.

The contents were then injected into the vibrating cell of the densitometer apparatus with a glass syringe. Care was taken to ensure that no air bubbles were present. The cell has two openings on the side of the apparatus so that the syringe is kept in place during the run. To ensure reproducibility of the T-values two to three runs were carried out on each of the solutions.

After each run, the cell was washed with acetone and dried with a fine stream of compressed air. The syringe were washed and dried similarly. Experimental runs were carried out at a temperature of 25°C accurate to  $\pm 0,003^{\circ}\text{C}$  by employing a Hallikainen temperature controller. This was considered necessary due for the following reasons:

Organic solvents have an average coefficient of expansion which requires temperature controls of within 0,01°C in order to determine the density of a mixture to within 0,00001 g cm<sup>-3</sup> (48). This would result in an accuracy of 5% in  $V^E$  results. The majority of liquid mixtures have volume changes less than 0,1% of the total volume of their components. Therefore an accuracy of 0,5% in excess volume requires density determinations to be accurate to 0,0001%. This requires temperature control to within 0,001°C.

The bath temperature was monitored by a Hewlett-Packard Quartz thermometer.

Table 3.2 THE LIQUIDS USED IN THIS THESES, THEIR SUPPLIERS AND THEIR DENSITIES

Liquid	Suppliers	GLC Minimum Assay	T-Value	Calculated Density (25,000°C)	Literature Density (20,0°C)
n-Hexane	BDH Chemicals	99,5%	1,727697	0,66858	0,6603
n-Heptane	Analyticals	99,5%	1,735492	0,68374	0,68376
n-Octane	BDH Chemicals	99,5%	1,745156	0,70263	0,7025
Petrol	Shell		1,757890	0,72768	
Methanol	PAL Chemicals		1,790712	0,79309	0,7914
Ethanol	NCP (reagent grade)		1,788353	0,78835	0,7893
n-Propanol	Analyticals	99,5%	1,786184	0,78878	0,8035
Isopropanol	PAL Chemicals		1,785521	0,78267	0,7855
1-Butanol	Analyticals	99,0%	1,799861	0,81156	0,8098
1-Methyl - 1-Propanol	Analyticals	99,0%	1,800669	0,81317	0,8080
2-Methyl - 1-Propanol	Analyticals	99,0%	1,805183	0,82231	0,8080
2-Methyl - 2-Propanol	Analyticals	99,0%	1,797799	0,80737	0,7887
1-Pentanol	BDH Chemicals		1,804823	0,82158	0,8144
1-Hexanol	BDH Chemicals		1,802331	0,81653	0,8136
Ethyl Acetate	Ethyl Corporation		1,841105	0,89588	0,9003
Ethylene Glycol	Merck	99,5%	1,911089	1,04335	1,1088
Sasol Alcohol	Sasol		1,795855	0,80346	



### 3.4.7 Results

The densities calculated for each of the liquids used in this thesis at 298,15 K are represented and compared with those at 293,15 K given in the Selected Values of Properties of Hydrocarbons and Related Compounds, American Petroleum Institute, Research Project 44, Thermodynamics Research, College Station, Texas. This comparison is shown in Table 3.2.

The excess volumes of mixing are presented in figures 3.8 - 3.10. Figure 3.8 shows the values obtained for ethanol, isopropanol and 1-propanol when mixed with n-heptane. Figure 3.9 compares the literature values of n-heptane + ethanol with those determined for petrol + ethanol <sup>(49)</sup>. Here the petrol  $V^E$  results are lower than those for n-heptane. This is obviously due to the effect of the hydrocarbon mixture in petrol.

Figure 3.10 compares the petrol-alcohol results. The conclusion is that the volume change is small on mixing petrol with alcohols. For a 10% ethanol in n-heptane mixture, the volume change is about 0,3%. For the mixture of 90% petrol with 10% alcohol blend the volume change is about 0,4% which is negligible.

Table 3.3 EXPERIMENTAL EXCESS MOLAR VOLUMES  $V_m^E$  FOR PETROL  
( $C_7H_{16}$ ) + ALCOHOL SYSTEMS AT 298,15 K

System: Petrol + Ethanol

Mass % petrol	$V_m^E / \text{cm}^3 \text{mol}^{-1}$
10,71	0,06876
20,72	0,11421
34,35	0,176448
42,11	0,195277
54,66	0,248102
63,94	0,294169
75,36	0,33359
90,03	0,34858
97,28	0,10242

---

System: Petrol + iso-Propanol

---

Mass % petrol	$V_m^E / \text{cm}^3 \text{ mol}^{-1}$
20,79	0,17880
30,50	0,29147
41,90	0,38257
54,58	0,46733
65,73	0,5522
75,89	0,5848
87,24	0,5467
95,29	0,22612

---

System: Petrol + 1-Butanol

---

Mass % petrol	$V_m^E / \text{cm}^3 \text{ mol}^{-1}$
11,18	0,030524
22,65	0,047432
32,65	0,08345
42,41	0,10496
63,87	0,11317
75,80	0,07511
87,21	0,04231

---

System: Petrol + Mixed Alcohol (70% Ethanol, 20% iso-Propanol + 10% 1-Butanol)

---

Mass % petrol	$V_m^E / \text{cm}^3 \text{ mol}^{-1}$
10,17	0,04525
22,94	0,104614
31,42	0,13194
43,67	0,17758
53,67	0,20945
64,68	0,23275
74,64	0,22713
87,99	0,20826

---

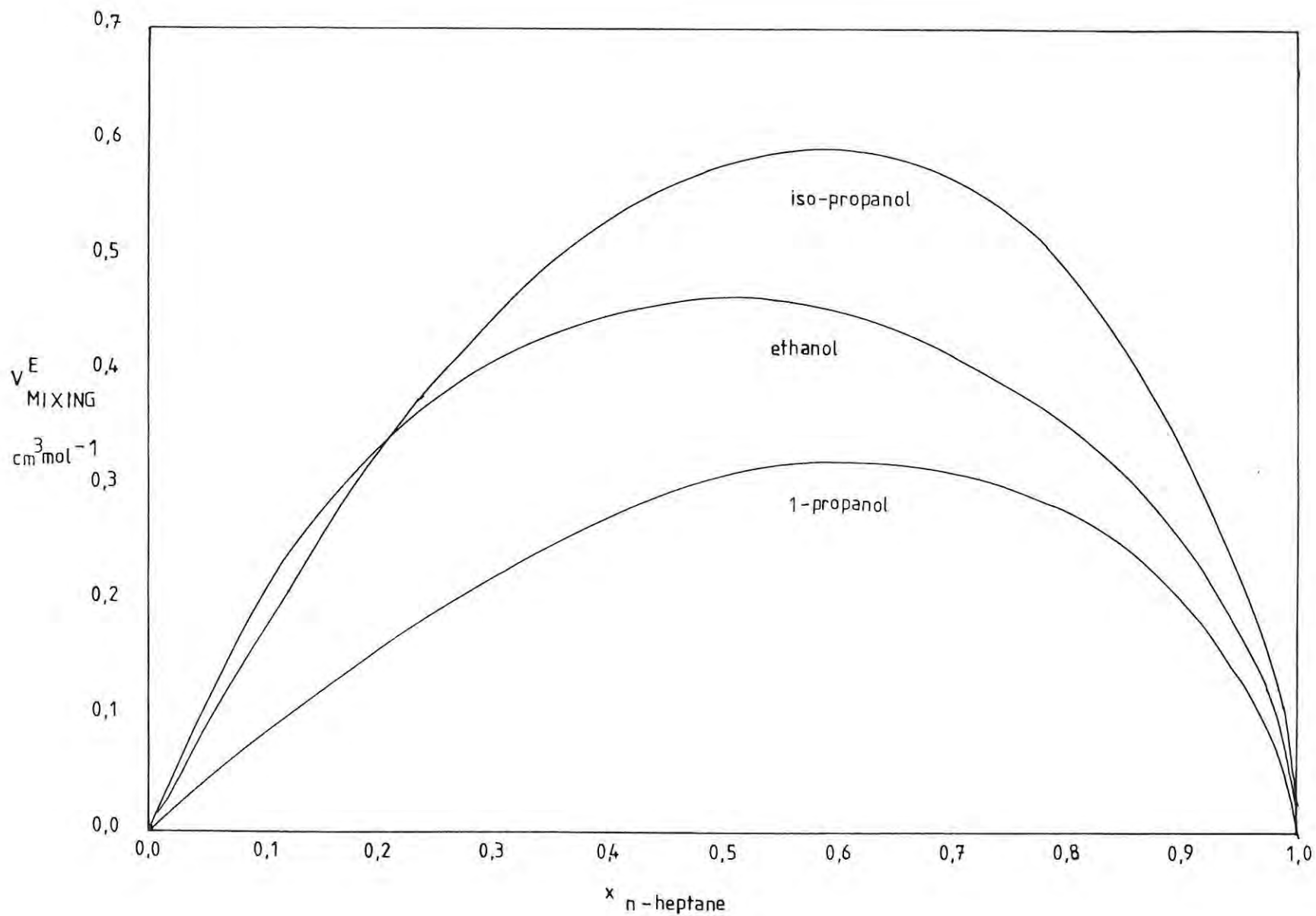


FIGURE 3.8 THE EFFECT OF INCREASING HYDROCARBON CHAIN OF THE ALCOHOL WHEN MIXED WITH N-HEPTANE AT 298,15 K

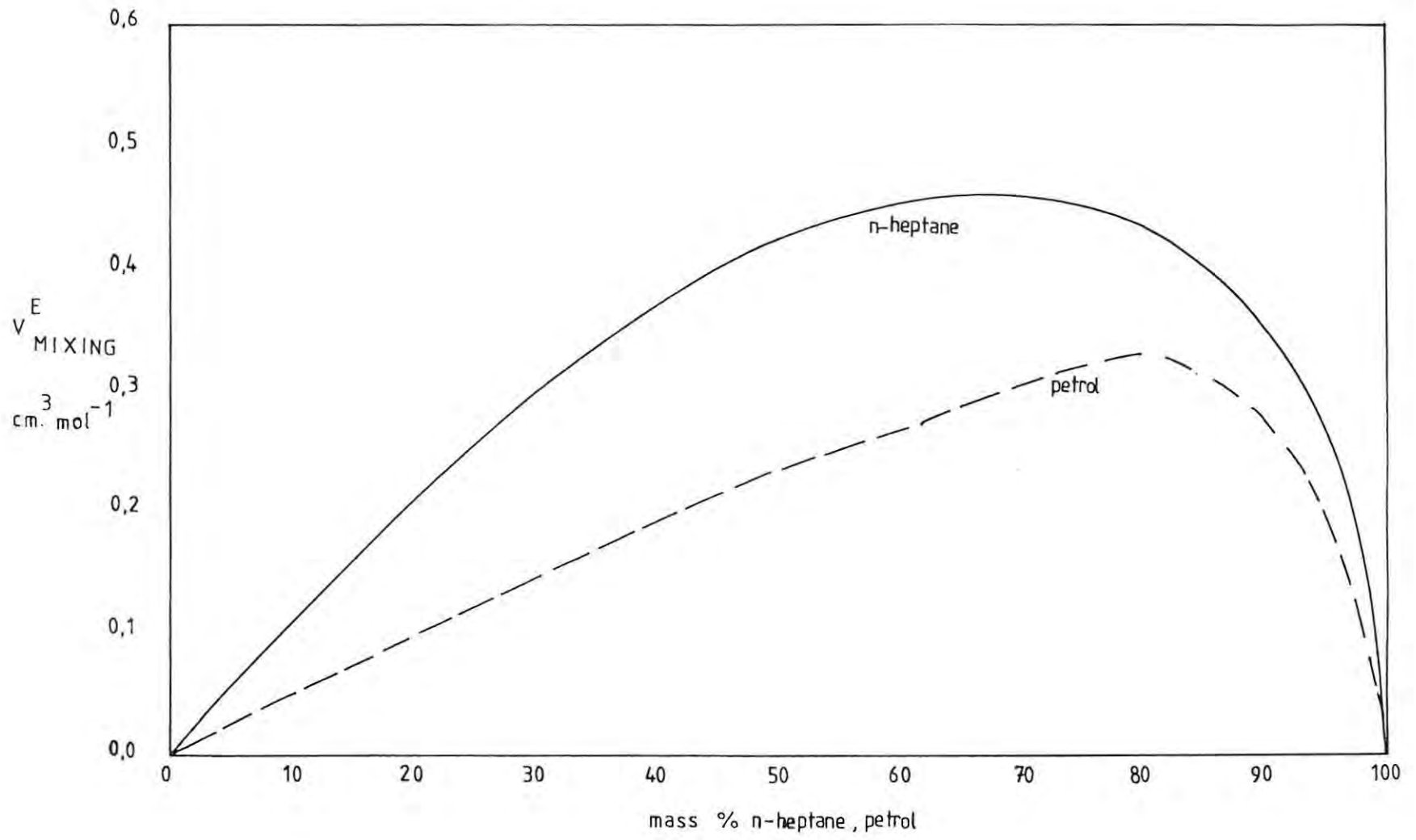


FIGURE 3.9 A COMPARISON OF  $V_M^E$  VALUES FOR THE SYSTEMS N-HEPTANE AND PETROL + ETHANOL AT 298,15 K

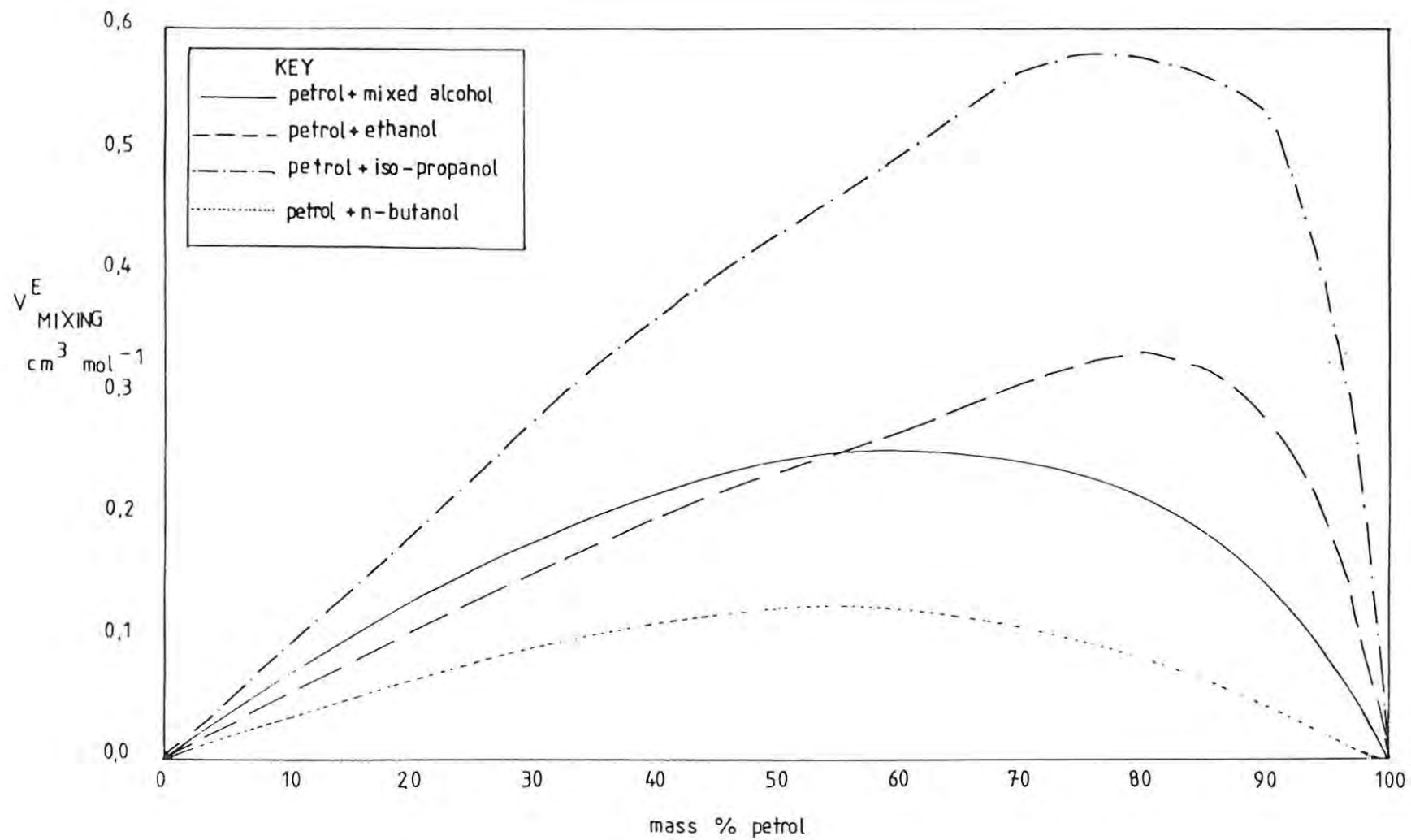


FIGURE 3.10 A COMPARISON OF  $V_M^E$  VALUES FOR THE PETROL + ALCOHOL SYSTEMS AT 298,15 K

### 3.4 DISCUSSION AND CONCLUSION

Excess enthalpies and volume measurements have shown that iso-propanol results in the greatest changes when mixed with petrol and n-heptane. This compares with literature results<sup>(50)</sup>. It can therefore be assumed that no significant problems relating to heating effects or volume changes occur when petrol and alcohols are mixed in bulk quantities.

#### 4 WATER SOLUBILITY STUDIES IN PETROL AND HEPTANE + ALCOHOL BLENDS

##### 4.1 INTRODUCTION

The ultimate goal of alternate fuel studies is to find a replacement for crude oil as the major source of transportation fuels. This would most likely result in extensive and costly changes in current methods and equipment for fuel manufacture and distribution. A transition period is foreseen when non-petroleum based fuels are used to supplement petroleum based supplies. Alcohols are the most likely replacement fuels of the future. Alcohol-petrol blends are already in use in different parts of the world both as a fuel and as an octane improver. The latter use of alcohols will become increasingly important as the use of lead compounds is withdrawn for health reasons.

In South Africa the SASOL process produces oxygenates as by-products <sup>(51)</sup>. Oxygenates, such as alcohols, aldehydes and ketones are formed simultaneously with the hydrocarbons in the synthesis process. The higher oxygenates are oil-soluble and are converted in the refining process to the corresponding hydrocarbons. The lower oxygenates, such as ethanol, propanol, butanol and acetone, are recovered separately and can be added to the transportation fuel pool. The SASOL blend of mixed alcohols used on the Witwatersrand include ethanol (65%), propanol (20%) and the higher alcohols, butanol, pentanol and hexanol, in lower proportions. This is mixed with petrol up to 15 percent by volume and used in unmodified vehicles.

Corrosion problems have been experienced by motorists using the SASOL fuel blend <sup>(52)</sup>. In all cases the corrosion took place in carburettors made of two different metals. As a result these problems are thought to be related to water contamination and the subsequent separation of a water-rich phase.

The solubility of water in petrol is very low and is estimated to be approximately 80 mg per 100g (i.e. less than 0,01%) <sup>(53)</sup>.



The addition of alcohol raises this significantly. A problem, however, arises when the water concentration increases beyond saturation. Methanol and ethanol both tend to absorb water from the atmosphere and while they are both fully miscible with water, the presence of relatively small amounts of water in petrol + alcohol blends causes phase separation. For example, a water content as low as 0,1% can cause separation of methanol from 10% blend at 293,15 K. The ethanol blend is less sensitive and a 10% ethanol blend can tolerate about 0,5% water at 293,15 K.

The absorption of water by pure methanol or ethanol fuels is not a major problem as they are fully miscible. However, the water does have the effect of cooling combustion, thereby increasing knock resistance. The main disadvantage of water in pure alcohol fuels is that the calorific value is reduced so that large proportions of water is undesirable.

In this work, the phase separation of alcohol-petrol-water blends was investigated in an attempt to understand the corrosion problems experienced by South African motorists using these fuels. Ternary phase diagrams and tielines have been determined for a number of alcohol-petrol-water systems at 298,15 K. These were compared to n-heptane-alcohol-water phase diagrams. The effect of temperature on the petrol phase diagrams was also examined.

Because the fuel blends used in South Africa contain between 10% and 20% alcohol it was considered necessary to obtain detailed solubility measurements at various temperature for blends in this composition range.

Corrosion will only take place in an environment in which two different metals are in contact with a highly conductive solution such as water. For this reason conductivity measurements were taken for some of the alcohol-water mixtures.

## 4.2 EXPERIMENTAL PROCEDURE

### 4.2.1 Materials

Table 3.2 (page 71) represents the chemicals used, their suppliers and their densities.

The alcohols, methanol, ethanol, 1-propanol and isopropanol were each distilled before use. The method of Lund and Bjerrum requiring magnesium metal activated with iodine was used <sup>(54)</sup>. The butanol isomers were dried with anhydrous calcium sulphate before the same distillation technique was applied. The petrol used was the high octane 98 grade obtained from a local Shell station (i.e. no SASOL product present).

### 4.2.2 Binodal Curve and Tie Line Measurements

Initial phase separation studies were carried out in 50 cm<sup>3</sup> measuring flasks fitted with tightly fitting caps. Binary mixtures of the two miscible liquids were made up and placed in a constant temperature bath set at 298,15 K for 1 hour to equilibrate. The third component (also equilibrated at 298,15 K) in this case, water, was then added to these consolute liquids until the mixture suddenly turned cloudy. The third component was added using a gas tight syringe capable of dispensing a drop weighing less than 0,01g. Care was taken to ensure complete mixing and water was added until one drop caused the clear solution to become cloudy. These results were used to obtain the binodal curve. To ensure that one phase existed when determining the refractive indices, a measured drop of alcohol was added to each mixture. This did not have a significant effect on the composition and the same composition was used to determine the "standard" curve refractive index composition.

A thermostatted Bellingham and Stanley refractometer (Abbe) was used for the refractive index measurements. This was controlled at a slightly elevated temperature of 298,25 K to ensure phase homogeneity. The "standard" curve for each system was obtained by relating the refractive index of each mixture on the binodal (co-existence) curve, to a "composition" which was determined by dropping a perpendicular from the binodal curve to the petrol or n-heptane composition axis of the ternary phase diagram.

The plot of refractive index and this composition formed the "standard" curve <sup>(55)</sup>. Figure 4.1 represents the laboratory arrangement.

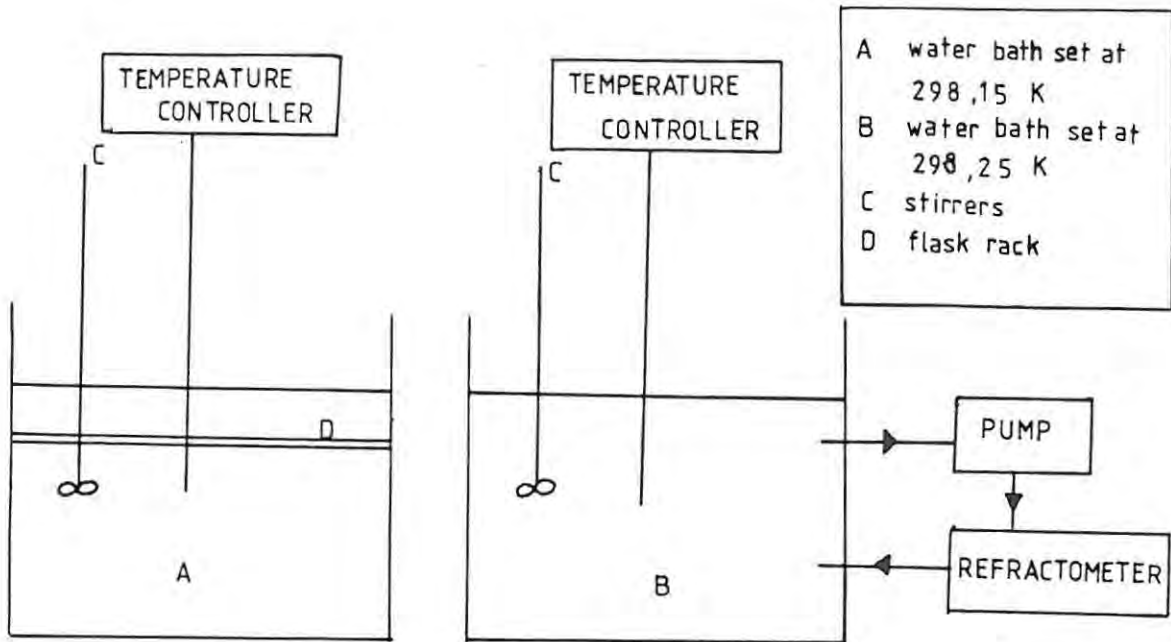


FIGURE 4.1 LABORATORY ARRANGEMENT FOR THE DETERMINATION OF THE BINODAL CURVE AND ITS TIE LINES

The tie lines were determined from carefully made-up solutions in the immiscible region of the phase diagram. The flasks were well-shaken and left for 2 hours to separate into two phases at 298,15 K. Refractive index measurements were then taken of each of the two separated phases by carefully withdrawing samples using a hypodermic syringe. The compositions of these mixtures on the binodal curve was then obtained by reference to the "standard" curve. Each tie line was checked to ensure that it passed through the composition of the overall mixture.

More precise measurements on the binodal curve were made on all the systems by weighing the components into a 50 cm<sup>3</sup> pyrex flask which was then sealed off under vacuum and dry air and liquid nitrogen temperatures. A calibrated mercury in glass thermometer was used to determine the consolute temperatures. This temperature was determined twice - once with increasing temperature and once with decreasing temperature.

The effects of temperature on the binodal curves were studied. Investigations were made at 275,15 K and 313,15 K in the manner described above.

The more detailed water solubility studies necessitated the use of a stock blend of each alcohol-petrol blend. 20 cm<sup>3</sup> aliquots of the petrol-alcohol mixtures were taken and allowed to equilibrate for 1 hour in a water bath set at 273,15 K. Water was added and the temperature kept constant until the blends became saturated. The temperature of the bath was then increased and the solubility of water determined again. The water was added by use of a hyperdermic syringe in the same way as that described above.

#### 4.2.3 Conductivity Measurements

Conductivity measurements were made using a Zeiss (CON602) conductivity meter. Alcohol-water mixtures were made up for the ethanol, iso-propanol, Sasol fuel alcohol and 1-pentanol systems and their conductivity measurements taken.

### 4.3 RESULTS

The composition of the points on the binodal curve at 298,15 K for the petrol/n-heptane - alcohol - water systems are given in tables 4.1 and 4.2. These results are graphed in figures 4.2 - 4.22. The results of the tie line determinations at 298,15 K are given in tables 4.3 and 4.4 and graphed in the figures above.

Table 4.5 presents the water concentration of the water rich layer as calculated from the tie lines of the binodal curves for the petrol-alcohol-water ternary systems. The petrol content of the blends was in each case 88 mass percent.

Table 4.6 represents the effect of temperature on the solubility of water in 10 percent and 20 percent methanol and ethanol petrol ternary systems. Figures 4.23 and 4.24 graphs these results.

Table 4.7 represents the conductivity measurement results.

Figure 4.25 compare the ternary phase diagrams for four systems at 273,15 K and 313,15 K

Table 4.1 EXPERIMENTAL DATA FOR THE BINODAL CURVES OF PETROL-ALCOHOL  
-WATER TERNIARY SYSTEM AT 298,15 K

The concentrations of petrol ( $C_p$ ), and water ( $C_w$ ) are given in mass percent. The alcohol concentration is determined from:  $100 - (C_p + C_w)$

System: Petrol + Methanol + Water	
$C_p$	$C_w$
0,83	31,36
2,36	22,20
3,00	19,92
5,62	14,40
9,99	9,67
14,21	6,92
18,07	5,35
25,22	3,67
34,17	2,26
44,13	1,25
68,92	0,87
85,15	0,28

System: Petrol + Ethanol + Water	
$C_p$	$C_w$
1,23	43,01
3,19	33,80
5,06	29,46
8,91	23,92
12,42	20,07
16,32	16,47
19,10	15,00
27,68	10,85
30,00	9,98
45,49	6,08
56,72	3,11
67,13	2,40
70,15	2,36
82,36	1,72
92,22	0,41

---

System: Petrol + 1-Propanol + Water

---

$C_p$	$C_w$
1,05	61,22
4,68	48,42
6,58	43,98
9,31	36,50
15,62	26,63
20,19	20,74
24,24	17,90
31,62	12,41
37,57	9,27
47,27	6,85
54,98	5,23
60,94	3,01
75,32	1,72
83,50	1,00

---

System: Petrol + iso-Propanol + Water

---

$C_p$	$C_w$
1,00	70,03
1,80	57,32
6,05	40,08
10,81	34,53
12,10	32,17
15,54	28,50
21,69	22,93
29,47	18,32
37,81	14,29
49,00	9,56
58,76	5,86
69,24	1,84

---

System: Petrol + 1-Butanol + Water

---

$C_p$	$C_w$
0,0	15,33
3,55	14,05
10,81	11,32
16,84	9,66
22,78	7,46
30,11	5,54
45,45	2,66
68,15	1,13
80,25	0,77

---

System: Petrol + sec-Butanol (1-methyl - 2-propanol)  
+ Water

---

$C_p$	$C_w$
0,0	23,13
6,43	21,49
15,21	14,69
26,07	10,00
45,80	5,23
66,40	1,39
89,29	0,59

---

System: Petrol + tert-Butanol (2-methyl - 2-propanol)  
+ Water

---

$C_p$	$C_w$
0,02	92,76
3,18	55,74
14,37	25,99
34,03	10,82
47,57	6,67
63,85	3,26
89,91	0,63



---

System: Petrol + 1-Pentanol + Water

$C_p$	$C_w$
0,0	10,52
8,16	8,25
18,29	6,72
24,46	5,47
30,53	3,89
48,41	2,86
70,69	0,67
79,52	0,52

---

System: Petrol + 1-Hexanol + Water

$C_p$	$C_w$
0,0	7,75
5,14	6,01
17,78	4,43
26,48	3,53
46,75	2,09
68,63	0,73

---

System: Petrol + Sasol Alcohol + Water

$C_p$	$C_w$
1,03	60,15
3,19	38,31
4,95	35,45
7,54	28,59
9,80	25,37
11,68	23,36
16,02	19,28
22,50	15,07
33,49	10,81
40,95	8,27
55,63	4,49
73,86	1,81
81,47	1,11

---

Table 4.2 EXPERIMENTAL DATA FOR THE BINODAL CURVES OF N-HEPTANE-ALCOHOL-WATER SYSTEMS AT 298,15 K  
(The concentration of n-heptane ( $C_h$ ), etc from Table 4.1)

System: n-Heptane + Methanol + Water	
$C_h$	$C_w$
0,14	92,99
0,28	53,92
0,80	28,64
5,53	10,92
7,96	7,06
11,26	4,43
25,53	0,90
93,64	0,00
93,81	0,00

System: n-Heptane + Ethanol + Water	
$C_h$	$C_w$
0,19	81,27
0,74	56,44
1,10	48,10
6,08	20,95
7,76	17,92
15,81	10,85
23,14	7,82
26,51	6,99
30,38	5,36
45,00	4,13
57,08	1,80
68,99	0,78
77,56	0,56
88,96	0,37

---

System: n-Heptane + 1-Propanol + Water

---

$C_h$	$C_w$
1,35	61,24
2,92	50,14
5,15	43,97
10,16	34,56
13,97	28,31
19,16	21,01
21,03	19,56
27,45	15,36
31,96	13,21
41,71	10,29
52,67	6,85
60,87	4,89
72,24	2,02
85,39	1,35

---

System: n-Heptane + iso-Propanol + Water

---

$C_h$	$C_w$
0,18	85,16
0,36	66,48
1,79	58,09
5,98	36,88
7,88	31,67
13,08	24,19
16,62	21,20
22,25	17,79
27,43	14,66
42,83	10,02
50,58	7,21
63,47	4,37
86,57	0,79

---

System: n-Heptane + 1-Butanol + Water

---

$C_h$	$C_w$
0,0	19,17
7,14	14,97
8,38	14,16
24,26	8,64
32,37	7,44
44,16	5,12
63,51	2,69
64,75	2,10
86,64	0,66
88,22	0,60

---

System: n-Heptane + sec-Butanol + Water

---

$C_h$	$C_w$
0,0	81,21
0,0	34,93
0,0	31,32
6,76	20,50
24,36	10,57
43,47	5,38
64,56	2,14
87,76	0,48

---

System: n-Heptane + tert-Butanol + Water

---

$C_h$	$C_w$
0,53	84,97
0,80	69,22
2,71	57,77
3,12	53,28
9,16	37,26

---

System: n-Heptane + tert-Butanol + Water (Continued)

---

$C_h$	$C_w$
21,11	18,74
22,26	17,38
32,23	12,03
42,02	8,27
65,76	2,86
82,33	1,51

---

System: n-Heptane + iso-Butanol (2-methyl-1-propanol)  
+ Water

---

$C_h$	$C_w$
0,0	17,26
7,69	12,99
24,67	7,17
47,76	3,82
66,35	1,46
86,97	0,83
0,0	92,64

---

System: n-Heptane + 1-Pentanol + Water

---

$C_h$	$C_w$
0,0	9,86
8,17	8,67
23,62	5,46
26,59	5,07
43,52	3,07
46,32	2,62
65,36	1,44
67,91	1,14
88,83	0,61
90,37	0,22

---

System: n-Heptane + 1-Hexanol + Water

---

$C_h$	$C_w$
0,0	6,83
8,81	5,30
25,50	2,96
26,75	2,94
43,87	2,08
46,39	1,59
68,29	0,65
89,75	0,06

---

System: n-Heptane + Sasol Alcohol + Water

---

$C_h$	$C_w$
0,0	98,83
1,20	45,01
7,33	23,20
15,74	14,15
43,84	5,20
87,11	0,85
26,14	9,77
65,31	2,48

---

Table 4.3 CONCENTRATIONS OF THE CONJUGATE TERNARY SOLUTIONS (a) AND (b) FOR THE PETROL TERNARY SYSTEMS AT 298,15 K. The symbols and units are the same as in Table 4.1

System: Petrol + Methanol + Water			
$C_p(a)$	$C_w(a)$	$C_p(b)$	$C_w(b)$
43,0	2,2	81,5	0,35
18,2	5,6	88,7	0,20
9,2	10,0	93,5	0,10
5,0	80,0	99,0	0,05

System: Petrol + Ethanol + Water			
$C_p(a)$	$C_w(a)$	$C_p(b)$	$C_w(b)$
5,1	29,7	94,0	0,6
9,7	22,8	89,0	1,0
20,2	14,2	68,7	2,0
30,8	10,0	57,6	3,0

System: Petrol + 1-Propanol + Water			
$C_p(a)$	$C_w(a)$	$C_p(b)$	$C_w(b)$
0,60	72,0	15,9	26,2
0,50	78,8	28,1	14,5
0,45	82,7	52,3	4,5
0,20	90,0	69,2	2,3

System: Petrol + iso-Propanol + Water			
$C_p(a)$	$C_w(a)$	$C_p(b)$	$C_w(b)$
11,5	33,5	57,5	6,5
5,2	44,2	63,5	5,2
2,0	53,5	75,0	2,7
1,0	63,0	88,0	0,6



---

System: Petrol + 1-Butanol + Water

---

$C_p(a)$	$C_w(a)$	$C_p(b)$	$C_w(b)$
0,0	100,0	13,7	10,2
0,0	100,0	46,0	2,8
0,0	100,0	74,1	0,9
0,0	100,0	90,0	0,2

---

System: Petrol + 1-Methyl-1-Propanol + Water

---

$C_p(a)$	$C_w(a)$	$C_p(b)$	$C_w(b)$
0,0	92,0	78,3	0,5
0,0	86,0	49,0	4,8
		25,1	10,8

---

System: Petrol + 2-Methyl-2-Propanol + Water

---

$C_p(a)$	$C_w(a)$	$C_p(b)$	$C_w(b)$
0,1	91,8	96,2	0,1
0,5	81,0	63,7	3,7
3,1	56,8	39,3	8,5

---

System: Petrol + 1-Pentanol + Water

---

$C_p(a)$	$C_w(a)$	$C_p(b)$	$C_w(b)$
0,0	99,0	88,0	0,0
0,0	99,0	67,1	1,3
0,0	99,0	31,4	4,7

---

System: Petrol + 1-Hexanol + Water

---

$C_p(a)$	$C_w(a)$	$C_p(b)$	$C_w(b)$
0,0	99,5	92,0	0,0
0,0	99,5	78,3	0,2
0,0	99,5	30,3	5,1

System: Petrol + Sasol Alcohol + Water			
$C_p(a)$	$C_w(a)$	$C_p(b)$	$C_w(b)$
19,0	18,7	49,5	6,9
6,2	31,7	62,6	4,1
2,1	43,3	69,7	3,1
0,5	62,0	77,6	2,0
0,4	69,5	86,8	0,8
0,2	79,0	95,0	0,3

Table 4.4 CONCENTRATIONS OF THE CONJUGATE TERNARY SOLUTIONS (a) AND (b) FOR THE HEPTANE TERNARY SYSTEMS AT 298,15 K

System: n-Heptane + Methanol + Water			
$C_h(a)$	$C_w(a)$	$C_h(b)$	$C_w(b)$
12,4	4,0	95,3	0,2
1,5	19,0	97,5	0,3
0,5	46,8	99,4	0,1

System: n-Heptane + Ethanol + Water			
$C_h(a)$	$C_w(a)$	$C_h(b)$	$C_w(b)$
0,7	70,4	96,5	0,2
2,2	34,5	94,5	0,3
10,0	15,8	90,5	0,5

System: n-Heptane + 1-Propanol + Water			
$C_h(a)$	$C_w(a)$	$C_h(b)$	$C_w(b)$
0,3	84,7	94,4	0,4
1,0	61,8	89,1	0,8
3,6	50,7	84,0	1,5
6,2	40,7	75,0	2,3

---

System: n-Heptane + iso-Propanol + Water

---

$C_h(a)$	$C_w(a)$	$C_h(b)$	$C_w(b)$
0,5	74,5	97,8	0,2
1,0	61,8	88,8	1,2
3,0	43,1	77,6	2,2

---

System: n-Heptane + 1-Butanol + Water

---

$C_h(a)$	$C_w(a)$	$C_h(b)$	$C_w(b)$
0,0	100,0	89,6	0,8
0,0	100,0	84,3	1,0
0,0	100,0	60,2	2,3
0,0	100,0	21,8	9,7
0,0	100,0	47,8	5,0

---

System: n-Heptane + 1-Methyl-1-Propanol + Water

---

$C_h(a)$	$C_w(a)$	$C_h(b)$	$C_w(b)$
0,2	93,3	89,7	0,3
0,3	89,7	81,4	0,6
0,35	76,65	50,4	4,0
0,4	83,1	15,0	15,0

---

System: n-Heptane + 2-Methyl-2-Propanol + Water

---

$C_h(a)$	$C_w(a)$	$C_h(b)$	$C_w(b)$
0,5	83,2	92,6	0,4
0,5	83,2	49,2	5,8
0,5	83,2	29,5	13,3

---

System: n-Heptane + 2-Methyl-1-Propanol + Water

---

$C_h(a)$	$C_w(a)$	$C_h(b)$	$C_w(b)$
0,0	97,8	99,7	0,0
0,2	93,7	57,9	2,5
0,2	93,7	13,1	11,0

---

System: n-Heptane + 1-Pentanol + Water

---

$C_h(a)$	$C_w(a)$	$C_h(b)$	$C_w(b)$
0,0	98,0	66,8	1,0
0,0	98,0	61,3	1,2
0,0	98,0	47,8	2,6
0,0	98,0	19,8	6,0

---

System: n-Heptane + 1-Hexanol + Water

---

$C_h(a)$	$C_w(a)$	$C_h(b)$	$C_w(b)$
0,0	100,0	14,0	4,3
0,0	100,0	48,9	2,1
0,0	100,0	88,0	0,4

---

System: n-Heptane + Sasol Alcohol + Water

---

$C_h(a)$	$C_w(a)$	$C_h(b)$	$C_w(b)$
00,0	86,6	99,0	0,1
00,0	75,8	98,5	0,1
0,8	50,2	95,6	0,2
9,8	19,7	80,2	1,5

---

Table 4.5 THE WATER CONCENTRATION  $C_w$  OF THE WATER RICH LAYER AS CALCULATED FROM THE TIE LINES OF THE BINODAL CURVES FOR THE PETROL-ALCOHOL-WATER TERNARY SYSTEMS AT 298,15 K. THE PETROL CONTENT OF THE BLENDS WAS IN EACH CASE 88 MASS PERCENT

Alcohol	$C_w$ /Mass Percent
Methanol	6
Ethanol	23
2-Propanol	63
Sasol Fuel Alcohol	70
1-Propanol	95
1-Butanol	100
1-Pentanol	99

Table 4.6 CONCENTRATION OF WATER,  $C_W$ , IN 10,0% AND IN 20,0% ALCOHOL-PETROL MIXTURES. ALL CONCENTRATIONS ARE IN MASS PERCENT UNITS

System: Petrol + Methanol + Water			
10% Methanol		20% Methanol	
T/K	$C_W$ /Mass %	T/K	$C_W$ /Mass %
275,91	0,092	276,15	0,140
283,48	0,116	282,07	0,220
291,35	0,142	293,35	0,325
301,05	0,171	302,93	0,410
309,96	0,205	314,12	0,533

System: Petrol + Ethanol + Water			
10% Ethanol		20% Ethanol	
T/K	$C_W$ /Mass %	T/K	$C_W$ /Mass %
275,01	0,448	274,60	1,35
282,50	0,475	279,95	1,44
289,57	0,499	287,56	1,56
300,98	0,540	293,15	1,64
308,36	0,570	307,12	1,85
313,14	0,587	311,65	1,92

System: Petrol + 1-Propanol + Water			
10% 1-Propanol		20% 1-Propanol	
T/K	$C_W$ /Mass %	T/K	$C_W$ /Mass %
273,94	0,492	275,65	1,62
278,05	0,508	280,57	1,69
288,69	0,550	288,36	1,84
293,22	0,569	299,95	2,02
299,66	0,594	311,65	2,21
310,20	0,637	314,24	2,24

System: Petrol + 1-Butanol + Water			
10% 1-Butanol		20% 1-Butanol	
T/K	C <sub>w</sub> /Mass %	T/K	C <sub>w</sub> /Mass %
278,66	0,217	274,03	0,62
278,78	0,250	287,00	0,74
297,25	0,287	294,23	0,79
306,25	0,320	302,26	0,88
312,15	0,346	311,65	0,98

Table 4.7 CONDUCTIVITY,  $\sigma$ , OF ALCOHOL-WATER MIXTURES OF WATER COMPOSITION C<sub>w</sub>. (THE WATER USED WAS GRAHAMSTOWN MUNICIPAL SUPPLY)

Ethanol	
C <sub>w</sub> /Mass %	$\sigma$ /mSm <sup>-1</sup>
100	87,1
95	71,0
84	43,2
72	26,1
51	12,5
30	6,0
10	1,5

iso-Propanol	
C <sub>w</sub> /Mass %	$\sigma$ /mSm <sup>-1</sup>
100	87,1
91	53,9
80	32,5
65	17,8
42	5,2
17	1,1

---

Sasol Alcohol

$C_w$ /Mass %	$\sigma$ mSm <sup>-1</sup>
100	87,1
93	63,0
88	51,2
79	35,5
58	16,0
36	7,0
19	2,5

---

1-Pentanol

$C_w$ /Mass %	$\sigma$ mSm <sup>-1</sup>
100	87,1
98,5	81,0

---



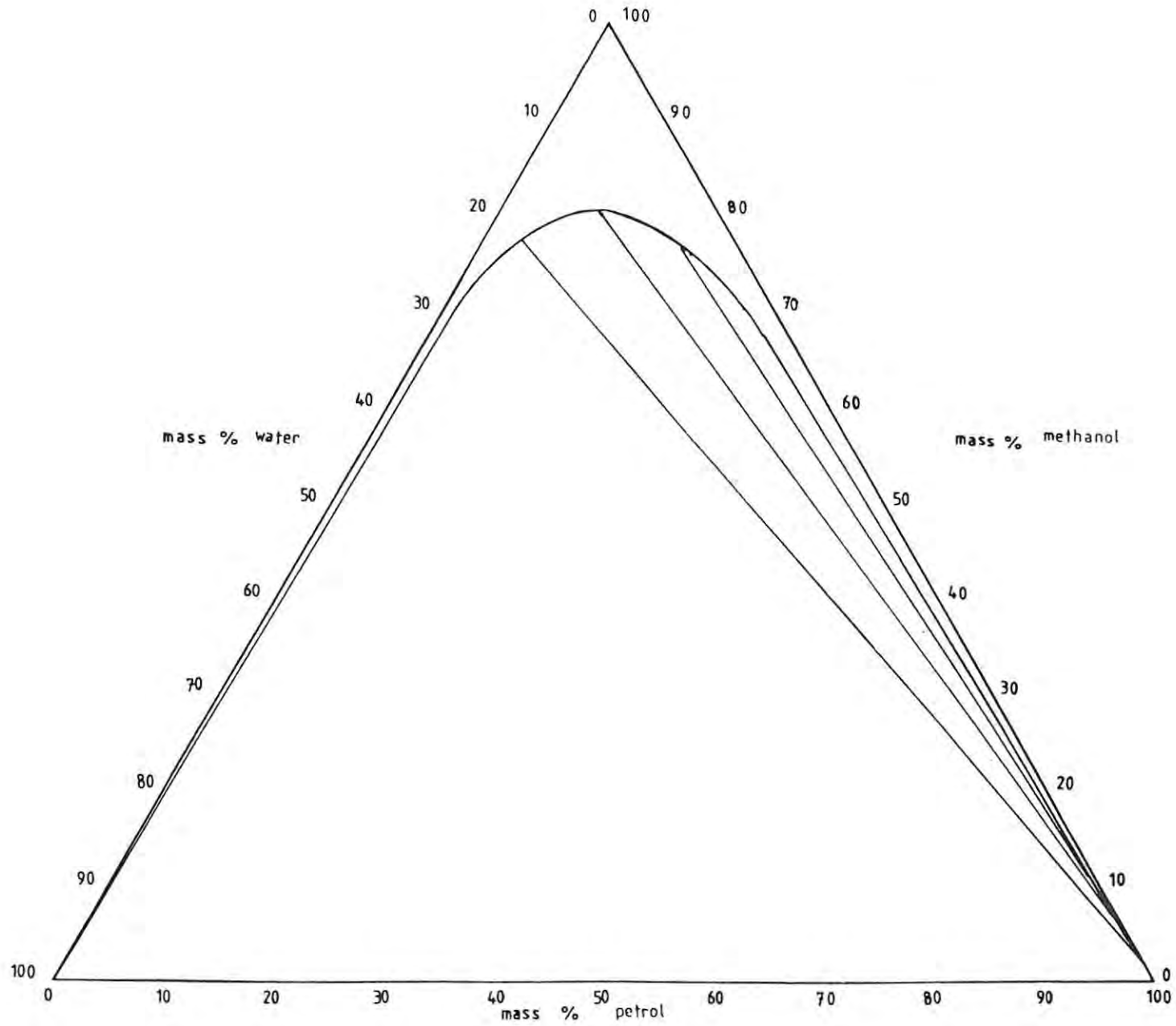


FIGURE 4.2 EXPERIMENTAL BINODAL CURVE FOR THE SYSTEM PETROL + METHANOL + WATER AT 298,15 K

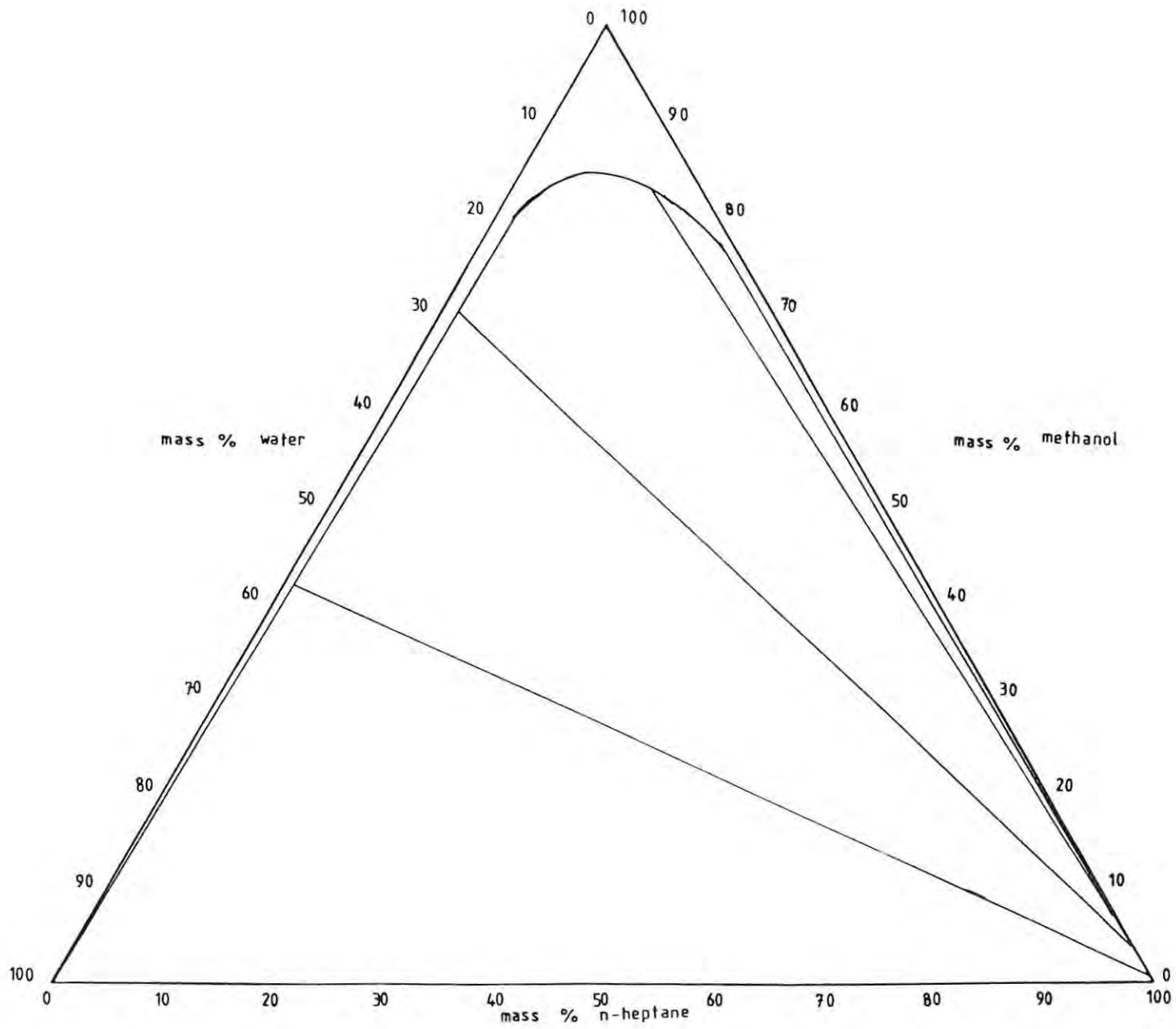


FIGURE 4.3 EXPERIMENTAL BINODAL CURVE FOR THE SYSTEM N-HEPTANE + METHANOL + WATER AT 298,15 K

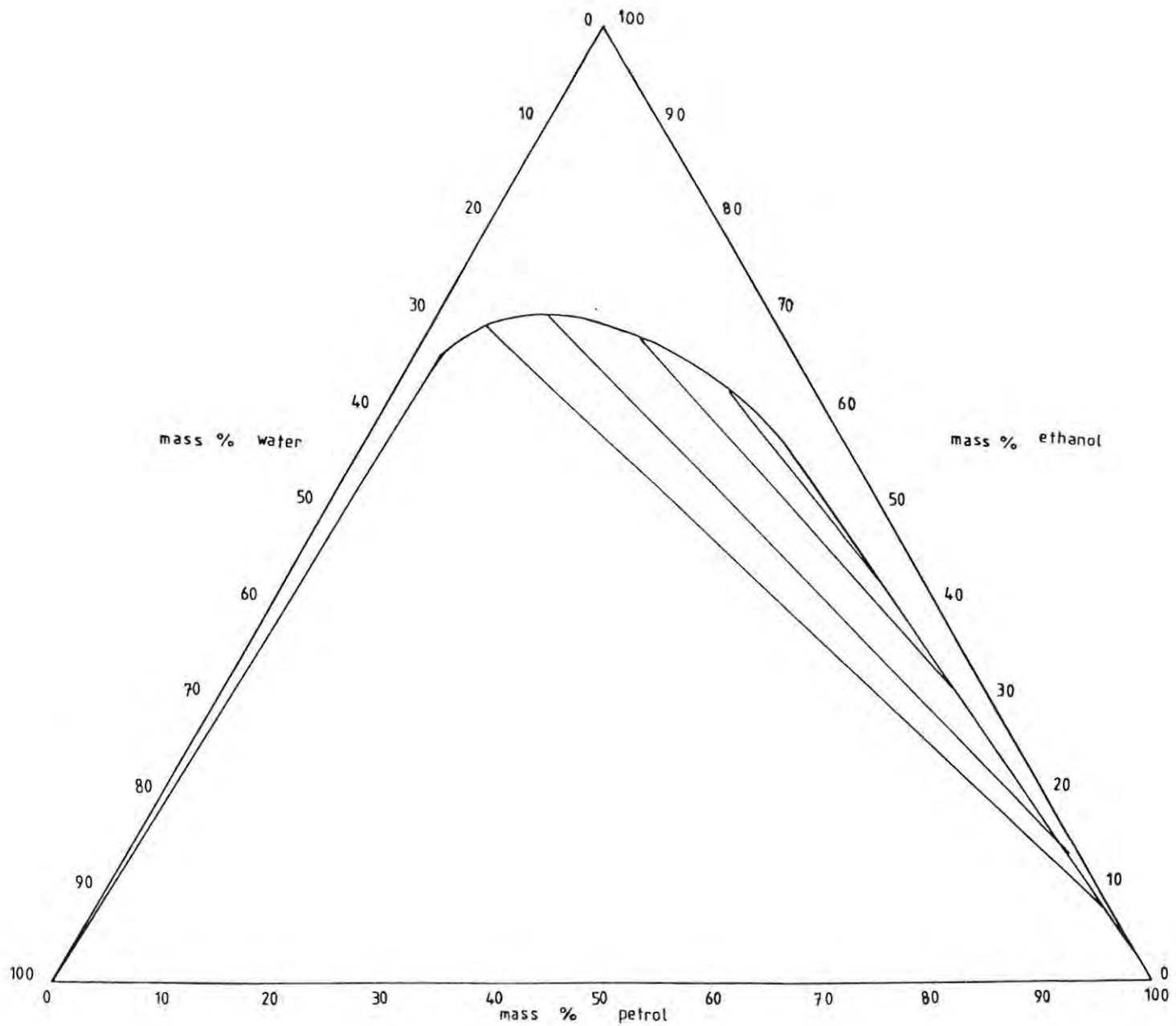


FIGURE 4.4 EXPERIMENTAL BINODAL CURVE FOR THE SYSTEM PETROL + ETHANOL + WATER AT 298,15 K

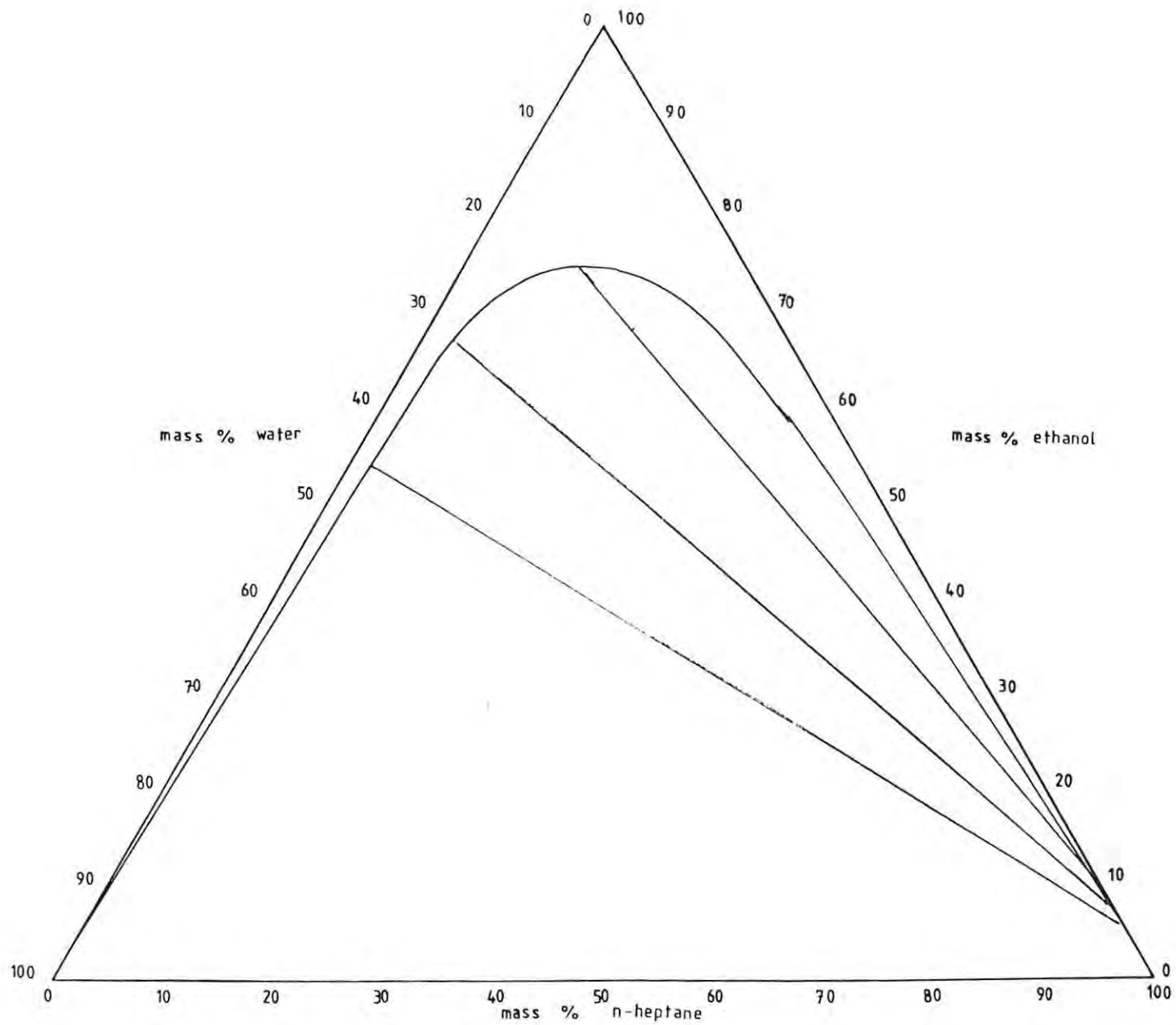


FIGURE 4.5 EXPERIMENTAL BINODAL CURVE FOR THE SYSTEM N-HEPTANE + ETHANOL + WATER AT 298,15 K

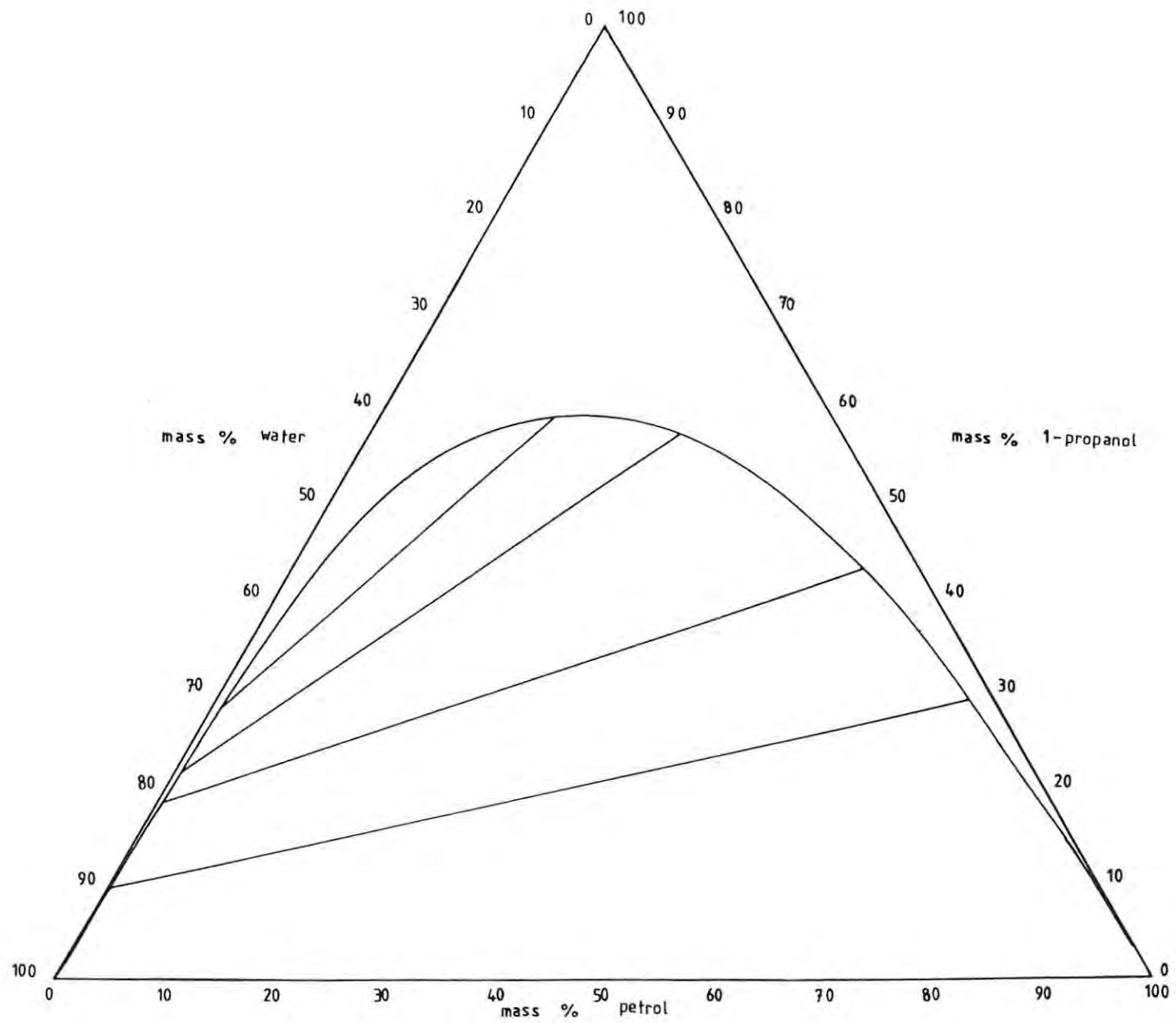


FIGURE 4.6 EXPERIMENTAL BINODAL CURVE FOR THE SYSTEM PETROL + 1-PROPANOL + WATER AT 298,15 K

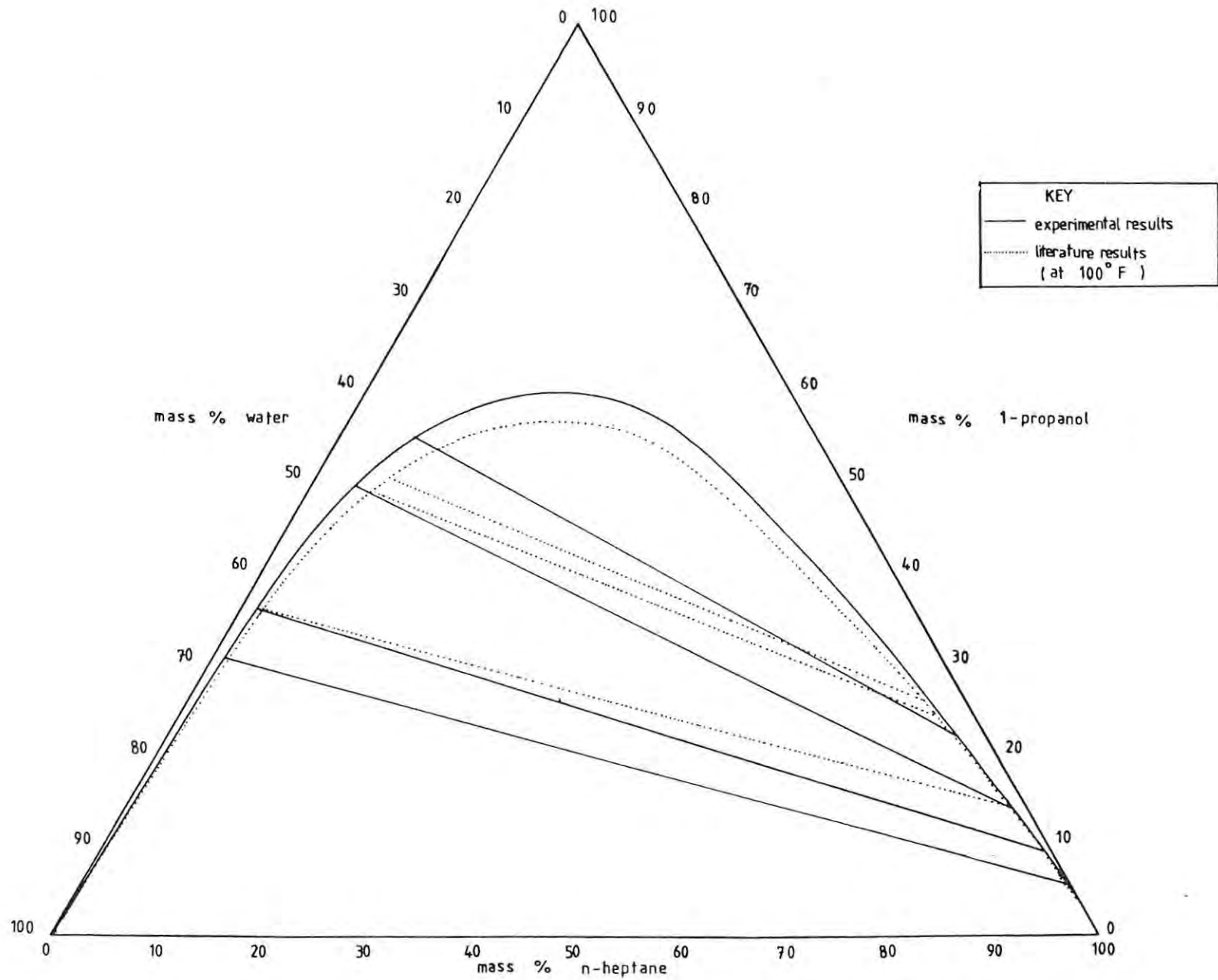


FIGURE 4.7 EXPERIMENTAL BINODAL CURVE FOR THE SYSTEM N-HEPTANE + 1-PROPANOL + WATER AT 298,15 K

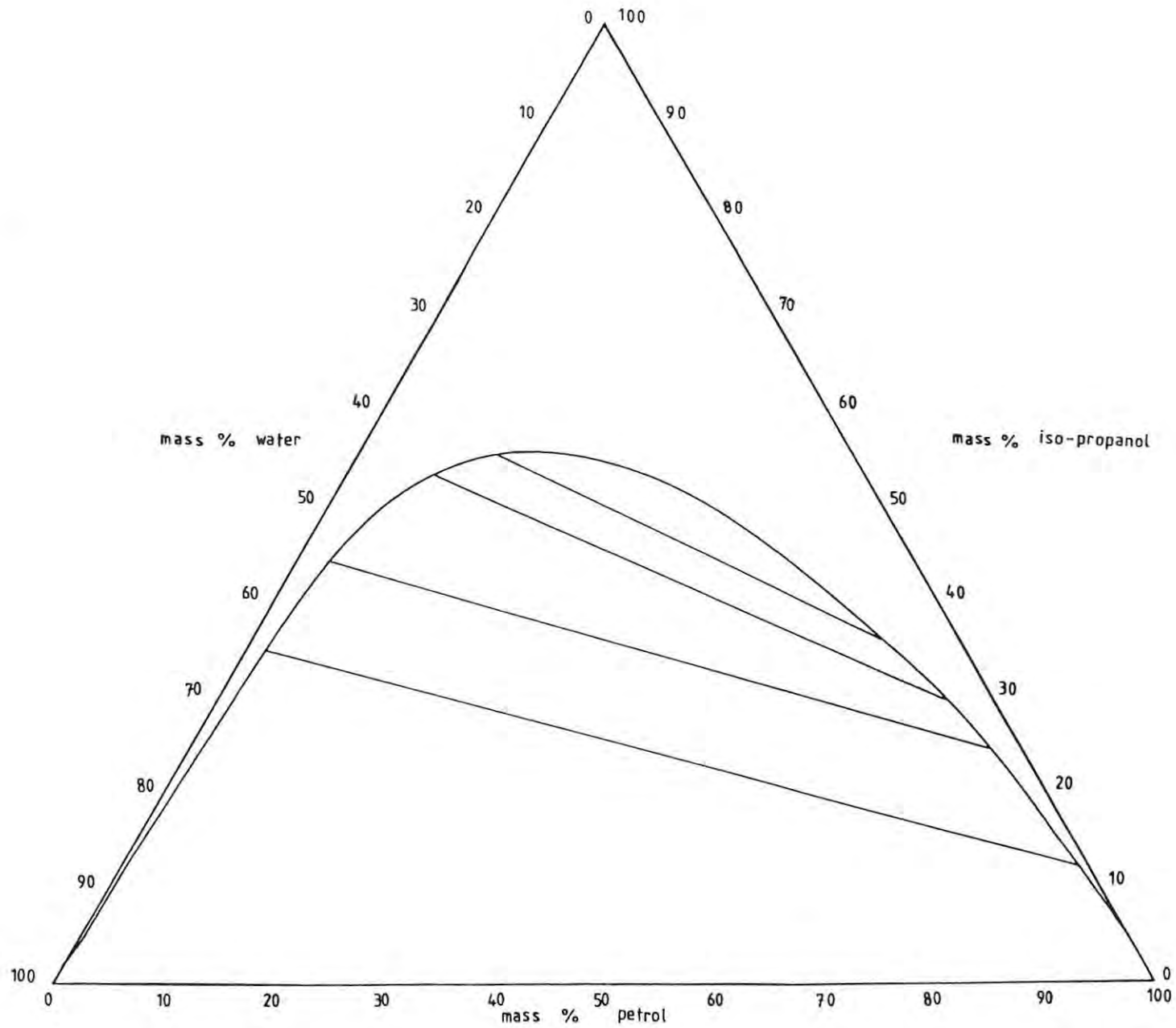


FIGURE 4.8 EXPERIMENTAL BINODAL CURVE FOR THE SYSTEM PETROL + ISO-PROPANOL + WATER AT 298,15 K



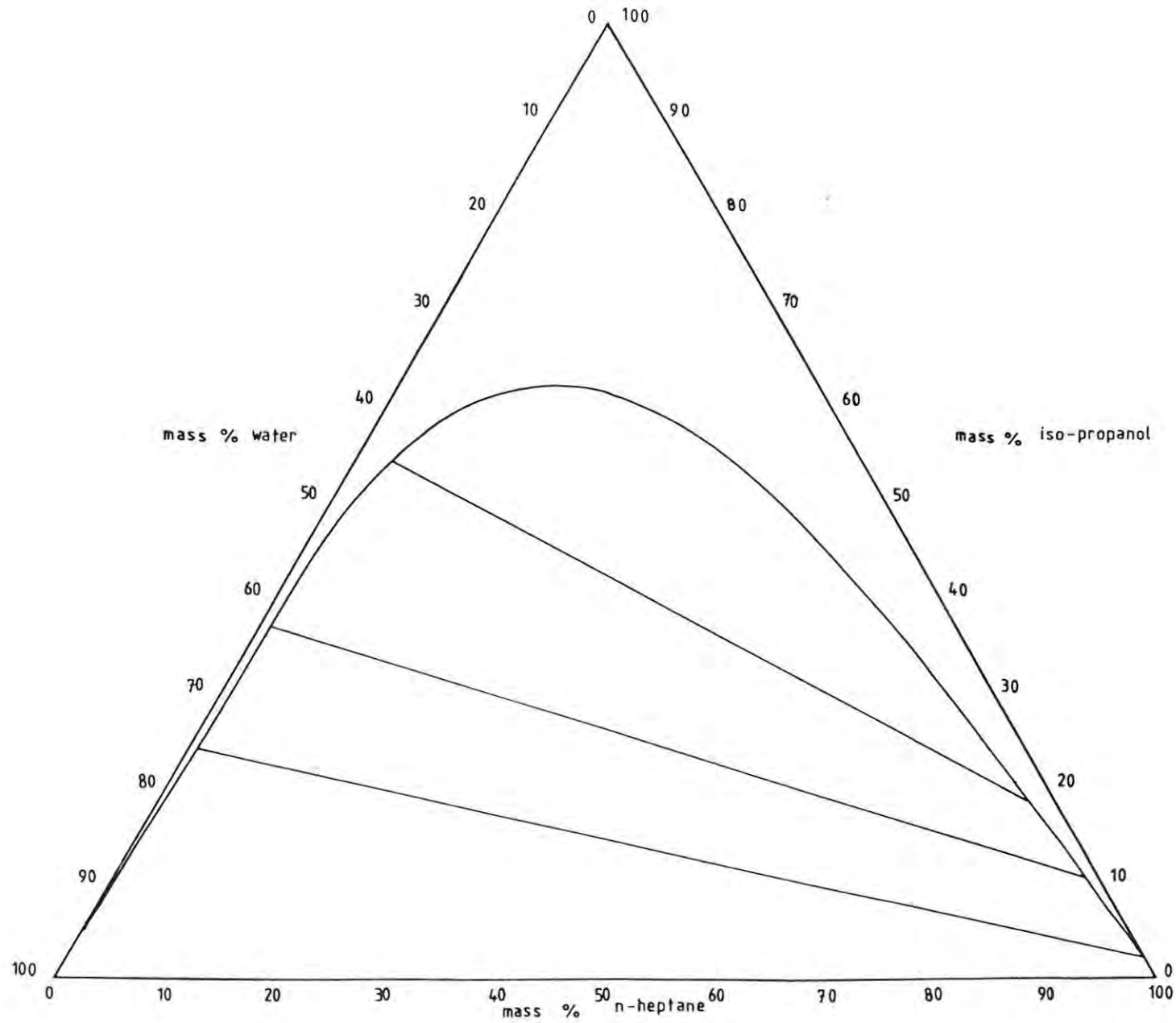


FIGURE 4.9 EXPERIMENTAL BINODAL CURVE FOR THE SYSTEM N-HEPTANE + ISO-PROPANOL + WATER AT 298,15 K

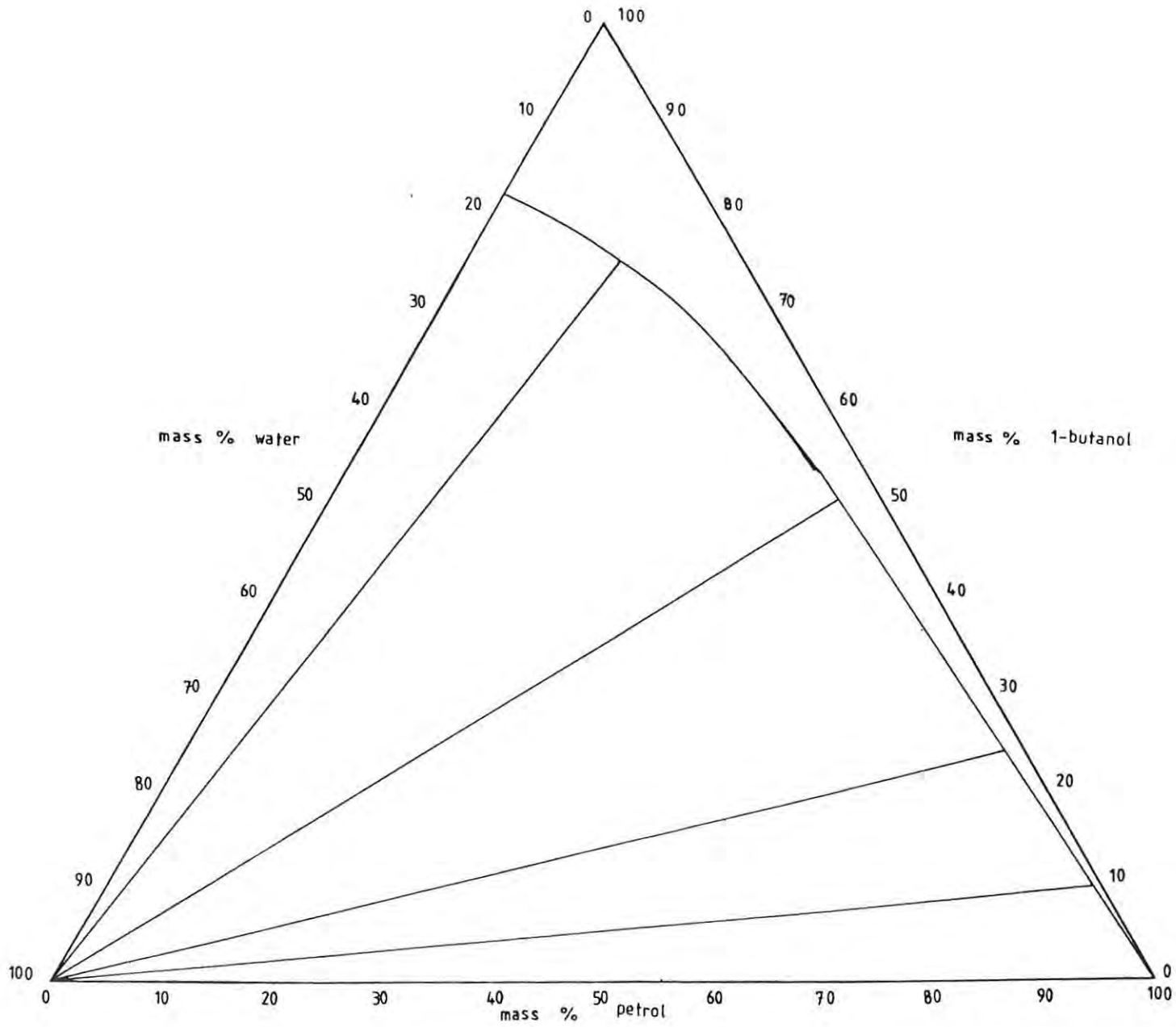


FIGURE 4.10 EXPERIMENTAL BINODAL CURVE FOR THE SYSTEM PETROL + 1-BUTANOL + WATER AT 298,15 K

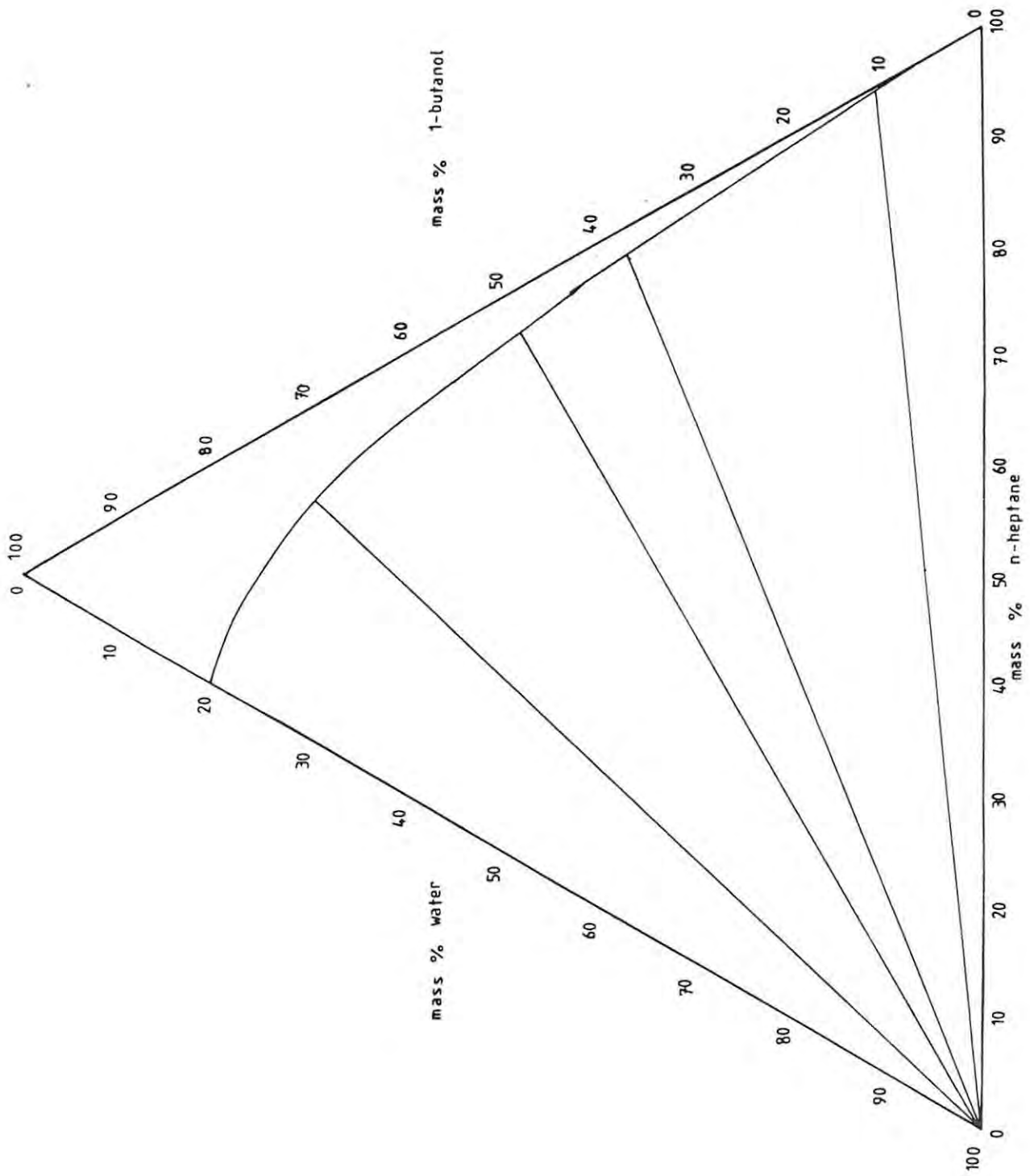


FIGURE 4.11 EXPERIMENTAL BINODAL CURVE FOR THE SYSTEM N-HEPTANE + 1-BUTANOL + WATER AT 298,15 K

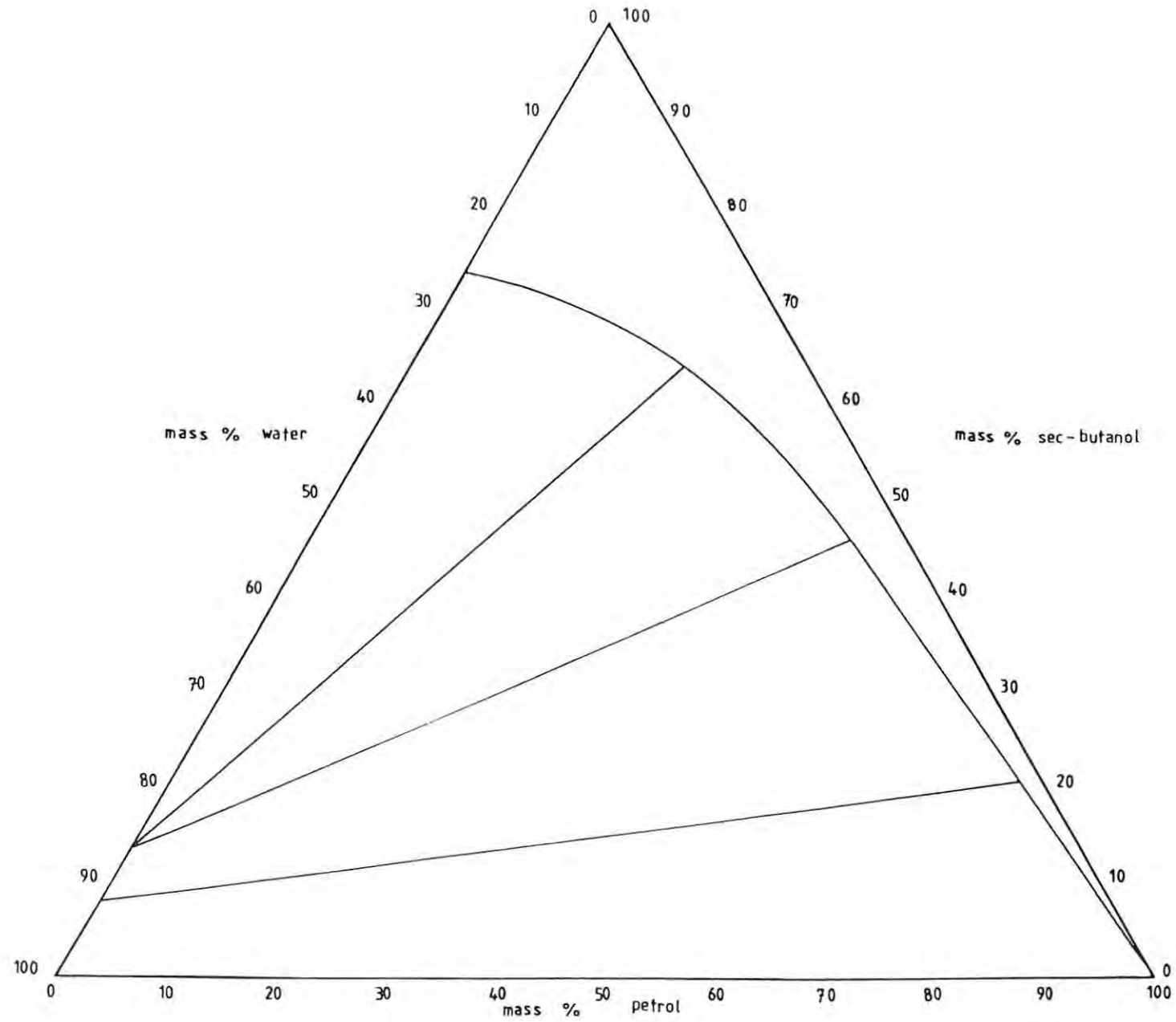


FIGURE 4.12 EXPERIMENTAL BINODAL CURVE FOR THE SYSTEM PETROL + SEC-BUTANOL + WATER AT 298,15 K

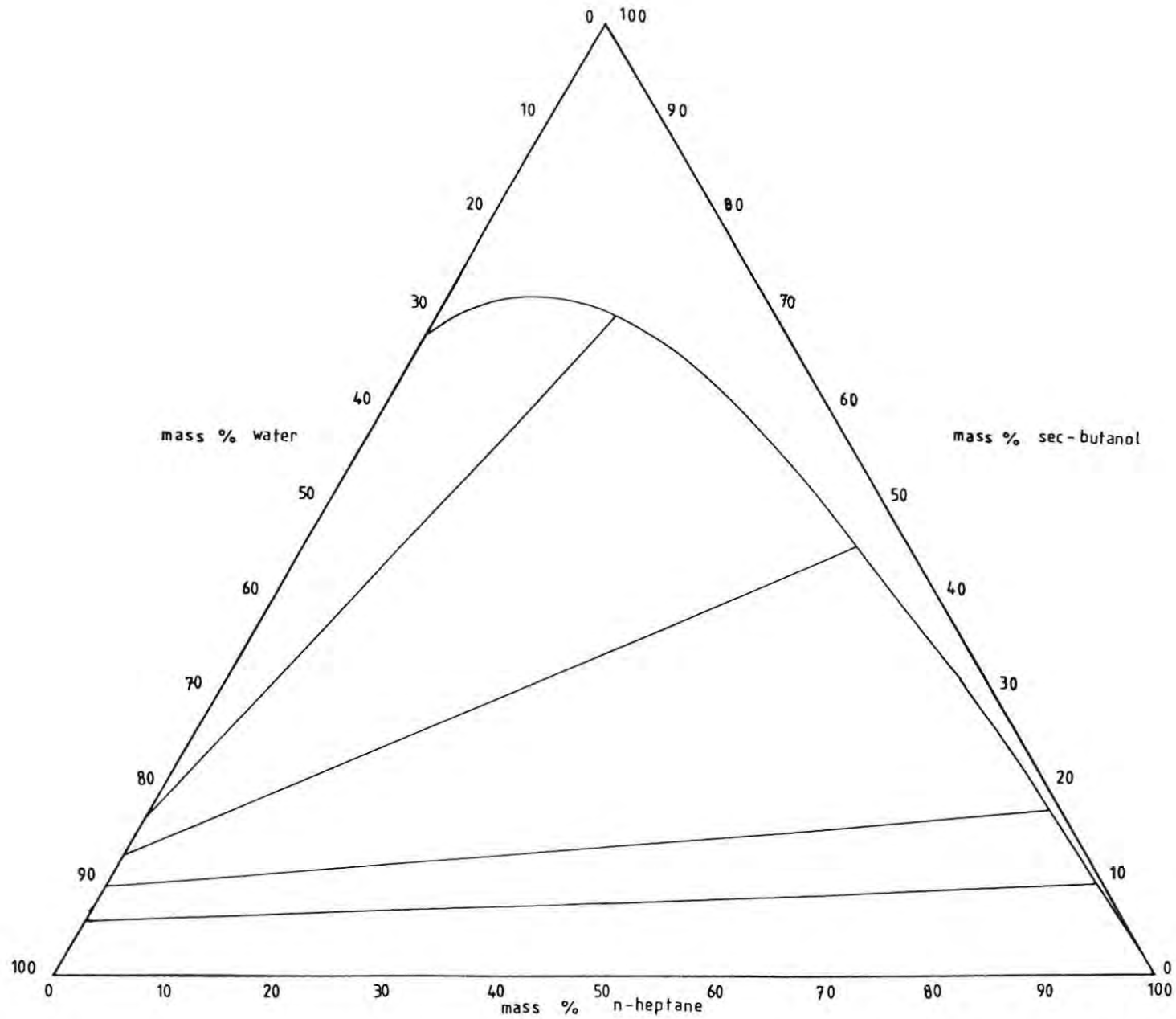


FIGURE 4.13 EXPERIMENTAL BINODAL CURVE FOR THE SYSTEM N-HEPTANE + SEC-BUTANOL + WATER AT 298,15 K

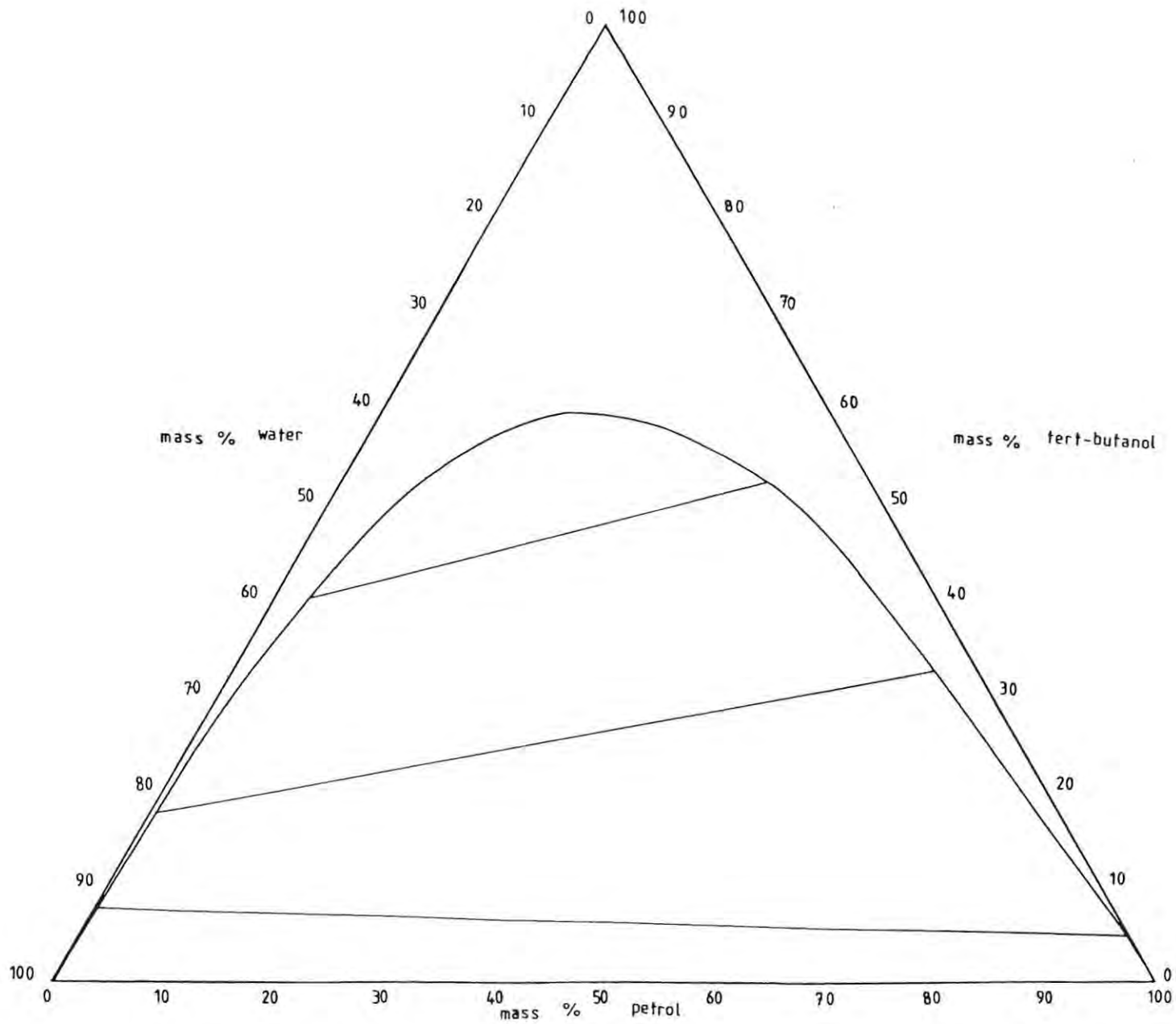


FIGURE 4.14 EXPERIMENTAL BINODAL CURVE FOR THE SYSTEM PETROL + TERT-BUTANOL + WATER AT 298,15 K

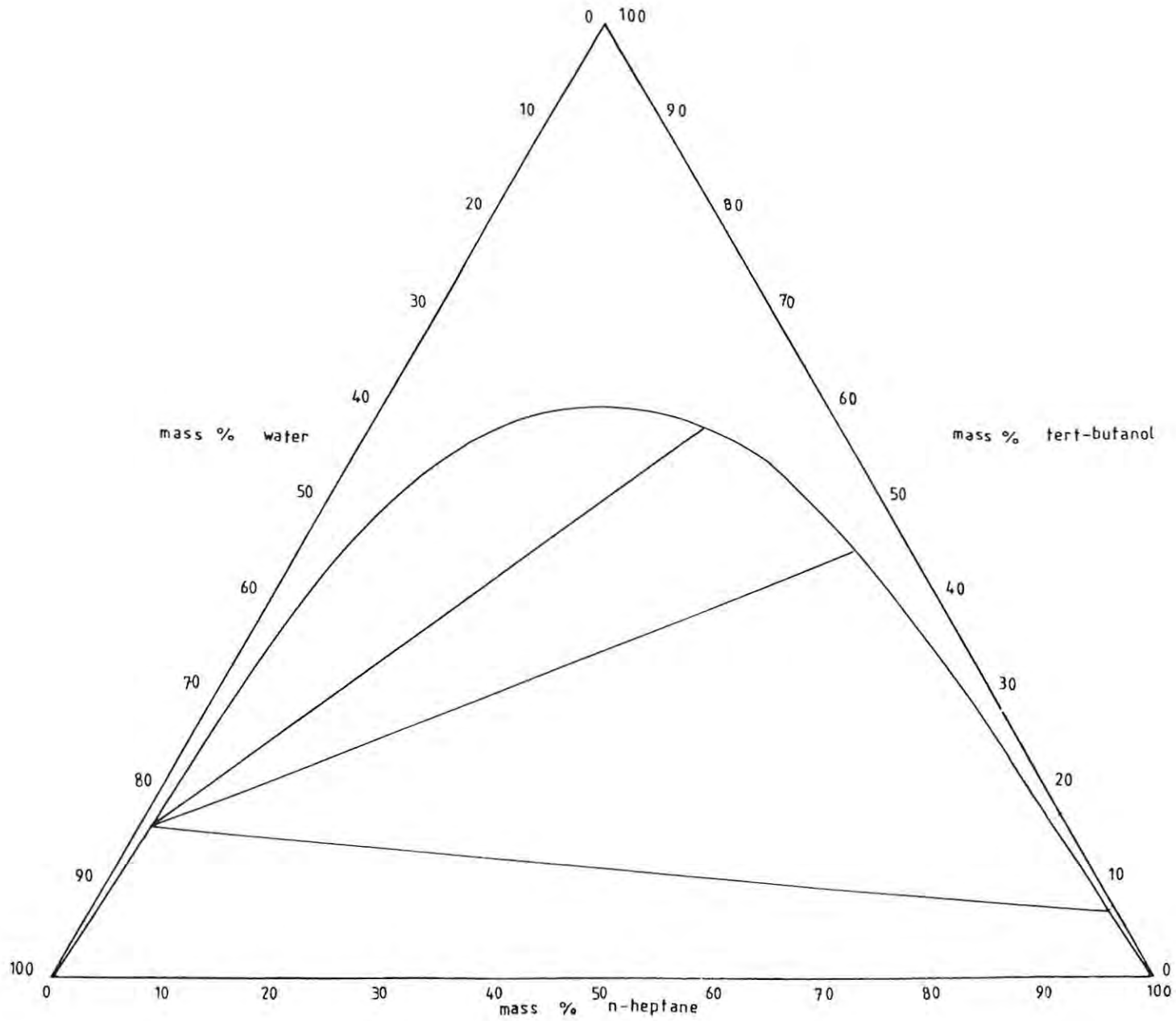


FIGURE 4.15 EXPERIMENTAL BINODAL CURVE FOR THE SYSTEM N-HEPTANE + TERT-BUTANOL + WATER AT 298,15 K

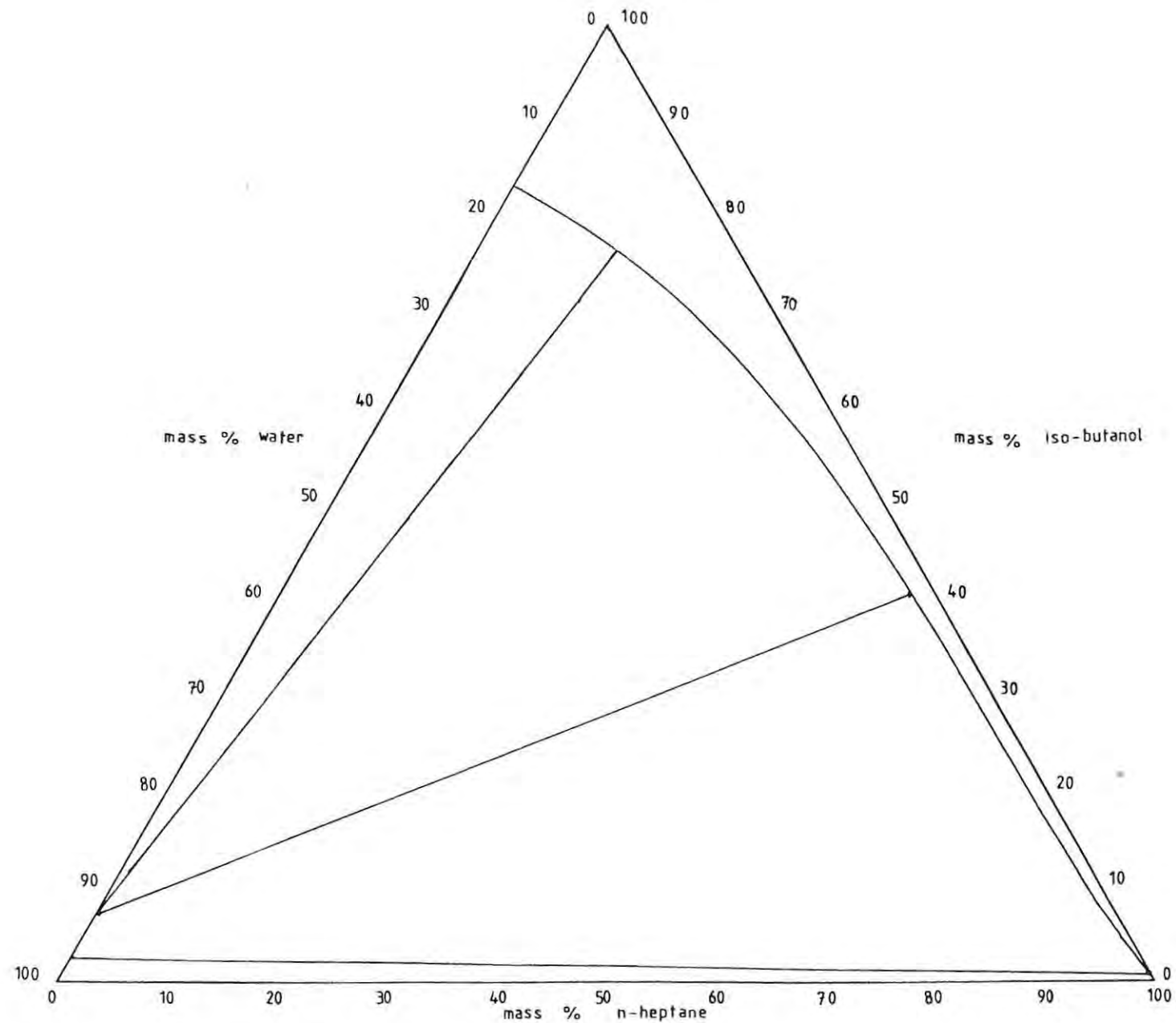


FIGURE 4.16 EXPERIMENTAL BINODAL CURVE FOR THE SYSTEM N-HEPTANE + ISO-BUTANOL + WATER AT 298,15 K



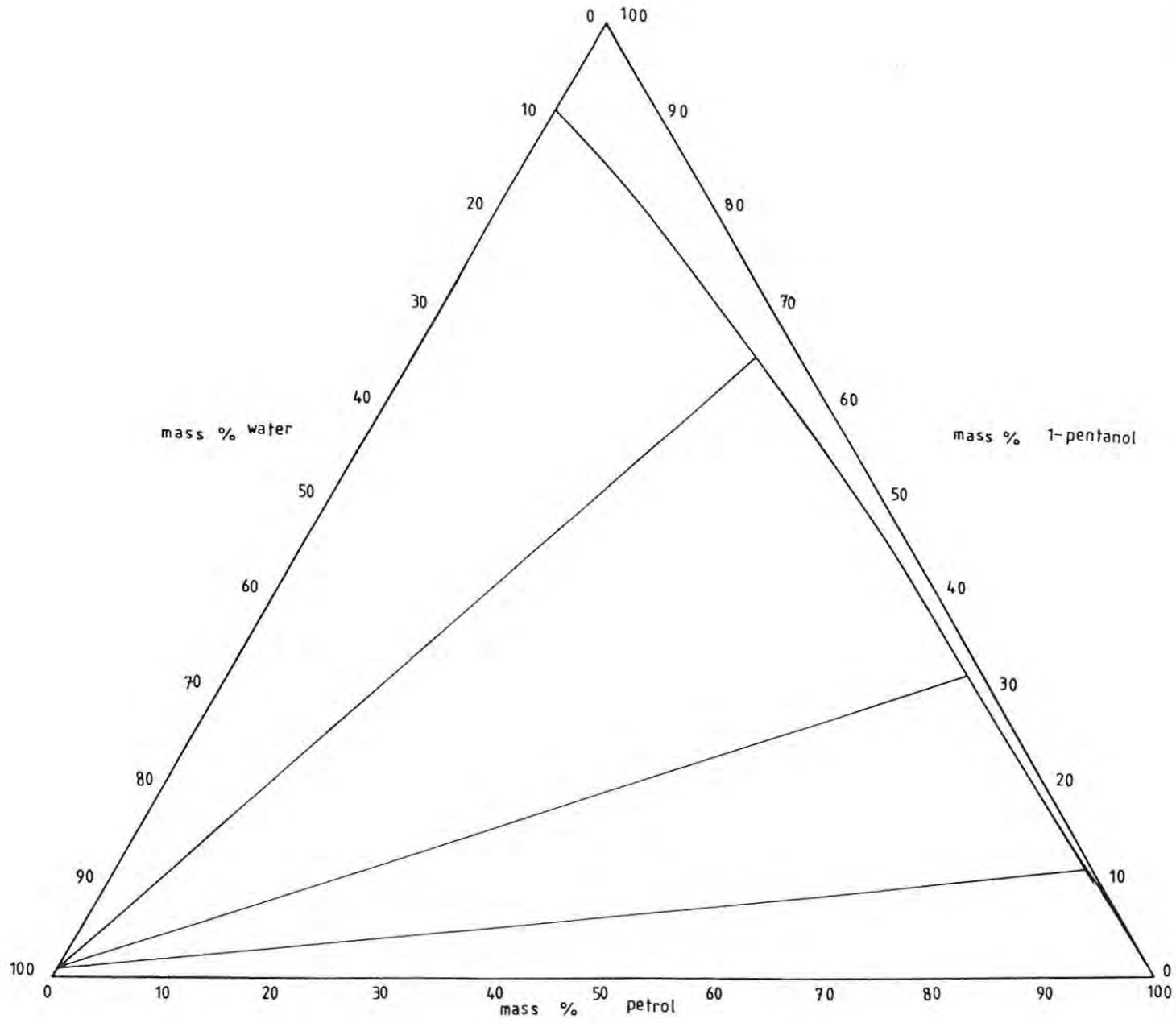


FIGURE 4.17 EXPERIMENTAL BINODAL CURVE FOR THE SYSTEM PETROL + 1-PENTANOL + WATER AT 298,15 K

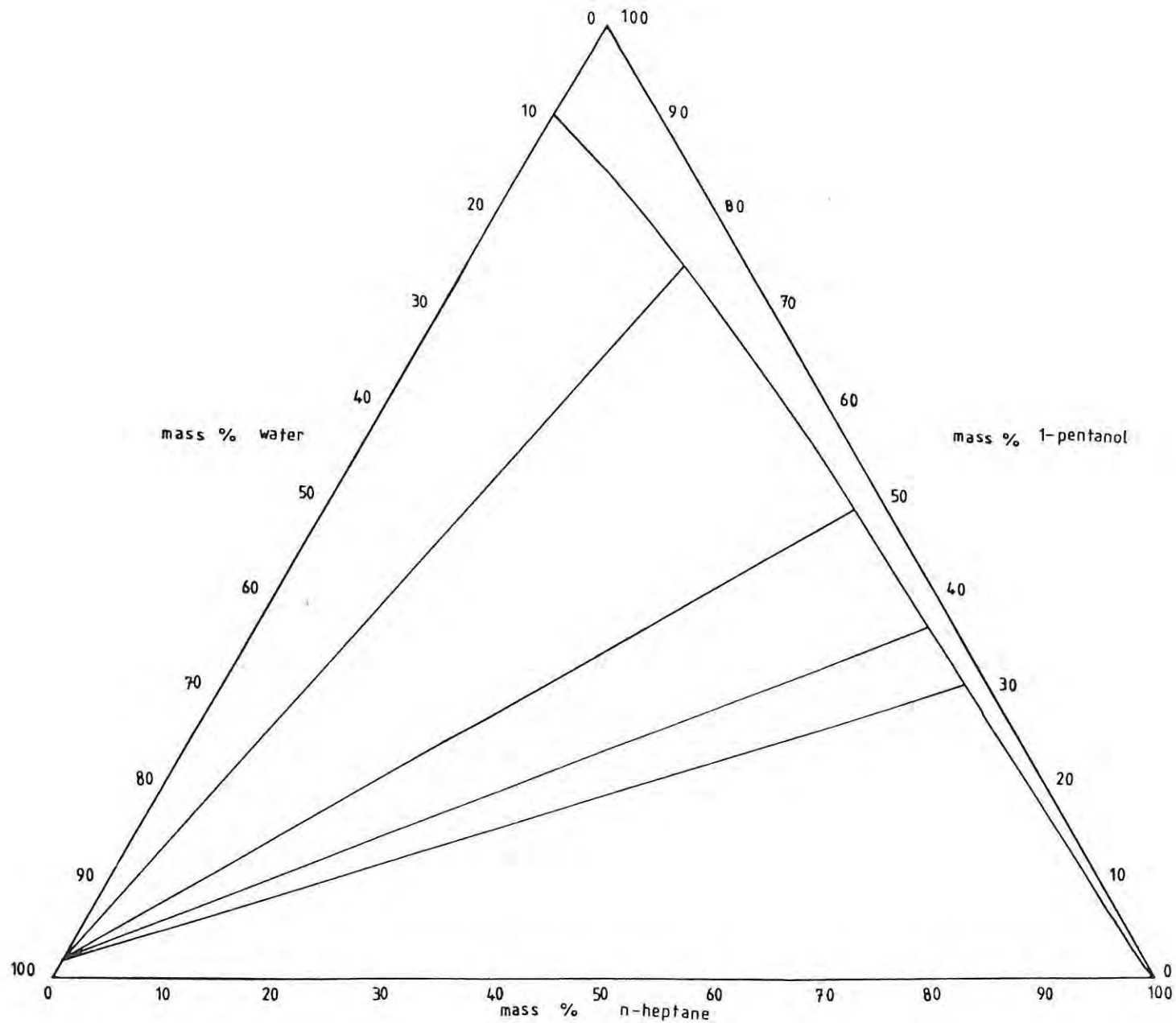


FIGURE 4.18 EXPERIMENTAL BINODAL CURVE FOR THE SYSTEM N-HEPTANE + 1-PENTANOL + WATER AT 298,15 K

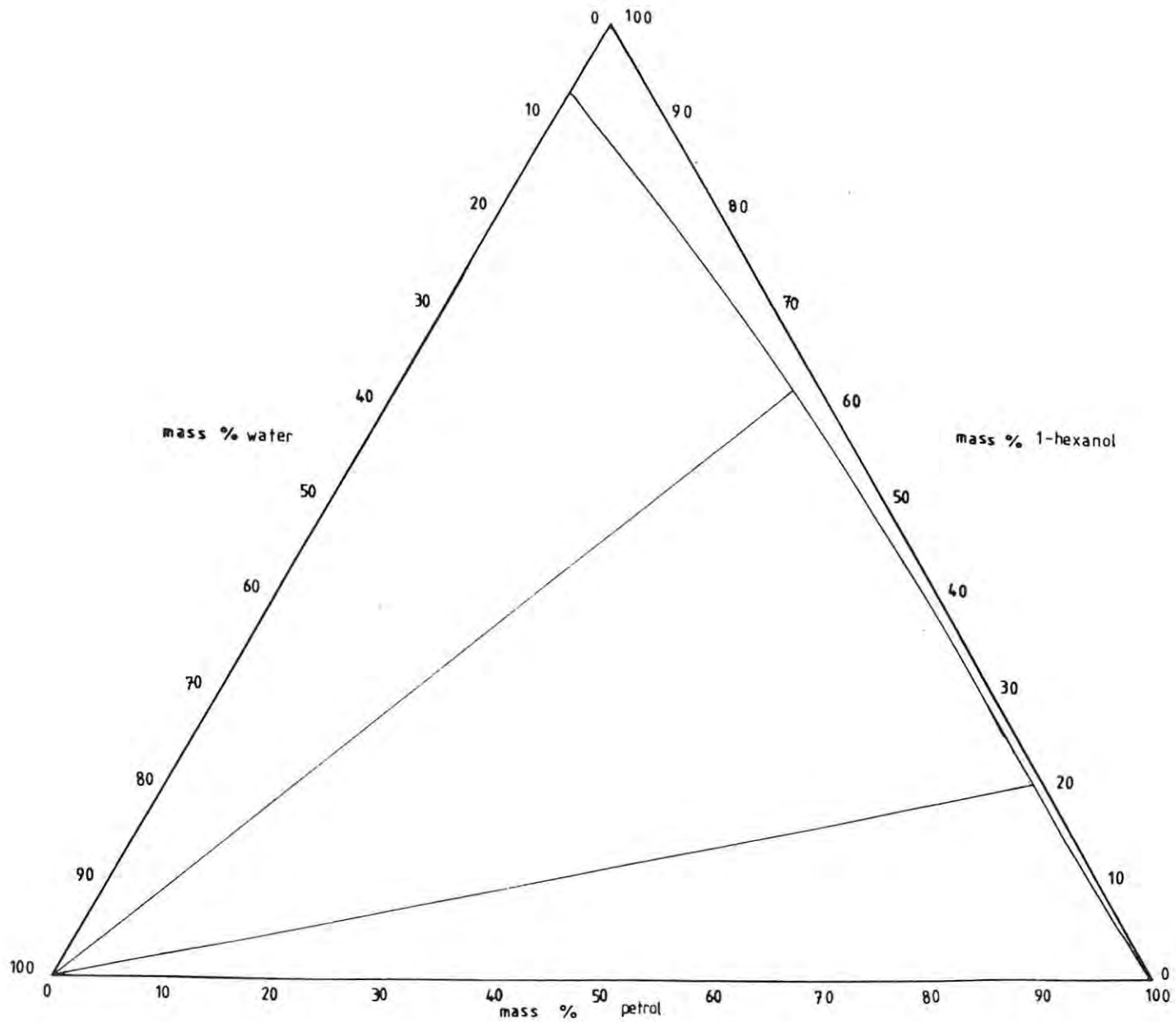


FIGURE 4.19 EXPERIMENTAL BINODAL CURVE FOR THE SYSTEM PETROL + 1-HEXANOL + WATER AT 298,15 K

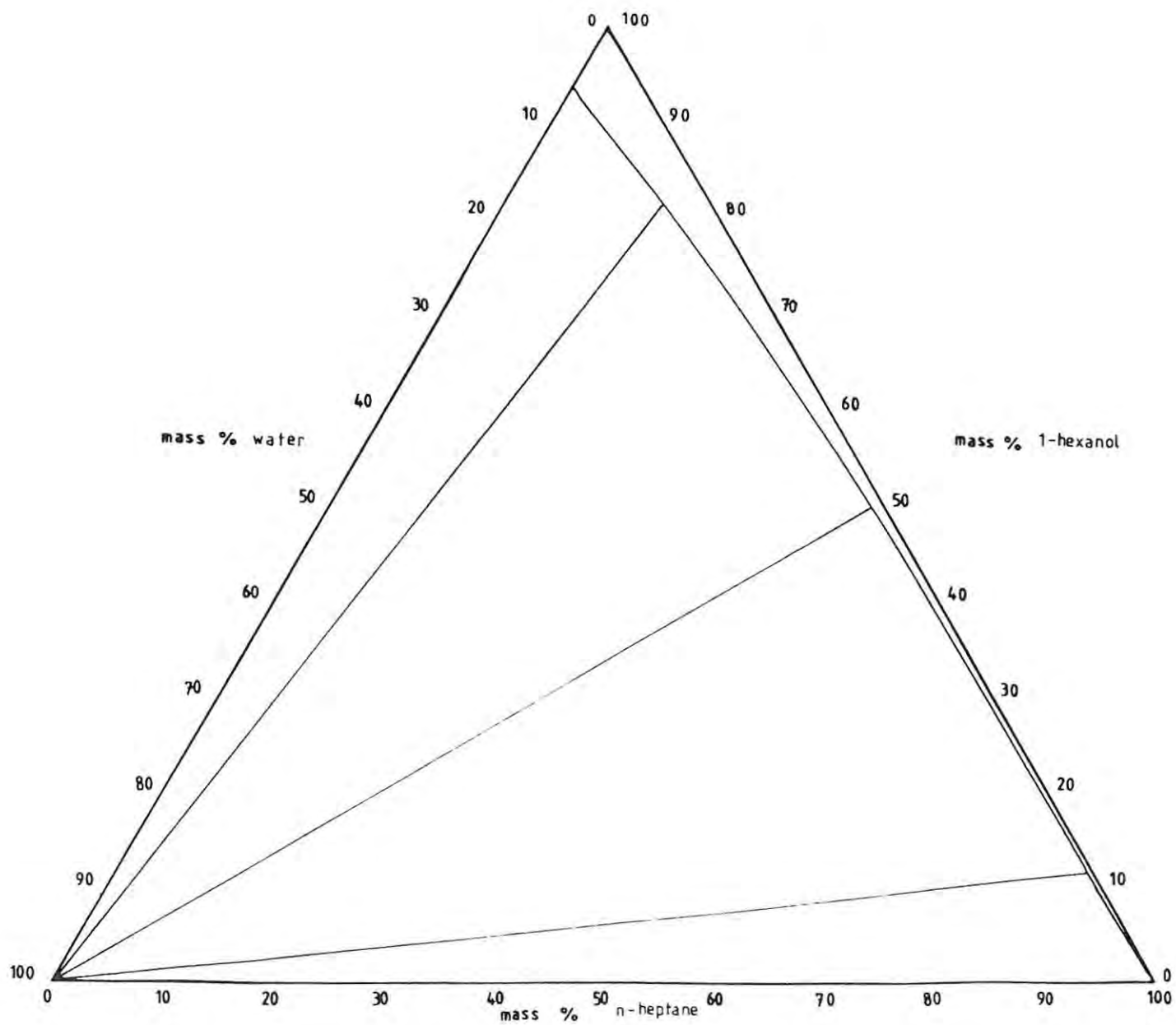


FIGURE 4.20 EXPERIMENTAL BINODAL CURVE FOR THE SYSTEM N-HEPTANE + 1-HEXANOL + WATER AT 298,18 K

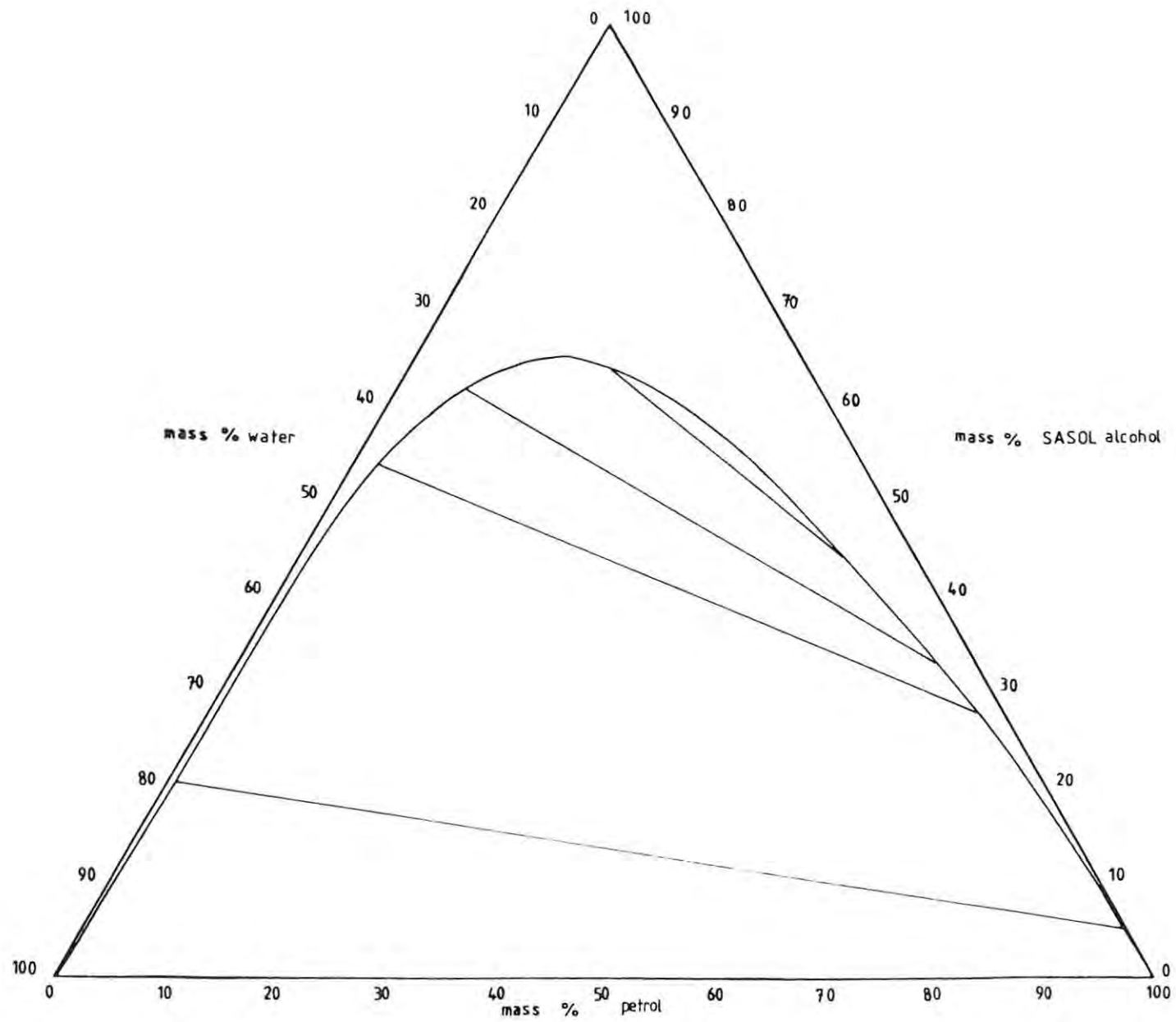


FIGURE 4.21 EXPERIMENTAL BINODAL CURVE FOR THE SYSTEM PETROL + SASOL ALCOHOL + WATER AT 298,15 K

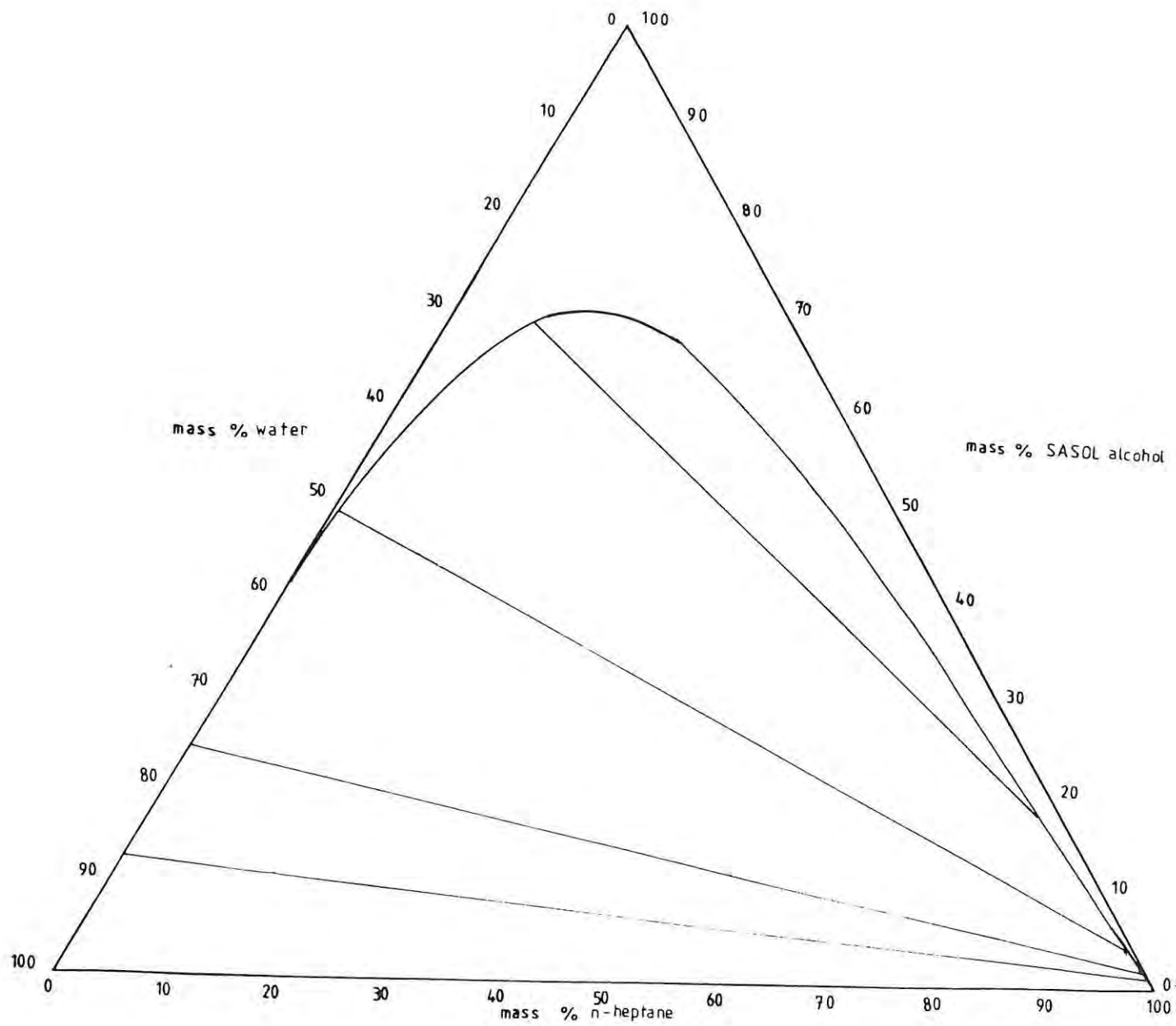
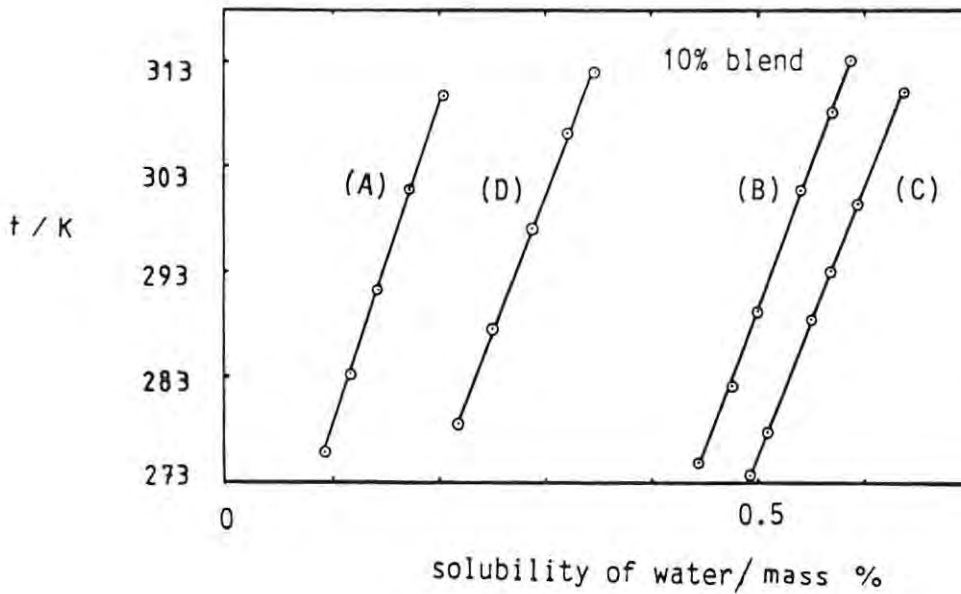
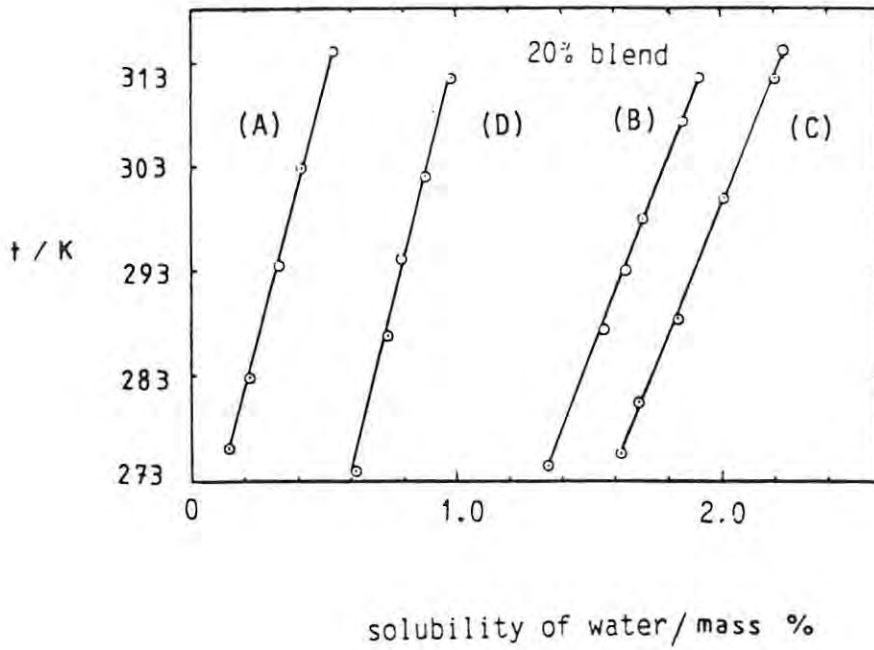


FIGURE 4.22 EXPERIMENTAL BINODAL CURVE FOR THE SYSTEM N-HEPTANE + SASOL ALCOHOL + WATER AT 298,15 K



FIGURES 4.23 AND 4.24 THE EFFECT OF TEMPERATURE ON THE SOLUBILITY OF WATER IN 10% AND 20% MIXTURES (BY MASS) OF ALCOHOL IN PETROL  
(A) METHANOL (B) ETHANOL  
(C) 1-PROPANOL (D) 1-BUTANOL

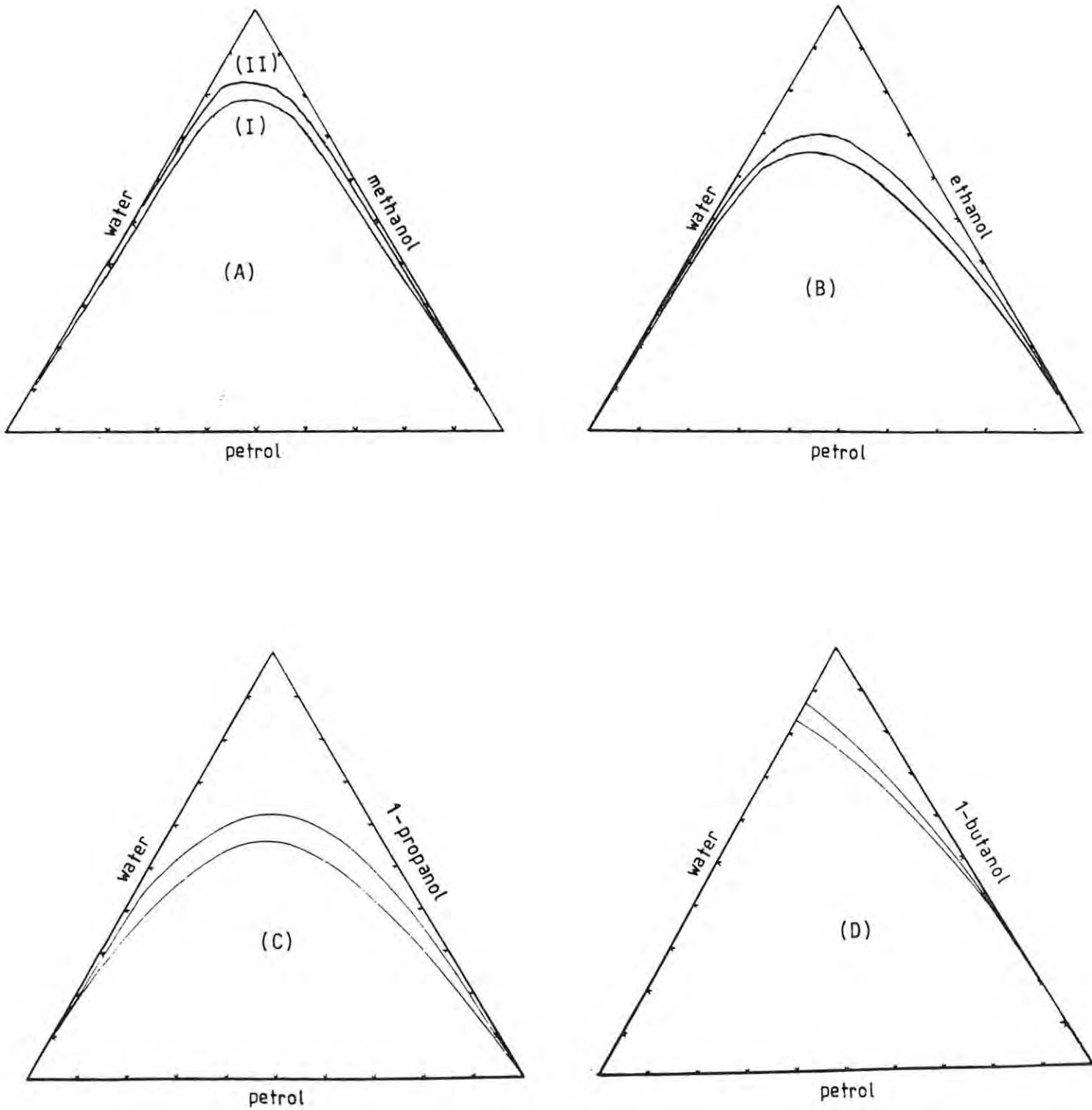


FIGURE 4.25 THE BINODAL CURVES FOR PETROL-ALCOHOL-WATER TERNARY SYSTEMS AT TWO TEMPERATURES 273,15 K (I) AND 313,15K (II)  
(A) METHANOL (B) ETHANOL  
(C) 1-PROPANOL (D) 1-BUTANOL



#### 4.4 DISCUSSION

The results reflected in tables 4.1 and 4.2 and figures 4.2 to 4.22 demonstrate that the miscibility of water in petrol-alcohol and n-heptane-alcohol blends is dependent on the type of alcohol. Water is more soluble, for example, in the iso-propanol blends than in the Sasol fuel alcohol blend or the ethanol blend for the same fraction of alcohol present.

Considering the n-heptane-alcohol-water results which serve as model systems for the petrol results, it is necessary to pay attention to the general trends in solvent classification. Although the solubility of water in solvents does not increase linearly with dielectric constant, there is a general trend in that direction <sup>(56)</sup> for example, heptane at 293,15 K has a dielectric constant  $\epsilon = 1,92$  and the solubility of water in mass percent is 0,015, whilst 1-butanol has an  $\epsilon$ -value of 17,1 at 298,15 K and the solubility of water is 20,5% by mass.

Dipole moment is another factor in solvent behaviour. It largely determines the orientation of a solvent around an organic solute molecule in the absence of specific solvent-solute interactions (which represents the case with the systems studied here). A solvent's dissolving power therefore depends on the effectiveness of electrostatic solvation. With ionic solutes, however, solvents of high dielectric constant facilitate dissolution by separating and solvating the ions. For the solubility of organic solutes the solvent dielectric constant is less of a critical factor. For this reason common solvents are classified according to their electrostatic factor,  $EF$  which is defined as the product of dielectric constant and the dipole moment .

Table 4.8 gives the relevant values for the systems studied <sup>(56)</sup>.

Table 4.8 ELECTROSTATIC FACTORS FOR PURE LIQUID COMPONENTS

Component	EF
n-Heptane	0,0
Water	144,44
Methanol	54,17
Ethanol	40,83
1-Propanol	33,37
iso-Butanol	31,69
iso-Propanol	30,75
1-Butanol	28,73
1-Pentanol	25,02
tert-Butanol	18,09

Table 4.9 represents the classification of solvents according to their electrostatic factor

Table 4.9 CLASSIFICATION TABLE

Class of Solvent	EF
Class I Hydrocarbon solvents	0-2
Class II Electron-donor solvents	2-20
Class III Hydroxylic solvents	15-50
Class IV Dipolar aprotic solvents	750

n-Heptane is a hydrocarbon solvent. Accordingly, electrostatic interactions between solute molecules and the solvent occur hardly at all, and this is represented by the weak dissolving abilities of the hydrocarbons. Water is classified as hydroxylic due to its structure. Class III solvents such as the alcohols prevent solvent association and allow for ready dissolution of organic solutes.

Another aspect of solubilisation is hydrogen bonding. Water and alcohols act as proton donors and acceptors whilst paraffins are non-hydrogen bonding. Pure alcohols or pure water are extensively associated via hydrogen bonding<sup>(57)</sup>. These two types of self-association are, however, quite different.

Infrared studies of alcohol-hydrocarbon systems have shown that n-heptane acts as an inert solvent for alcohols and that hydrogen bonding in alcohols leads to short lived aggregates <sup>(58)</sup>. In liquid water hydrogen bonded clusters or clathrates are being formed. The addition of water to alcohol will disrupt the structure arrangement of both components.

It has been suggested that alcohols can be divided into three classes regarding water solubility, <sup>(57)</sup> methanol to propanol being totally water soluble, butanol to heptanol moderately soluble, and the higher alcohols poorly soluble.

The tie lines for each of the systems studied are included in figures 4.2 - 4.22. The tie lines for the petrol-methanol and ethanol blends slope in the opposite direction to the tie lines for the petrol-1-propanol and 1-butanol blends. This suggests that methanol and ethanol are each more soluble in water than in petrol while 1-propanol and 1-butanol are each more soluble in petrol than in water.

The composition of the water-rich phase, for mixtures in the immiscible regions in the petrol-alcohol-water blends will be relatively richer in water the higher the carbon number of the alcohol. For 1-butanol, 1-pentanol and 1-hexanol this is indeed the case and the water-rich phase is almost pure water.

A study of figure 4.6 reveals that as the total amount of 1-propanol is increased in the system, the increase in solubility of the 1-propanol in the petrol-rich layer is greater than that in the water-rich layer. The slopes of the tie lines for this system change in sign as is the case with all the systems studied. Such systems are called solutropic <sup>(59)</sup>.

The phase splitting of petrol-water-1-propanol or 1-butanol or higher alcohol blends result in a phase which is very rich in water. This we believe has an important part to play in the corrosive nature of alcohol fuel blends. The higher the carbon number of the straight chained alcohol used in blending with petrol, the greater will be the water concentration in the water-rich layer which forms when phase splitting takes place.

It is suggested that phase separation takes place in the hot carburettor i.e. after the vehicle has been running as a result of evaporation of the more volatile alcohols.

The apparent change in behaviour for isomers of the n-alcohols is important and is emphasised by the ternary phase diagrams of butanol isomers. Isobutanol was unable to solubilise water in petrol blends whereas tertiary butanol resulted in a ternary phase diagram with the lines sloping in the same direction as those for 1-propanol. This is due to the fact that the tertiary butanol is soluble in petrol at all compositions. The electrostatic factor for tertiary butanol in Table 4.9 allows it to be classified as an electron donating solvent so that interactions with the positive end of a dipole as in water is possible which increases solvation and the solubility of the solute.

Table 4.5 shows that the composition of the water-rich layer for petrol blends containing 12 mass percent of alcohol is very dependent on the type of alcohol. For methanol and ethanol blends, the water content of the water-rich phase is low. However, for iso-propanol (63 mass %) 1-propanol (95 mass %) and higher alcohols the water content is high. For Sasol fuel alcohol the water content is also high (70 mass %), an expected figure, considering its composition.

Table 4.7 represents the results of conductivity measurements for some of the alcohol-water mixtures. Conductivity is very much dependent on the water content and rises sharply for mixtures containing over 80 mass percent of water. Mixtures which on phase separation result in high water concentration therefore have the potential to promote corrosion. In order to reduce the corrosive nature of alcohol blended petrol, alcohols higher than ethanol should not be used or their concentration should be reduced as much as possible.

Figures 4.23 and 4.24 show the effect of temperature on the water solubility of 10 and 20 mass percent methanol and ethanol petrol blends. There is a gradual increase in the water content for all systems between 273,15 K and 313,15 K. This is supported by the Figure 4.25.

## 5 DIESEL-ALCOHOL BLENDS

### 5.1 INTRODUCTION

Diesel engines are able to tolerate variations in fuel quality<sup>(60)</sup>. This is evident from the vast amount of literature advocating different replacement fuels. In the diesel engine there is no spark to aid combustion and the fuel-air mixture is first induced into the cylinder, then vaporised and brought to a high temperature by compression before it self-ignites. This ability to self-ignite at the temperatures caused by compression is the most important property of diesel engine fuel.

A common measure of the auto-ignition quality of a fuel is the cetane number. A low cetane number (long ignition delay) will result not only in late combustion, but also in high peak combustion pressures and in severe knock (which can affect engine durability).

The main drawback of the alcohols methanol and ethanol from a diesel fuel point of view is their low cetane number<sup>(61)</sup>. The cetane number of methanol is about 3, that of ethanol is 8, while that of commercial diesel is between 45 and 50.

The higher alcohols e.g. propanol are reasonably good diesel fuels but can not be produced economically in large enough quantities to be sold as a transport fuel. Only methanol or ethanol can be produced economically in such quantities. As a result this discussion will be restricted to these two alcohols.

A problem with methanol and ethanol is that they do not mix with diesel in all proportions at all temperatures. A co-solvent or bridging agent is necessary to ensure a stable single phase mixture of diesel and methanol or ethanol<sup>(62)</sup>.

In this work ethyl acetate was chosen although it is not the best bridging agent but it is readily available and cheap so could be used commercially. The effect on the ternary phase diagram of water as a likely commercial contaminant was also investigated.



The addition of ethanol and ethyl acetate to diesel has a deleterious effect on the cetane number so that octyl nitrate known to have a cetane value of 250<sup>(63)</sup> must be added. The effect of this on ordinary ternary phase behaviour was investigated as was the cetane number of the mixtures.

## 5.2 EXPERIMENTAL PROCEDURE

### 5.2.1 Materials

The diesel used was Shell diesel purchased in Grahamstown in the summer months of 1983-1984 and 1984-1985. The alcohols and ethyl acetate sources are given in table 3.2. The octyl nitrate used was Ethyl Corporations DII3 (Diesel Ignition Improver 3) which is primarily 3-methyl-heptyl-nitrate. AECI supplied two samples of cetane improvers which were also studied.

### 5.2.2 Method

The ternary phase diagrams were determined in a manner discussed in Section 4.2. The effect of the addition of 1 and 4 mass percent octyl nitrate to the diesel was interpreted on ternary axes. The effect of small amounts of water on the phase diagrams was also studied.

The cetane numbers presented in this work were established by the Chemical and Analytical services of SASOL 1 (Pty) Limited on their C.F.R. engine. The precision and reproducibility is within 2 cetane numbers in 45. The blends were made up by volume and are correct to within 2 percent.

## 5.3 RESULTS

The phase diagram results at 298,15 K are given in table 5.1 and graphed in figures 5.1 - 5.2. Table 5.2 and figure 5.3 demonstrate the effect on cetane numbers of adding ethanol and ethyl acetate to diesel. Cetane numbers of these blends plus 1 to 4 volume percent octyl nitrate are given in table 5.3.4 and graphed in figure 5.4. The degree of cetane enhancement per one percent of octyl nitrate is plotted against percent diesel composition in figure 5.5. The results for the AECI cetane improvers are given in table 5.4 and figure 5.6.

Tables 5.1 EXPERIMENTAL DATA FOR THE BINODAL CURVES OF DIESEL-ALCOHOL-ETHYL ACETATE TERNARY SYSTEM AT 298,15 K  
The concentrations of diesel ( $C_d$ ), and ethyl acetate ( $C_{ea}$ ) are given in mass percent. The alcohol concentration is determined from  $100 - (C_d + C_{ea})$

---

System: Diesel + Methanol + Ethyl Acetate

---

$C_d$	$C_{ea}$
0,0	99,01
0,15	0,55
0,43	17,12
0,45	24,99
9,50	36,10
13,42	44,61
17,86	47,16
37,29	39,95
59,82	27,18
84,34	11,67

---

System: Diesel + (Methanol + 1% Water) + Ethyl Acetate

---

$C_d$	$C_{ea}$
0,46	13,03
4,58	30,75
14,82	46,09
20,43	48,24
38,50	40,40
60,81	27,47
89,08	8,34

---

System: Diesel + (Methanol + 5% Water) + Ethyl  
Acetate

---

$C_d$	$C_{ea}$
0,84	11,33
3,97	31,71
9,27	47,62
22,08	52,26
39,60	42,63
64,37	28,82
89,10	10,09

---

System: Diesel + Ethanol + Ethyl Acetate

---

$C_d$	$C_{ea}$
21,88	0,0
29,92	3,89
40,13	6,35
58,76	5,01
80,71	0,0

---

System: Diesel + (Ethanol + 5% Water) + Ethyl  
Acetate

---

$C_d$	$C_{ea}$
5,10	0,0
6,45	4,27
14,00	31,57
29,06	30,64
44,20	27,86
64,30	21,24
99,30	0,0



---

System: (Diesel + 4% Octyl Nitrate) + Ethanol  
+ Ethyl Acetate

---

$C_d$	$C_{ea}$
24,39	0,0
40,50	4,19
59,81	2,60
71,07	0,0

---

System: (Diesel + 4% Octyl Nitrate) + (Ethanol  
+ 5% Water) + Ethyl Acetate

---

$C_d$	$C_{ea}$
2,07	0,0
9,44	15,99
23,98	29,59
27,66	29,51
43,07	26,31
59,33	20,99
75,36	16,47
97,85	0,0

Table 5.2 CETANE NUMBERS FOR DIESEL + ETHANOL + ETHYL ACETATE BLENDS. THE CONCENTRATIONS (C) REFER TO VOLUME/VOLUME PER CENT (The ratio of ethanol to ethyl acetate is between 2 and 1,5)

---

$C$ (diesel) Volume %	$C$ (ethanol) Volume %	$C$ (ethyl acetate) Volume %	cetane number
100	0	0	49,2
89	7	4	44,0
85	10	5	42,0
80	12	8	40,5
75	17	8	38,0
60	25	15	34

---

Table 5.3 CETANE NUMBERS FOR DIESEL + ETHANOL + ETHYL ACETATE + OCTYL NITRATE BLENDS

C(diesel) Volume %	C(ethanol) Volume %	C(ethyl acetate) Volume %	C(octyl nitrate) Volume %	cetane number
61,0	25,0	12,5	1,5	39,0
59,0	24,0	14,0	3,0	44,6
59,0	23,0	14,0	4,0	48,5
58,0	22,0	15,0	5,0	53,5
66,0	20,0	13,0	0,95	40,5
67,0	21,5	10,0	1,5	45,0
57,0	21,0	10,0	2,05	47,7
66,0	23,5	7,5	3,0	53,0
71,0	18,0	11,5	0,5	42,5
71,0	18,0	10,0	1,0	46,0
72,0	17,5	9,0	1,5	50,5
80,0	15,0	5,0	0,0	40,0
80,0	14,5	5,0	0,5	46,0
80,0	14,0	4,0	1,0	52,5

Table 5.4 CETANE NUMBERS FOR BLENDS CONTAINING OCTYL NITRATE (ON) OR AECI SAMPLES 1 AND 2

$c$ (diesel) Volume %	$c$ (ethanol) Volume %	$c$ (ethyl acetate) Volume %	$c$ (ON) Volume %	$c$ (sample 1) Volume %	$c$ (sample 2) Volume %	cetane number
61,0	25,0	13,0	1,0	0,0	0,0	37,0
61,0	25,0	13,0	0,0	1,0	0,0	38,2
61,0	25,0	13,0	0,0	0,0	1,0	38,9
60,0	23,0	15,0	2,0	0,0	0,0	40,8
60,0	23,0	15,0	0,0	2,0	0,0	41,8
60,0	23,0	15,0	0,0	0,0	2,0	45,0
80,0	15,0	5,0	0,0	0,0	0,0	40,0
80,0	14,5	5,0	0,5	0,0	0,0	46,0
80,0	14,5	5,0	0,0	0,5	0,0	47,5
80,0	14,5	5,0	0,0	0,0	0,5	49,5
80,0	12,0	7,0	1,0	0,0	0,0	52,5
80,0	12,0	7,0	0,0	1,0	0,0	54,6
80,0	12,0	7,0	0,0	0,0	1,0	59,5

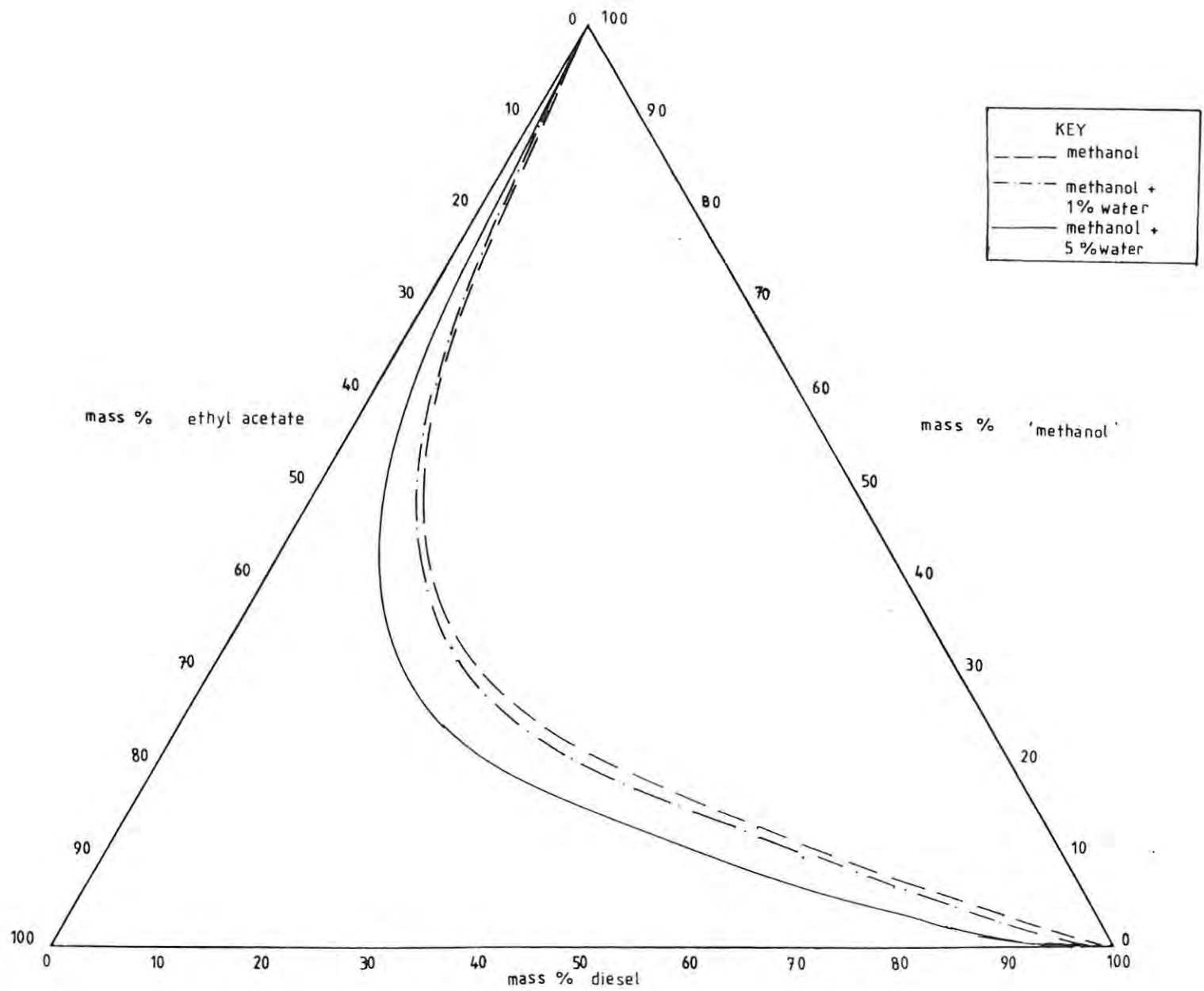


FIGURE 5.1 BINODAL CURVES FOR DIESEL-METHANOL-ETHYL ACETATE SYSTEMS

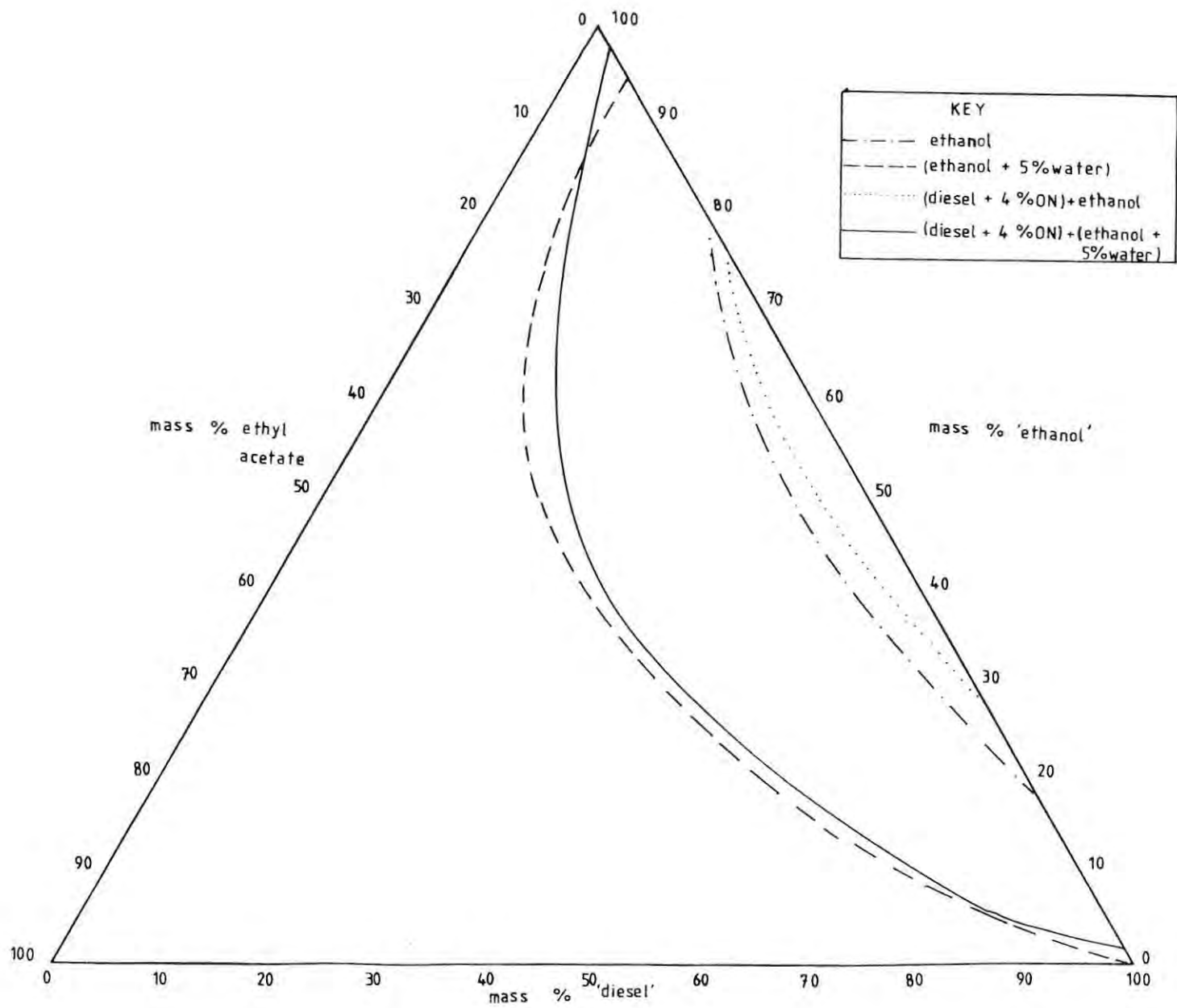


FIGURE 5.2 BINODAL CURVES FOR DIESEL-ETHANOL-ETHYL ACETATE SYSTEMS

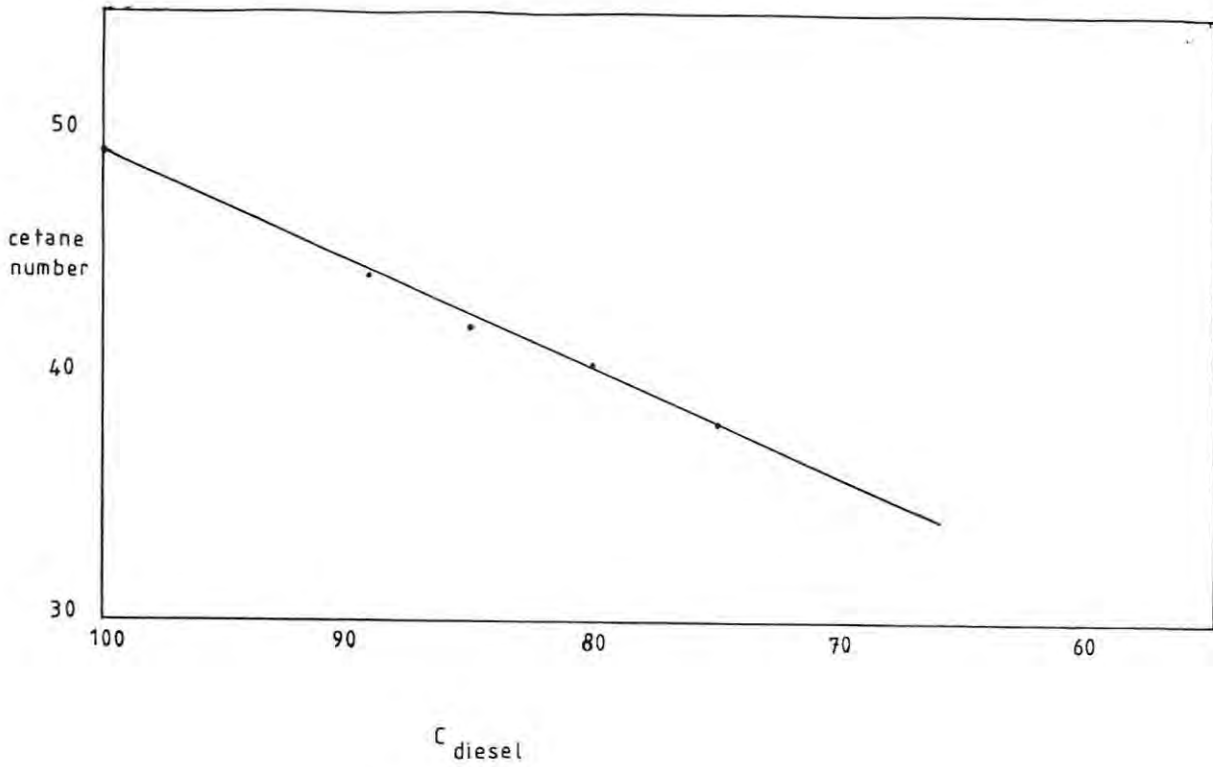


FIGURE 5.3 CETANE NUMBER PLOTTED AGAINST DIESEL CONCENTRATION

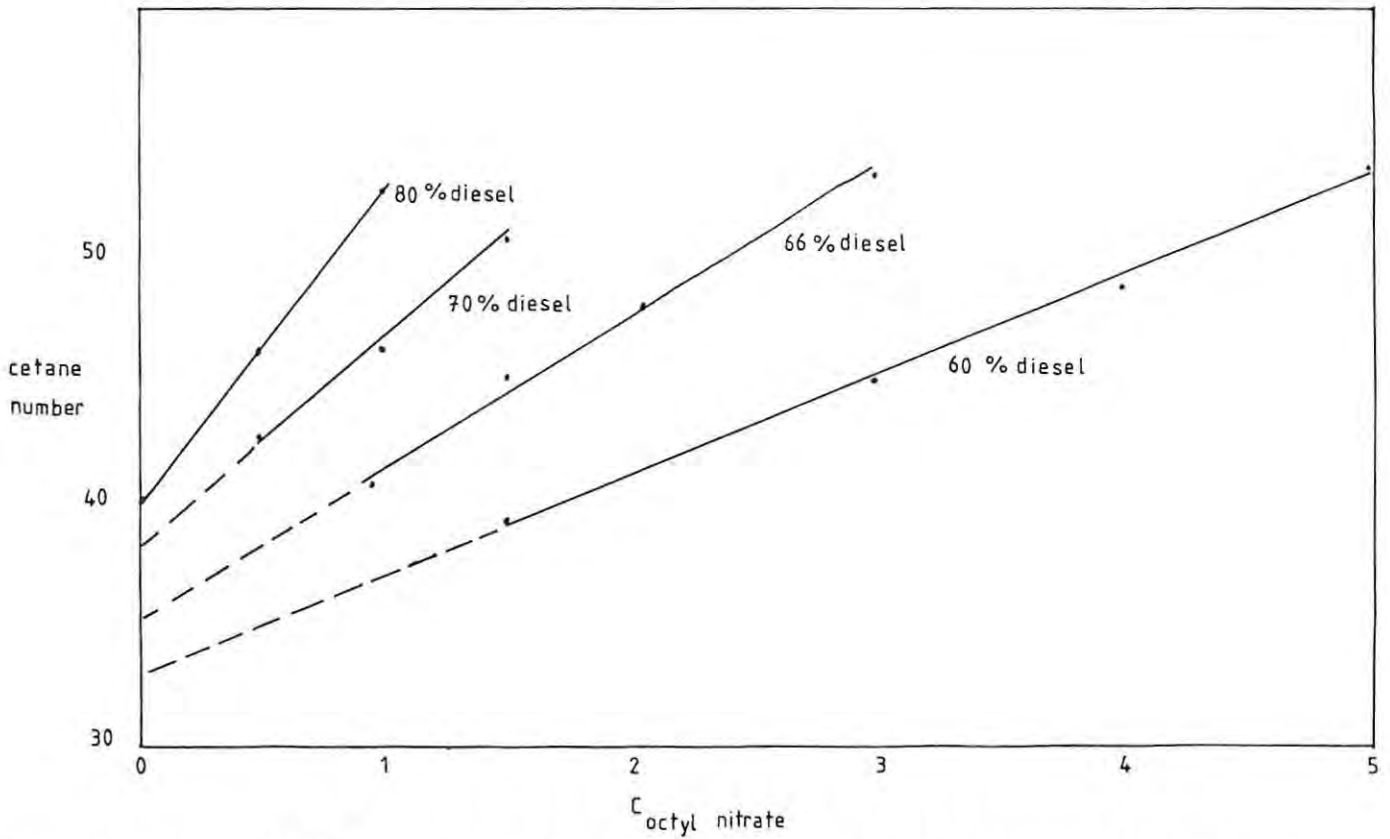


FIGURE 5.4 CETANE NUMBER AS A FUNCTION OF OCTYL NITRATE CONCENTRATION FOR DIFFERENT CONCENTRATIONS OF DIESEL

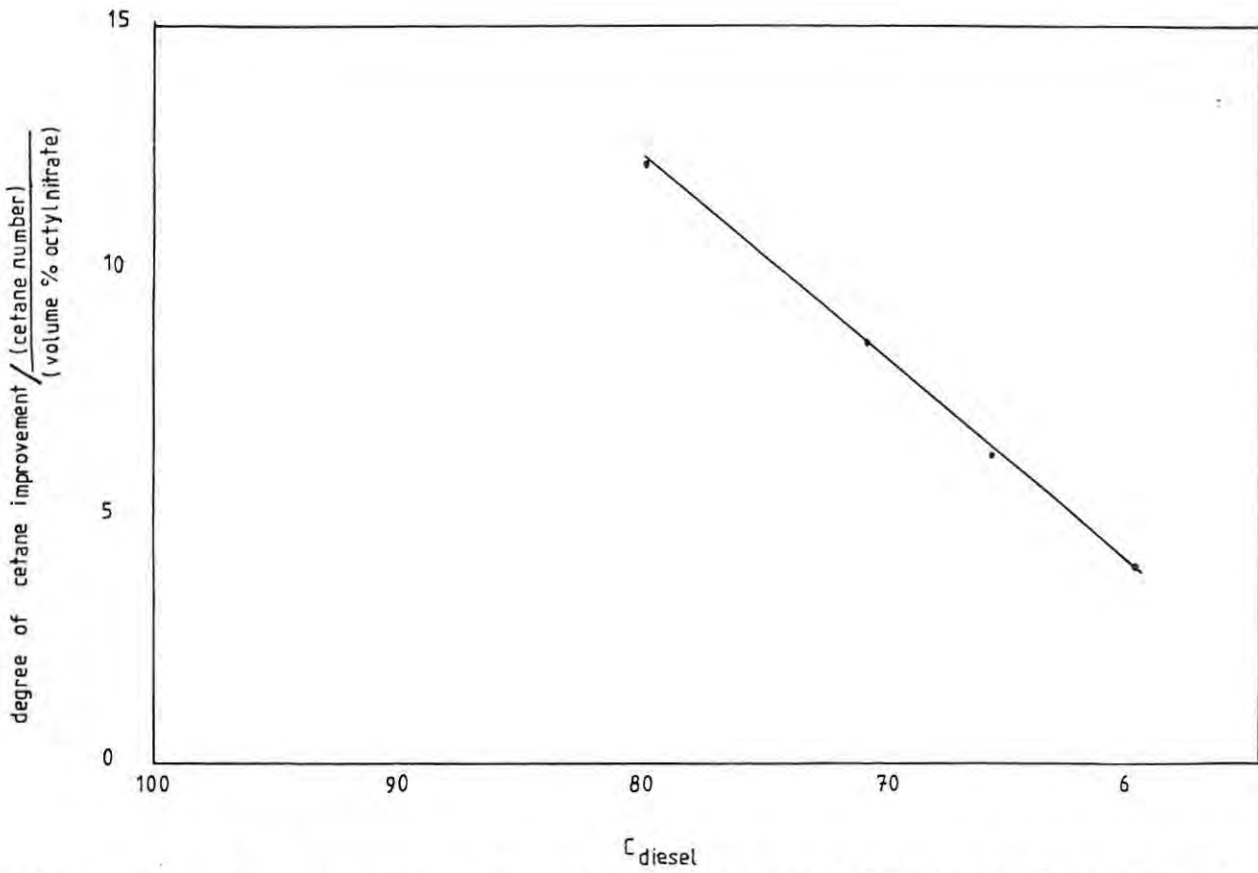


FIGURE 5.5 THE DEGREE OF CETANE IMPROVEMENT PER PERCENT OF OCTYL NITRATE PLOTTED AGAINST THE DIESEL CONCENTRATION

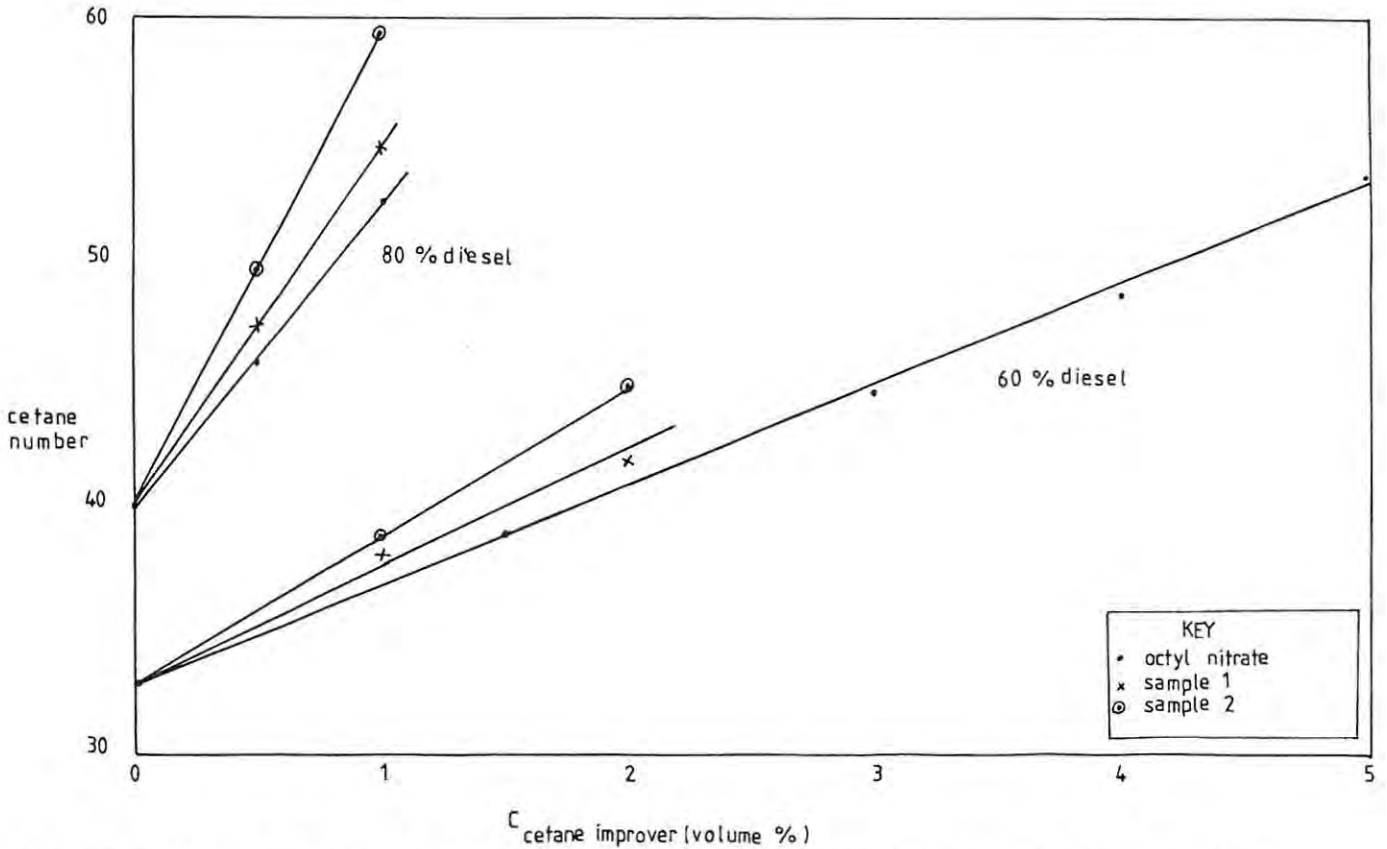


FIGURE 5.6 THE CETANE NUMBER PLOTTED AGAINST CETANE IMPROVER CONCENTRATION FOR 60% AND 80% DIESEL CONCENTRATION

#### 5.4 DISCUSSION

It is important first to consider the properties of ethyl acetate (ethyl ethanoate). It is an important industrial solvent and is able to dissolve in both polar and non-polar organic liquids. The relevant electrostatic factor is 10,90<sup>(56)</sup> indicative of its electron-donating ability. The solubility of water in ethyl acetate at 298,15 K is 3,19 mass percent<sup>(56)</sup>. Therefore it would be expected that the inclusion of 5 percent water in a blend would necessitate a relatively large increase in the concentration of ethyl acetate to prevent phase separations.

It is evident from figure 5.1 that methanol and diesel are unable to mix in any reasonable proportions. To achieve miscibility a high percentage of ethyl acetate is added. The inclusion of water in the system increases the immiscibility and more ethyl acetate must be added to bring about a homogeneous mixture. These miscibility characteristics indicate that methanol is not a suitable blending fuel for diesel.

Of the two alcohols studied, ethanol is the more appropriate blending fuel. It is more soluble in diesel and to achieve miscibility in all proportions at 298,15 K, 5 volume percent ethyl acetate is required. The addition of 5 volume percent water increases this need dramatically to 30 percent.

The effect of the ignition improver octyl nitrate on the phase diagram (refer to table 5.1 and figure 5.2) is insignificant. It would appear that octyl nitrate has some solubilising ability as slightly less ethyl acetate is required to ensure miscibility. This effect is not evident for the mixtures containing water.

An important observation was made for the ternary blends of diesel-ethanol-ethyl acetate at low diesel composition and low temperatures. A white, waxy solid precipitated. This was assumed to be the higher molecular mass hydrocarbons separating out from solution as a result of the presence of alcohol. This precipitate is difficult to dissolve but would not cause any deleterious effect on a fuel blend at temperatures generally experienced in South Africa as it could be filtered out and will dissolve and melt at temperatures greater than 278,15 K.



Ethanol and ethyl acetate seem to behave similarly in reducing the cetane number of a blend.

Table 5.3 and figure 5.4 illustrate the effectiveness of octyl nitrate as a booster of the cetane number. The effectiveness was shown to be strongly dependent on the percentage of substituted fuel in the blend.

Table 5.4 and figure 5.5 compare the cetane improvement achieved by octyl nitrate to that of AECI's two samples. The results show that sample 2 is possibly a better cetane improver than sample 1 which in turn is a better cetane improver than octyl nitrate.

Cetane numbers for commercial diesel fuels vary between 40 and 60. A high cetane number indicates a low propensity for diesel engine knock <sup>(60)</sup>. Alcohols have low cetane numbers and one reason for this is their high heats of vaporisation which lowers mixture temperatures and increases ignition delays. Cetane improvers, usually organic nitrates, are added to diesel-alcohol blends to increase cetane number. These compounds are able to auto-ignite very easily at low temperatures and therefore provide an ignition source for the alcohols <sup>(60)</sup>.

## 6 CONCLUSION

Prediction of liquid-liquid equilibria of ternary mixtures based on the constituent binaries is a rigorous test of an activity coefficient equation. The modified UNIQUAC model was used and found to approximate the experimental phase behaviour of the selected system. n-Heptane-1-propanol-water represents a Group 1 system and serves as a model system for petrol-alcohol-water phase behaviour investigations.

Excess enthalpies and excess volumes of petrol/n-heptane-alcohol binary systems were studied in order to obtain an idea of the heating and volume effects that take place on mixing. The results showed that negligible heat and volume changes occurred.

Water contamination of alcohols presents a significant problem when blended with petrol as fuel extenders. Phase separation must be prevented and for this reason water solubility in various petrol-alcohol blends was studied. Ternary phase diagrams and tie lines were determined for a number of petrol-alcohol-water systems.

The results show that the solubility of water in the petrol-alcohol blends and the concentration of water in the water-rich phase which forms on phase separation is strongly dependent on the type of alcohol. Sasol fuel alcohol allowed a 70 mass percent water composition on phase separation in a 88 mass percent petrol blend which could be linked to the corrosion problems experienced by motorists on the Witwatersrand.

Diesel-alcohol blends were included in this research. Methanol and ethanol were compared as possible diesel fuel extenders using ethyl acetate as a co-solvent. The ternary phase diagrams were determined and the effect of small additions of water to the alcohol on the miscibility studied. Cetane numbers of diesel-ethanol-ethyl acetate blends with and without cetane improvers were determined. The cetane improvers assessed were found to be effective.

## 7 FUTURE STUDIES

The alkane-alcohol-water systems can be further investigated in order to determine the nature of alcohol-water interactions. Backlund et al<sup>(64)</sup> have studied similar systems as possible model systems for micelles. It was suggested that water may enter the alkane phase hydrogen bonded to the hydroxyl group of the alcohol and thus solubilised alcohol molecules may carry water into the micellar interior.

This would be achieved by creating a two phase mixture and analysing this partitioning. The partition coefficient  $K_x$  could be calculated by the equation

$$K_x = \frac{x_a^o}{x_a^w} \quad \text{eqn. 7.1}$$

where  $x_a^o$  and  $x_a^w$  are the mole fractions of alcohol in the organic phase and in the water phase, respectively. By assuming ideal behaviour the Gibbs energy of transfer can be calculated according to

$$G_{tr}^o = - RT \ln K_x \quad \text{eqn. 7.2}$$

This can be compared for the different chain lengths alcohol as well as for diols.

An alternative approach exists for the prediction of phase equilibria. Ternary liquid-liquid equilibria can be predicted from excess enthalpies via the method of Rowley and Batter<sup>(65)</sup>. Excess enthalpies would be determined experimentally for each of the constituent binaries. This excess enthalpy data could be fitted using a suitable data reduction program to an enthalpy-based local composition model such as UNIQUAC to predict liquid-liquid equilibria for a type 1 ternary system.

Recently attention <sup>(66)</sup> has been drawn to isomer effects and the effects of molecular size and shape on thermodynamic behaviour of non-electrolyte mixtures. It would be, therefore, of interest to investigate the effect of the butanol isomers on excess volumes when mixed with n-heptane. The interactions between polar and non-polar molecules and the effect of branching of the chain of an alcohol on excess volumes would lead to a better understanding of the associations between alcohols.

REFERENCES

1. Kolb, D., J. Chem. Ed., 1979, 56, 465 - 469.
2. Choucri, N., Technology Review, 1980, October, 36 - 45.
3. Flower, A.R., Scientific American, 1978, 238, 42 - 49.
4. Thompson, R., Energy and Chemistry, Whitstable, 1981.
5. Thring, R.H., SAE Transactions, 1974, 91, 30 - 33.
6. Technology Review, 1981, July 68 - 79.
7. Mullins, P.J., Automotive Industries, 1980, January, 57 - 59.
8. Automotive Engineering, 1979, 87, 69 - 73.
9. Olree, R.M., Lenane, D.L., SAE Paper 840108, 1984.
10. Courtney, R.L., Newhall H.K., SAE Paper 790809, 1979.
11. Haggin, J., Chem. Eng. News, 1983, 60 11 - 14.
12. Harker, J.H., Backhurst, J.R., "Fuel and Energy", Academic Press, London, 1981.
13. Chem. Eng. News, 1983, 60, 23.
14. Lee, B., Chem. Eng. News, 1982, 59, 28.
15. Ward's Engine Update, 1981, 7, 3 - 6.
16. Swift, H.E., American Scientist, 1983, 71, 616 - 620.
17. Meyer, R., Automotive Engineering, 1980, 88, 95 - 99.
18. Hall, D., New Scientist, 1981, 524 - 526.

REFERENCES - Continued

19. Hurn, R.W., SAE Paper, 770759, 1977.
20. Hammond, A.L., Science, 1977, 195 564 - 567.
21. Daniels, J., Motor, 1981, 43 - 45.
22. Murayame, T., et al, "A Method to improve the Solubility and Combustion Characteristics of Alcohol-Diesel Fuel Blends", International Off Highway Meeting and Exposition, Milwaukee, Wisconsin, September, 1982
23. Chem. Eng. News, 1983, 61, 20 - 21.
24. Callahan, J.M., Automotive Industries, 1984, 27 - 28.
25. Advertisement, ARCO Chemical Company.
26. Anderson, E., Chem. Eng. News, 62, 31 - 33.
27. Bertodo, R., SAE Paper 790430, 1979.
28. Ogstone, A., Automotive Engineering, 1980.
29. Letcher, T.M., Chem SA, 1981, February, 35 - 37
30. Schwab, A.W., Fattore, R.S., Pryde, E.H., J. Disp. Sci. Tech., 1982, 3, 45 - 60.
31. Thring, R.H., SAE Paper 831685, . 1983.
32. Lawrason, G.C., SAE Paper SP-254, 1964, 1 - 13.
33. Prausnitz, J.M., "Molecular Thermodynamics of Fluid Phase Equilibria", Prentice-Hall Inc., New York, 1969.
34. Reid, R.C., Prausnitz, J.M., Sherwood, T.K., "The Properties of Gases and Liquids", Third Edition, McGraw - Hill Book Company, 1977.
35. Prausnitz, J.M., Abrams, D.S., A.I. Ch. E. Jour., 1975, 21, 116 - 128.

REFERENCES - Continued

36. Anderson, T.F., Prausnitz, J.M., Ind. Eng. Chem., Process Des. Dev., 1978, 17, 552 - 560.
37. Anderson, T.F., Prausnitz, J.M., Ind. Eng. Chem., Process. Des. Dev., 1978, 17, 561 - 567.
38. IMSL Library Handbook.
39. Bancroft, W.D., Hubard, S.S., 1942, JACS. 64, 347.
40. Nagata, I., et al, Fluid Phase Equilibria, 1977/1978, 1, 267 - 275.
41. Maurer, G., Prausnitz, J.M., Fluid Phase Equilibria, 1978, 2, 91 - 99.
42. Letcher, J.M., Chem SA, 1975, 226 - 231.
43. Monk, P., Wadso, I., Acta Chem. Scand., 1968, 22, 1842.
44. Instruction Manual: Microcalorimetry System 2107, LKB, Sweden
45. Christensen, J.J., Hanks, R.W., Izatz, R.M., "Handbook of Heats of Mixing", Wiley Interscience Publication, New York, 1982.
46. Savini, C.G., Winterhalter, D.R., Van Ness, H.C., J. Chem. Eng. Data, 1965, 10, 168 - 171.
47. DMA - Digital Precision Meters - Operating Instructions, Anton Paar, Austria.
48. Battino, R., Chem. Reviews., 1971, 7, 5.
49. Van Ness, H.C., Soczek, C.A., Peloquin, G.C., Machado, R.L., J. Chem. Eng. Data, 1967, 12, 217 - 224.
50. Bagley, E.B., Nelson, T.P., Scigliano, J.A., J. Phys. Chem, 1975, 77, 2794.



REFERENCES - Continued

51. Hoogendoorn, J.C., Energy Progress, 1982, 2, 32 - 36.
52. CAR, 1985, July, 33 - 35.
53. Koenig, A., Menrad, H., Bernhardt, W., "Alcohols in Automobiles", Alcohol Fuels Conference, Inst. Chem. Eng., Sydney, August 1978.
54. Vogel, "Vogel's Textbook of Practical Organic Chemistry", Revised by Fruniss, B.S., Hannaford, A.J., Rogers, K., Smith, P.W.G., Tatchell, A.R., Fourth Edition, Longmans, London, 1978, 268.
55. Briggs, S.W., Comings, E.W., Ind. Eng. Chem., 1943, 35, 411.
56. Dack, M.R.J., "Solutions and Solubilities", Part II Techniques of Chemistry, Wiley-Interscience Publication, 1977.
57. Backlund, S., Hoiland, H., Vikholm, I., J. Sol. Chem., 1984, 13, 749 - 755.
58. Van Ness, H.C., Van Winkle, J., Richtol, H.H., Hollinger, H.B., J. Phys. Chem., 1967, 71, 1483 - 1489.
59. McCants, J.F., Jones, J.H., Hopson, W.H., Ind. Eng. Chem., 1953, 45, 454 - 456.
60. Roddy, J.W., Coleman, C.F., Ind. Eng. Chem. Fund., 1981, 20, 250 - 254.
61. Adelman, H., SAE Paper 790956, 1979.
62. Bandel, W., "Problems in the Application of Ethanol as Fuel for Utility Vehicles", Proceedings of the International Symposium on Alcohol Fuel Technology, Methanol and Ethanol, Wolfsburg, Federal Republic of Germany, November, 1977.
63. Private Correspondence, Ethyl Corporation, Baton Rouge, Louisiana, U.S.A.
64. Backlund, S., Horland, H., Ljosland, E., Vikholm, I., Fluid Phase Equilibria, 1985, 20, 249 - 256.



REFERENCES - Continued

65. Rowley, R.L., Battler, J.R., Fluid Phase Equilibria, 1985, 18, 111.
66. Chaudhari, S.K., Katti, S.S., J. Chem. Therm., 1985, 17, 101 - 104.

## APPENDIX 1

Crude oil consists of many components as indicated in table 1.A.1. The products from crude oil are separated by distillation and the boiling ranges are also given in the above table. Crude oil is usually liquid at room temperature and is completely soluble in organic solvents such as benzene and also carbon disulphide. On combustion it produces significantly less residual ash than coal. There are four major components in crude oil.

### 1. HYDROCARBONS

These form the greater part of most crudes and are present in a wide range of molecular masses, varying from dissolved gases to solid waxes. The main groups of hydrocarbons in crudes are the paraffins and the branched paraffin. In addition, crude oil contains cyclic compounds such as the naphthenes and aromatic compounds including dicyclic compounds such as naphthalene and pyridine. Olefins are present which also exist as both normal straight chain structures and as isomers. These readily polymerise which affects chemical processes such as cracking as they may form gums.

### 2. OXYGEN COMPOUNDS

Organic compounds containing oxygen are present in small amounts. One important group is the naphthenic acids, which are carboxylic acids containing a naphthene ring. These may present problems in distillation processes and, in addition, corrosion problems since they provide the formation of an emulsion of water in oil in the presence of alkalis.

### 3. SULPHUR COMPOUNDS

The amount varies and for fuel oils these compounds must be removed.

### 4. INORGANIC COMPOUNDS

The inorganic elements are usually in the oil as either suspended particles of mineral matter or dissolved organometallic salts.

Small amounts of water, often containing inorganic salts may be present in the crude, frequently as a suspension or an emulsion if natural emulsifiers are present. These emulsions may be quite stable and elaborate techniques exist for breaking them and removing the water.

TABLE 1.A.1 - IMPORTANT PRODUCTS FROM CRUDE OIL

	Boiling Range (K)	Composition	Manufactured by	Principal uses	Notes
Natural Gas		Mainly methane, some nitrogen depending on source	Natural sources	Fuel gas, also reformed to synthesis gas	Calorific value 38 MJ m <sup>-3</sup>
Liquefied petroleum gas (LPG)	Propane, butane		Stripped from "wet" natural gas or from cracking operations	Domestic and industrial fuel-production of coal gas, synthetic chemicals	Calorific value 100 MJ m <sup>-3</sup>
Primary Flash Distillate (PFD)	Varies	Propane & butane dissolved in gasoline-kerosene range of liquids	Preliminary distillation of crude petroleum	Manufacture of synthesis gas	
Gasoline	300 - 450	Complex mixture of materials. Petrol contains additives to improve performance but no sulphur or polymerizable components	Primary distillation, cracking and reforming processes	Spark ignition internal combustion engines	Octane number indication of performance SG 0.795
Kerosene	410 - 575	Paraffinic hydrocarbons with substantial proportion of aromatics, low sulphur content	Distillation, cracking	Agricultural tractors, lighting, heating and aviation gas turbines	Tractor vaporizing oil (TVO)-aromatics are an advantage-not the case with petrol engines. SG 0.793
Gas Oil	450 - 620	Saturated hydrocarbons	Distillation, hydrodesulphurization	Diesel fuel, heating & furnaces. Feed to cracking units	Initially used for absorbing benzol from coal gas

TABLE 1.A.1 - IMPORTANT PRODUCTS FROM CRUDE OIL - CONTINUED

	Boiling Range (K)	Composition	Manufactured by	Principal uses	Notes
Diesel Fuel	450 - 650	Saturated hydrocarbons, often with high sulphur	Distillation cracking	Diesel engines, furnace heating	Quality of fuel & boiling point range are a function of the duty. Low-speed engine, high-sulphur, high boiling point. SG 0.870
Fuel Oils	500 - 700+		Residue of primary distillation, blended with distillates	Large-scale industrial heating	Require atomizing wide range of viscosities SG 0.89 - 0.95
Lubricating Oils	Wide range	Three types: mainly aromatic, mainly aliphatic or mixed	Vacuum distillation of primary distillation residue solvent extraction	Lubrication	Wide variation in quality from say grease in marine applications to sewing machine oil. Control of viscosity important
Wax		Paraffins	Chilling residue from vacuum distillation	Toilet preparations, food, candles petroleum jelly	
Bitumen		Wide variation	Residue from vacuum distillation or oxidation of residue from primary distillation ("blown" bitumen)	Road surfacing, water-proofing	Wide variation in softening point. NB. "asphalt" in UK is bitumen + mineral filler

The calorific values of the liquid end products from crude oil are compared in Table 1.A.2. to those of methanol and ethanol.

TABLE 1.A.2 - PROPERTIES OF LIQUID FUELS

Fuel	Relative Density	Composition (% by mass)				Calorific value (MJ) Kg <sup>-1</sup>	
		C	H	S	O+N+ash	Gross	Net
<b>Light</b>							
Distillate	0.68	84.10	15.85	0.05		47.8	44.5
Kerosene	0.78	85.8	14.1	0.1		46.5	43.5
Gas Oil	0.83	86.1	13.2	0.7		45.6	42.8
Light Fuel Oil	0.93	85.6	11.7	2.5	0.2	43.5	41.1
<b>Medium Fuel</b>							
Oil	0.95	85.6	11.5	2.6	0.3	43.1	40.8
<b>Heavy Fuel</b>							
Oil	0.96	85.4	11.4	2.8	0.4	42.9	40.5
Methanol	0.796	37.5	12.5		50.0*	22.69	19.94
Ethanol	0.794	52.2	13.0		34.8*	30.15	27.23
Petrol	0.72-0.76	850-885	11.5-15.0	0.1		44.8-46.9	41.9-44.0
T.V.O.	0.815	86.9	12.9	0.2		46.0	43.2
Diesel Fuel	0.840	86.5	13.2	0.3		45.7	42.9

\* Oxygen only.

The basic refining operations of the crude oil is represented in figure 1.A.1.

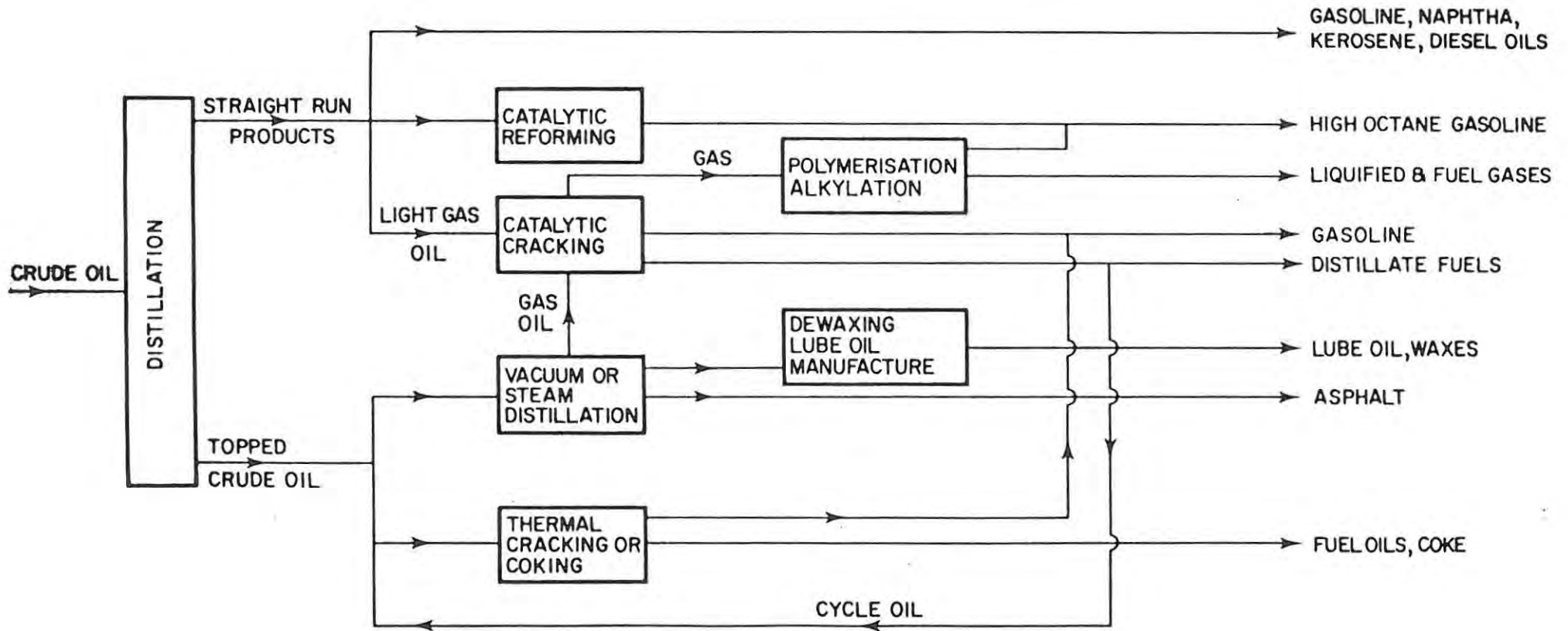


FIGURE 1.A.1 - BASIC REFINING OPERATIONS

APPENDIX 2 - COMPUTER PROGRAMS

```
PROGRAM NONLIN(INPUT,OUTPUT,PLOTFIL=1030/1030,
& TAPE1=INPUT,TAPE2=OUTPUT,TAPE6=PLOTFIL)
PARAMETER (M=29)
PARAMETER (N=2)
PARAMETER (IX = ((N+1)*N)/2 )
PARAMETER (IW = 5*N + 2*M + IX )
EXTERNAL EXAMPL
DIMENSION X(N),F(M),XJAC(M,N),XJTJ(IX),WORK(IW)
DIMENSION PARM(4),Y(29),V(29)
DIMENSION GX(1002),GY(1002),IG(2,4)
CHARACTER*20 HT,XT,YT
COMMON /DATAPT/Y,V

NSIG=4
EPS=0.0
DELTA=0.0
MAXFN=1000
IOPT=1

DO 5 I=1,N
5 X(I)=0.5

DO 10 I=1,M
10 READ(1,*)V(I),Y(I)
CONTINUE

CALL 7XSSQ(EXAMPL,M,N,NSIG,EPS,DELTA,MAXFN,IOPT,PARM,X,SSQ,F,
& XJAC,M,XJTJ,WORK,INFER,IER)

DO 20 I=1,N
20 WRITE(2,*)' X(' ,I,') = ',X(I)
CONTINUE
WRITE(2,*)' SSQ = ',SSQ
WRITE(2,*)' INFER = ',INFER
WRITE(2,*)' IER = ',IER

PRINT*, 'ABCISSA ', 'MEASURED ', 'FITTED ', 'DIFFERENCE '
SUM=0.0
DO 30 I=1,M
30 AB=V(I)
AM=Y(I)
FT=FJUNC(X,N,AR)
DF=FT-AM
SUM=SUM+(DF**2)
PRINT*,AB,AM,FT,DF
CONTINUE
STD=SQRT(SUM/(M-1))
PRINT*, 'STD = ',STD
```



```
NG=2  
DO 40 I=1,M  
GX(I)=V(I)  
GY(I)=Y(I)  
CONTINUE
```

```
IG(1,1)=4  
IG(2,1)=1000-M  
IG(1,2)=-1  
IG(2,2)=0  
IG(1,3)=1  
IG(2,3)=1  
IG(1,4)=1  
IG(2,4)=1
```

```
XRANGE=GX(M)-GX(1)  
XDIFFF=XRANGE/FL0AT(1000-M)  
XPOINT=GX(1)  
DO 50 I=M+1,1000  
GX(I)=XPOINT  
GY(I)=FUNC(X,N,XPOINT)  
XPOINT=XPOINT+XDIFFF  
CONTINUE
```

```
HT='NON LINEAR FIT'  
IHT=14  
XT='-- X --'  
IXT=7  
YT='GAMMA'  
IYT=5  
XSIZE=30.0  
YSIZE=20.0
```

```
CALL PLOTS(0,0,6)  
CALL PLOT(2.,3.,-3)  
CALL GRAPH(GX,GY,NG,IG,HT,IHT,XT,IXT,YT,IYT,XSIZE,YSIZE)  
CALL PLOT(32.0,-20.0,999)
```

```
STOP  
END
```

```
SUBROUTINE EXAMPL(X,M,N,F)  
DIMENSION X(N),F(M)  
DIMENSION Y(29),V(29)  
COMMON /DATAPT/Y,V  
  
DO 5 I=1,M  
F(I) = Y(I)-FUNC(X,N,V(I))  
CONTINUE  
RETURN  
END
```

```
FUNCTION FUNC(X,N,V)
DIMENSION X(N)
DATA R,T/8.314,298.15/
DATA Z,R1,R2,Q1,Q2/10.0,3.97,4.50,3.01,3.86/
V1=V
V2=1.0-V
T1=(V1*Q1)/((V1*Q1)+(V2*Q2))
T2=(V2*Q2)/((V1*Q1)+(V2*Q2))
W1=(V1*R1)/((V1*R1)+(V2*R2))
W2=(V2*R2)/((V1*R1)+(V2*R2))
B1=((Z/2)*(R1-Q1))-(R1-1)
B2=((Z/2)*(R2*Q2))-(R2-1)
```

```
S1=W1/V1
P1=LOG(S1)
S2=T1/W1
P2=LOG(S2)
P3=(Z/2)*Q1*P2
P4=(R1/R2)*B2
P5=W2*(B1-P4)
P6=EXP(-X(2)/(R*T))
PRINT*, 'X(2)=', X(2)
PRINT*, 'P6=', P6
P7=T1+(T2*P6)
P8=-Q1*LOG(P7)
P9=T2*Q1
P10=P6/P7
P11=EXP(-X(1)/(R*T))
PRINT*, 'X(1)=', X(1)
P12=T2+(T1*P11)
P13=P11/P12
P14=P9*(P10-P13)
P15=P1+P3+P5+P8+P14
FUNC=EXP(P15)
```

```
RETURN
END
```

11.10.33.UCLP, SA, SLP01 , 0.271KLNS.

```
PROGRAM UNIQUAC(INPUT,OUTPUT,DATA,SOLU7,TAPES=DATA,TAPES6=SOLU7)
C
  DIMENSION A(2),B(2),W(2),T(2),TT(2),F(12)
  DIMENSION S(10),VX(2),R(2),Q(2),QQ(2),LNGAMA(2),GAMMA(2)
  REAL B,W,T,TT,S,GAMMA,TEMP,P,W1,W2,T1,T2,TT1,TT2,B1,B2
  REAL S7,S8,VX,LNGAMA,S1,S2,S3,S4,S5,S6,S9,S10
  REAL P1,P2,P3,P4,P5,P6,P7,P8,P9,P10,P11,P12
  CHARACTER*80 LINE
C
  READ(5, '(A80)')LINE
  READ(5,*)(A(I),I=1,2)
  READ(5,*)(R(I),I=1,2)
  READ(5,*)(Q(I),I=1,2)
  READ(5,*)(QQ(I),I=1,2)
  READ(5,*)TEMP
  READ(5,*)Z
C
  WRITE(6,100)
  WRITE(6,105)LINE
  WRITE(6,110)(A(I),I=1,2)
  WRITE(6,115)(R(I),I=1,2)
  WRITE(6,120)(Q(I),I=1,2)
  WRITE(6,125)(QQ(I),I=1,2)
  WRITE(6,130)TEMP
  WRITE(6,135)Z
100  FORMAT(T2,'SYSTEM IS: ')
105  FORMAT(A80)
110  FORMAT(T2,'A VALUES ARE: ',T20,F9.4,T30,F9.4)
115  FORMAT(T2,'R VALUES ARE: ',T20,F9.4,T30,F9.4)
120  FORMAT(T2,'Q VALUES ARE: ',T20,F9.4,T30,F9.4)
125  FORMAT(T2,'QQ VALUES ARE: ',T20,F9.4,T30,F9.4)
130  FORMAT(T2,'TEMP IS: ',T20,F9.4)
135  FORMAT(T2,'Z VALUE IS: ',T20,F9.4)
C
  WRITE(6,1)
  WRITE(6,5)
  1  FORMAT(T2,'UNIQUAC EQUATION FOR BINARY PARAMETERS')
  5  FORMAT(T4,'X1',T19,'X2',T40,'GAMMA 1',T55,'GAMMA 2')
C
C
  VX(1)=0.05
10  VX(2)=1.0-VX(1)
C
  W1=(VX(1)*R(1))/((VX(1)*R(1))+(VX(2)*R(2)))
  W2=(VX(2)*R(2))/((VX(1)*R(1))+(VX(2)*R(2)))
  T1=(VX(1)*Q(1))/((VX(1)*Q(1))+(VX(2)*Q(2)))
  T2=(VX(2)*Q(2))/((VX(1)*Q(1))+(VX(2)*Q(2)))
  TT1=(VX(1)*QQ(1))/((VX(1)*QQ(1))+(VX(2)*QQ(2)))
  TT2=(VX(2)*QQ(2))/((VX(1)*QQ(1))+(VX(2)*QQ(2)))
  B1=((Z/2)*(R(1)-Q(1)))-(R(1)-1)
  B2=((Z/2)*(R(2)-Q(2)))-(R(2)-1)
```

```
S1=(W1/VX(1))
P1=LOG(S1)
S2=(W2/VX(2))
P2=LOG(S2)
S3=(T1/W1)
P3=LOG(S3)
S4=(T2/W2)
P4=LOG(S4)
P5=(Z/2)*Q(1)*P3
P6=(Z/2)*Q(2)*P4
S5=(R(1)/R(2))*B2
P5=(Z/2)*Q(1)*P3
P6=(Z/2)*Q(2)*P4
S5=(R(1)/R(2))*B2
P7=W2*(B1-S5)
S6=(R(2)/R(1))*B1
P8=W1*(B2-S6)
```

```
S7=EXP(-A(1)/TEMP)
S8=EXP(-A(2)/TEMP)
P9=Q(1)*(LOG(TT1+(TT2*S8)))
P10=Q(2)*(LOG(TT2+(TT1*S7)))
S9=S7/((TT2+(TT1*S7)))
S10=S8/((TT1+(TT2*S8)))
P11=TT2*Q(1)*(S10-S9)
P12=TT1*Q(2)*(S9-S10)
LNGAMA(1)=P1+P5+P7-P9+P11
LNGAMA(2)=P2+P6+P8-P10+P12
GAMMA(1)=EXP(LNGAMA(1))
GAMMA(2)=EXP(LNGAMA(2))
```

```
C
WRITE(6,15)VX(1),VX(2),GAMMA(1),GAMMA(2)
15 FORMAT(T2,F4.2,T17,F4.2,T32,F15.7,T47,F15.7)
VX(1)=VX(1)+0.05
IF(VX(1).LT.1.00) GOTO 10

STOP
END
```